BUILDING THERMOREGULATION BASED ON THE ADAPTIVE BUILDING ENVELOPE

A Dissertation
Presented to
The Academic Faculty

by

Zhaoyun Zeng

In Partial Fulfillment
of the Requirements for the Degree
Doctor of Philosophy in the
School of Architecture

Georgia Institute of Technology
May 2020

BUILDING THERMOREGULATION BASED ON THE ADAPTIVE BUILDING ENVELOPE

Approved by:

Godfried Augenbroe, Co-Advisor
School of Architecture
Georgia Institute of Technology

Dr. Jason Brown, Co-Advisor
School of Architecture
Georgia Institute of Technology

Dr. Xinyi Song
School of Building Construction
Georgia Institute of Technology

Dr. Jan Hensen
Department of the Built Environment
Eindhoven University of Technology

Dr. Pieter de Wilde
School of Architecture
University of Plymouth

Dr. Ajla Aksamija
Department of Architecture
University of Massachusetts Amherst

Date Approved: December 12, 2019

This thesis is dedicated to my parents,
Guangqing Zeng and Rui Li,
who have been supporting me with their love all along

ACKNOWLEDGEMENTS

I would like to express my sincere gratitude to my co-advisor Prof. Godfried Augenbroe, who shows me what a deep and critical thinker should be like and has guided me with his wisdom and experience on my way to becoming a qualified researcher. He also set an outstanding example for me of how to educate the young generation of researchers. I will always be proud of being one of his students.

I would also like to express my deep gratitude to my co-advisor Dr. Jason Brown, who has given me valuable advice on how to think logically and rigorously.

I would like to extend my sincere thanks to my committee members for their invaluable suggestions on my thesis. They are Dr. Xinyi Song, Dr. Jan Hensen, Dr. Pieter de Wilde, and Dr. Ajla Aksamija.

The selective reflective coating in Section 5.2 was developed by Dr. Natalie Stingelin and Mr. Alex Balzer. I cannot finish this section without their exceptional work and support.

TABLE OF CONTENTS

ACKNOWLEDGEMENTS	**iv**
LIST OF TABLES	**viii**
LIST OF FIGURES	**ix**
LIST OF SYMBOLS AND ABBREVIATIONS	**xiii**
SUMMARY	**xx**
CHAPTER 1. Introduction	**1**
1.1 Inspiration	**1**
1.2 The Definition of the Adaptive Building Envelope	**4**
1.2.1 Counter-Load Energy, Natural Energy, and Artificial Energy	5
1.2.2 Intrinsic Control and Extrinsic Control	6
1.2.3 Two Functions of Building Systems	7
1.2.4 Passive System and Active System	8
1.2.5 Static Passive System and Dynamic Passive System	12
1.2.6 The Definition of ABE	12
1.3 A Review of ABE Technologies	**13**
1.3.1 Classification of ABE Technologies	13
1.3.2 Glazing Technology	14
1.3.3 Opaque Technology	32
1.3.4 Bridge Technology	42
1.3.5 A Finite-Difference Model of ABE Technologies	48
1.4 Research Questions	**51**
1.5 The Structure of This Thesis	**52**
CHAPTER 2. Energy Saving Potential of ABE	**54**
2.1 Weather Variables that Determine Energy Saving Potential	**54**
2.2 Methods of Calculating the Energy Saving Potential	**59**
2.2.1 Building Model	59
2.2.2 Outdoor Dry-bulb Temperature	60
2.2.3 Outdoor Wet-bulb Temperature	62
2.2.4 Sky Temperature	64
2.2.5 Solar Radiation	66
CHAPTER 3. Modelling Methods of ABE Systems	**70**
3.1 The General Structure of Modelling Methods of ABE Systems	**70**
3.1.1 Control Module and Interface	72
3.1.2 Actuator	76
3.2 Glazing Technology	**78**
3.2.1 Dynamic Shading Device	78
3.2.2 Switchable Window	82

3.2.3 Double Skin Façade (DSF) 84
3.2.4 Movable Insulation 86
3.3 Opaque Technology 87
3.3.1 Dynamic Façade 87
3.3.2 Radiative Coating 93
3.3.3 Thermal Storage 94
3.4 Bridge Technology 96
3.4.1 Thermodiode 96
3.4.2 Evaporative Cooling 98

CHAPTER 4. The Optimization of ABE 101
4.1 A Critical Review of Previous ABE Optimization Studies 101
4.1.1 Categorization of Previous ABE Optimization Studies 101
4.1.2 Comments on Previous ABE Optimization Studies 104
4.2 A Generic Optimization Framework for ABE 106
4.3 Product Development 108
4.3.1 Design Variable 112
4.3.2 Constraint 113
4.3.3 Objective Function 114
4.4 Building Design 119
4.4.1 Selection of a Set of Technologies 120
4.4.2 Design Variable 122
4.4.3 Constraint 123
4.4.4 Objective Function 125
4.5 Building Operation 126
4.5.1 The Nested Optimization Framework 127
4.5.2 Model Predictive Control 128

CHAPTER 5. Application Studies 132
5.1 Application Study 1: Optimization of a Façade with Movable Insulation 132
5.1.1 Overview 132
5.1.2 Problem Description 133
5.1.3 The Building Model of This Study 134
5.1.4 Formulation of the Optimization Problem 136
5.1.5 Control of Movable Insulation 141
5.1.6 Results of Scenario 1 145
5.1.7 Revision of the Formulation of the Optimization Problem 148
5.1.8 Cost Model of Scenario 2 151
5.1.9 Results of Scenario 2 154
5.2 Application Study 2: Optimization of a Selective Reflective Coating 158
5.2.1 Overview 158
5.2.2 Problem Description 159
5.2.3 The Building Model of This Study 162
5.2.4 Formulation of the Optimization Problem 164
5.2.5 Results 169
5.3 Application Study 3: Optimization of a Ventilated Façade with MPC 171
5.3.1 Overview 171

5.3.2 Problem Description 172
5.3.3 Model Predictive Control Parameters 174
5.3.4 The Finite-Difference Model of This Study 175
5.3.5 Verification of the Finite-Difference Model 182
5.3.6 Explicit Constraint and Implicit Constraint 184
5.3.7 Design Optimization with Nested MPC 192

CHAPTER 6. Closure 198
6.1 Contributions of This Thesis 198
6.1.1 The Energy Saving Potential of ABE Technologies 198
6.1.2 Modelling Methods for ABE Technologies 199
6.1.3 A Generic Optimization Framework for ABE 199
6.2 Limitations of This Thesis 200
6.2.1 Solving ABE Optimization Problems 200
6.2.2 Cost Model 201
6.2.3 Characteristics of the Selective Reflective Coating 201
6.3 Future Work 202
6.3.1 The Energy Saving Potential of ABE Technologies 202
6.3.2 The Selection of ABE Technologies 202
6.3.3 MPC 203

REFERENCES 205

LIST OF TABLES

Table 1	– The similarities between the heat balance of the human body and that of the building	1
Table 2	– The classification of different ABE technologies	13
Table 3	– The variables associated with each family of ABE technology	51
Table 4	- The weather variables and the ABE technologies	55
Table 5	– Cities chosen as examples for the outdoor dry-bulb temperature case	61
Table 6	– The four scenarios of utilizing the sky temperature for cooling	65
Table 7	– Cities chosen as examples for the solar radiation case	68
Table 8	– Explanation of the four approaches to the optimization of ABE	102
Table 9	– The differences of the freedom of changing the design variables between different optimization approaches	104
Table 10	– Summary of incompatible ABE technologies	121
Table 11	– Summary of the three application studies	132
Table 12	– Formulation of the optimization problem of application study 1	136
Table 13	– The properties of different window configurations in scenario 1	139
Table 14	– Cost of double-glazed windows of different sizes	152
Table 15	– Cost of materials used in the insulation layer	153
Table 16	– Cost of items used in the control system	153
Table 17	– The properties of the bare window that the selective reflective coating is applied to	168
Table 18	– Comparison of the four control methods	187
Table 19	– Design variables and their levels for the nested optimization	193

LIST OF FIGURES

Figure 1	– The roadmap of developing the new definition of the ABE	5
Figure 2	– The three ways of distinguishing between passive systems and active systems	10
Figure 3	– The configuration of an electrochromic device	16
Figure 4	– The transmittance curves of a full WO3-based electrochromic device (Y. Wang et al., 2016)	18
Figure 5	– Spectral reflectance (a) and transmittance (b) for a 0.05-µm-thick VO2 film in semiconducting and metallic states (S. Y. Li, Niklasson, & Granqvist, 2012)	26
Figure 6	– The configuration of a sliding movable insulation	32
Figure 7	– Exploded view and section of a type of dynamic insulation façade (Koenders et al., 2018)	35
Figure 8	– The configuration and working mechanism of the breathing wall in the winter (Imbabi, 2012)	37
Figure 9	– The working mechanism of a bi-directional thermodiode (Chun et al., 2002)	44
Figure 10	– (a) Direct evaporative cooling and (b) indirect evaporative cooling (Riangvilaikul & Kumar, 2010)	46
Figure 11	– (a) The principle of the M-cycle (Wani, Ghodke, & Shrivastava, 2012) and (b) the psychrometric representation of the M-cycle	47
Figure 12	– The configuration of an M-cycle cooler (Rogdakis & Tertipis, 2015)	48
Figure 13	– (a) The nodal representation of the finite-difference model; (b) the matrix representation of the glazing envelope model; and (c) the matrix representation of the opaque envelope model	50
Figure 14	– The structure of this thesis	53
Figure 15	– (a) Geometry and (b) thermal zoning of the small office building model	60

Figure 16	– Proportion of the cooling need removed by cooling the indoor air down to the outdoor dry-bulb temperature	61
Figure 17	– Proportion of the cooling need removed by cooling the indoor air down to the outdoor wet-bulb temperature	63
Figure 18	– The proportion of cooling need removed by using nighttime radiative cooling + thermal storage	66
Figure 19	– The proportion of heating need removed with solar energy	69
Figure 20	– The general structure of modelling methods of ABE systems	70
Figure 21	– A simple configuration of BCVTB that connects Matlab and EnergyPlus	76
Figure 22	– Specifying overhangs with different tilt angles in the Shading: Building: Detailed object	79
Figure 23	– The rendering of the overhang at different tilt angles	79
Figure 24	– (a) Double skin façade system opening conditions and (b) air nodes in EnergyPlus (D. Kim et al., 2018)	86
Figure 25	– The diagram of the ventilated slab model	89
Figure 26	– Schematic process of adapting the ventilated slab model to a closed-loop dynamic insulation system (Koenders et al., 2018)	92
Figure 27	– The nodal model of thermodiode	98
Figure 28	– The connection of three indirect evaporative coolers and one direct evaporative cooler to model an M-cycle system	100
Figure 29	– The relationship between the four approaches to the optimization of ABE	103
Figure 30	– A generic optimization framework for ABE (The focus of this chapter is highlighted by blue boxes.)	107
Figure 31	– Overview of the technology readiness level scale (Mankins, 2009)	111
Figure 32	– The nested optimization framework for building design optimization	128
Figure 33	– Relationship between different optimization horizons (Corbin et al., 2013)	131

Figure 34	– Structure of application study 1	134
Figure 35	– The residential building model used in application study 1	135
Figure 36	– Different layouts of the south façade	136
Figure 37	– The control system for movable insulation	142
Figure 38	– The EUI colour map for static windows	146
Figure 39	– The EUI colour map for windows with movable insulation	148
Figure 40	– The position of the points at which the illuminance is measured for application study 1	149
Figure 41	– The average UDI colour map for the double-glazed window	150
Figure 42	– The utility function colour map for static windows	151
Figure 43	– Lowest LCC and the corresponding window configuration for different WWRs	155
Figure 44	– LCC colour map for four typical WWRs	156
Figure 45	– The structure of DBRs	160
Figure 46	– The modulation of the width, height, and position of the high-reflectance band (Bachevillier et al., 2019)	160
Figure 47	– Comparison of the original forward approach workflow and the modified forward approach workflow	162
Figure 48	– The adapted single-zone building model for application study 2	164
Figure 49	– The position of the points at which the illuminance is measured for application study 2	166
Figure 50	– The Pareto optimal set of the selective reflective coating	170
Figure 51	– The feasible region of the selective reflective coating	171
Figure 52	– The configuration and control states of the ventilated façade	173
Figure 53	– Diagram of the finite-difference model used in application study 3	178
Figure 54	– Linear regression of fan power versus flow rate	182

Figure 55 – A comparison between the hourly ideal cooling energy in May of the EnergyPlus model and the finite-difference model 183

Figure 56 – A comparison between the indoor air temperature in May of the EnergyPlus model and the finite-difference model 184

Figure 57 – A thermostat that measures mean radiant temperature 186

Figure 58 – The comparison of operative temperature between the four control methods (The solid olive line marks the thermal comfort threshold (21°C) and the dashed olive lines mark the beginning of the occupied hours each day (6:00).) 189

Figure 59 – The comparison of control decisions of the three control methods 190

Figure 60 – The comparison of energy cost between the four control methods 192

Figure 61 – The optimized control decisions of different design cases 194

Figure 62 – The total HVAC energy cost (U.S. $) of different design cases 195

LIST OF SYMBOLS AND ABBREVIATIONS

HVAC	Heating, ventilation and air conditioning
ABE	Adaptive building envelope
ABF	Adaptive building façade
LC	Liquid crystal
SPD	Suspended particle device
DSF	Double skin façade
DRC	Daytime radiative cooling
SHGC	Solar heat gain coefficient
Tr_{vis}	Visible transmittance
Tr_{sol}	Solar transmittance
PCM	Phase change material
DEC	Direct evaporative cooling
IEC	Indirect evaporative cooling
η_{wb}	Wet-bulb effectiveness
$T_{o,db}$	Outdoor dry-bulb temperature [°C]
$T_{p,o}$	Temperature of the product stream at the outlet of an evaporative cooling system [°C]
$T_{o,wb}$	Outdoor wet-bulb temperature [°C]
$\mathbf{A}$, $\mathbf{B}$, $\mathbf{D}$	Coefficient matrices
$\mathbf{C}$, $\mathbf{E}$	Source vectors
$\mathbf{T}$	Temperature vector
A	Surface area [m^2]
h	Heat transfer coefficient [W/(m^2·K)]

k	thermal conductivity [W/(m·K)]
T	Temperature [°C]
Q	Heat transfer rate [W] or temperature [°C]
Δt	Time step [s]
c	Specific heat [J/(kg·K)]
$\dot{m}$	Mass flow rate [kg/s]
DOP	Degree of perfection
COP	Coefficient of performance
η_c	Carnot efficiency
Q_c	Cooling power output of a refrigeration system [W]
P_e	Electric power input of a refrigeration system [W]
T_H	Temperature of the high-temperature heat reservoir [K]
T_L	Temperature of the low-temperature heat reservoir [K]
PNNL	Pacific Northwest National Laboratory
$T_{cl,n}$	New cooling setpoint [°C]
$T_{cl,o}$	Original cooling setpoint [°C]
Φ_r	Radiative heat loss to the sky from the inside [W]
R_{se}	External surface heat resistance of the building envelope element considered, $m^2 \cdot K/W$
U_c	Thermal transmittance of the element [$W/(m^2 \cdot K)$]
A_c	Projected area of the element [m^2]
h_{or}	External radiative heat transfer coefficient [$W/(m^2 \cdot K)$]
$\Delta\theta_{er}$	Average difference between the external air temperature and the apparent sky temperature [°C]
$\Phi_{sol,k}$	Solar energy transferred to the inside through surface k

$F_{sh,ob,k}$	Shading reduction factor for external obstacles for the solar effective collecting area of surface *k*
$A_{sol,k}$	Effective collecting area of surface *k* with a given orientation and tilt angle, in the considered zone or space [m^2]
$I_{sol,k}$	Solar irradiance, the mean energy of the solar irradiation over the time step of the calculation, per square meter of collecting area of surface *k*, with a given orientation and tilt angle [W/m^2]
$F_{r,k}$	Form factor between the building element and the sky
BCVTB	Building Controls Virtual Test Bed
LBNL	Lawrence Berkeley National Laboratory
PDE	Partial differential equation
k_0	Thermal conductivity at 20°C [W/(m·K)]
k_1	Change in conductivity per degree temperature difference from 20°C [$W/(m \cdot K^2)$]
$T_{o,r}$	Outdoor mean radiant temperature [°C]
T_{op}	Outdoor panel temperature [°C]
T_{ip}	Indoor panel temperature [°C]
T_i	Indoor temperature [°C]
h_{eq}	Equivalent heat transfer coefficient of a thermodiode [$W/(m^2 \cdot K)$]
NASA	National Aeronautics and Space Administration
TRL	Technology Readiness Level
$F(\mathbf{x})$	Objective function
$\mathbf{x}$	Vector of design variables
$g_i(\mathbf{x})$	*i*th inequality constraint
$h_j(\mathbf{x})$	*j*th equality constraint
Utility	Utility function
n	Number of objective functions

w_i	Weight of the *i*th objective function
$F_i(\mathbf{x})$	*i*th objective function
F_i^o	Utopia point
p	An exponent for a global criterion
$\mathbf{X}$	Feasible design space
$\mathbf{F}$	Vector of objective functions
$F^*(\mathbf{x})$	Penalty function
α_i, β_j	Penalty parameters
RBC	Rule-based control
MPC	Model predictive control
RHC	Receding horizon control
WWR	Window-to-wall ratio
EUI	Energy use intensity
LCC	Life-cycle cost
XPS	Extruded polystyrene
R_{grid}	Source-site ratios for grid electricity
R_{ng}	Source-site ratios for natural gas
E_c	Annual electricity consumption for cooling [kWh]
E_f	Annual electricity consumed by fans in the HVAC system [kWh]
E_h	Annual natural gas consumption for heating [kWh]
A_f	Total floor area of the buildings [m^2]
U_t	Total U-factor of the window with an additional insulation layer [$W/(m^2 \cdot K)$]
U_g	U-factor of the glazing layer [$W/(m^2 \cdot K)$]
R_I	Thermal resistance of insulation layer [$m^2 \cdot K/W$]

C_{HVAC} Total operation cost of the HVAC system [U.S. $]

n Number of years considered

$C_{HVAC,1}$ Operation cost of the HVAC system for the first year [U.S. $]

d Discount rate

Ab_{sol} Solar absorptance

I_{sol} Incident solar radiation [W/m^2]

h_{oc} Outside surface convection heat transfer coefficient [W/(m^2·K)]

h_i Inside surface heat transfer coefficient [W/(m^2·K)]

U_{eq} Equivalent thermal conductance of the glazing system [W/(m^2·K)]

Q_{c0} Conduction heat flux through the window [W/m^2]

Q_{s0} Solar radiation transmitted through the window [W/m^2]

Q_0 Total heat transfer rate through the window when the movable insulation is open [W/m^2]

Q_1 Conduction heat flux through the window when the movable insulation is closed [W/m^2]

UDI Useful daylight illuminance

nEUI Normalized energy use intensity

A_w Area of the window [m^2]

U_w U-factor of the window [W/(m^2·K)]

l_{XPS} Thickness of XPS [cm]

TMM Transfer-matrix method

NREL National Renewable Energy Laboratory

nE_{HAVC} Normalized source HVAC energy consumption

$E_{c,id}$ Annual ideal cooling energy need [kWh]

$E_{h,id}$ Annual ideal heating energy need [kWh]

η_h Efficiency of the heating system

Re_{sol}	Solar reflectance
Re_{vis}	Visible reflectance
Ab_{vis}	Visible absorptance
C_{elec}	Unit price of grid electricity [$/kWh]
E_{fan}	Total electricity consumption of the ventilated façade fan [kWh]
C_{ng}	Unit price of natural gas [$/kWh]
Nu	Nusselt number
Ra	Rayleigh number
AR	Aspect ratio of the cavity
h_{rad}	Radiative heat transfer coefficient [W/(m^2·K)]
σ	Stefan-Boltzmann constant, 5.67×10^{-8} [W/(m^2·K^4)]
ε_1, ε_2	Emissivity of the two walls
Re	Reynolds number
Pr	Prandtl number
v_{air}	Air velocity [m/s]
A_{sec}	Sectional area of the air channel [m^2]
ρ_{air}	Density of air [kg/m^3]
c_{air}	Specific heat of air [J/(kg·K)]
T_m	Temperature of the *m*th air stream node [°C]
T_{w1}, T_{w2}	Temperatures of the two walls [°C]
h_{conv}	Convective heat transfer coefficient [W/(m^2·K)]
A_w	Area of the air channel wall [m^2]
T_{op}	Operative temperature [°C]
T_{mr}	Mean radiant temperature [°C]
$T_{i,a}$	Indoor air temperature [°C]

T_{ht} Heating setpoint [°C]

ANOVA Analysis of variance

SUMMARY

In contrast to the traditional building envelope, which tries to block the thermal and mass exchange between the indoor and outdoor environments as much as possible, the adaptive building envelope (ABE) can admit the favorable environmental factors while block the adverse ones to reduce the building load as well as improve the thermal and visual comfort of the occupants. This thesis is intended to facilitate the research of ABE by (1) Clarifying the definition of ABE and offer conceptualizations that are important to the research. (2) Investigating the energy saving potential of ABE technologies by associating these technologies with four weather variables. The results of this investigation can be used in the selection of ABE technologies. (3) Summarizing the existing modelling methods for ABE technologies. If the modelling methods for certain ABE technologies do not exist, they will be developed in this thesis. (4) Reviewing and categorizing the optimization approaches adopted in previous studies on ABE. Recommendations are also made for choosing the appropriate optimization approaches in different application scenarios. (5) Developing a generic optimization framework for ABE that can guide the formulation of optimization problems in different application scenarios. (6) Conducting three application studies that can enrich the optimization framework and serve as paradigms for using the optimization framework in different application scenarios.

CHAPTER 1. INTRODUCTION

1.1 Inspiration

The Thermoregulation, according to the Merriam-Webster dictionary, means "The maintenance or regulation of temperature; specifically: the maintenance of a particular temperature of the living body". Despite the extremely wide variations of environments that humans are exposed to, the thermoregulation of the human body is able to maintain the core body temperature accurately around 37°C (Arens & Zhang, 2006; Downey & Lemons, 1994; Loonen, Trcka, Costla, & Hensen, 2013). Looking closely, we found astonishing similarities between the heat balance of the human body and that of the building, which are summarized in Table 1.

Table 1 – The similarities between the heat balance of the human body and that of the building

Human body	Building
Respiration	Ventilation
The skin separates the internal and external environments of the human body	The envelope separates the indoor and outdoor environments of the building
Convective and radiative heat transfer between the skin and the environment	Convective and radiative heat transfer between the envelope and the environment
Diffusion of moisture through the skin	Diffusion of moisture through the envelope
The anterior hypothalamus is the central receptor and regulator of temperature	In most buildings/rooms, a central thermostat and a central temperature controller is used
Sweating	Evaporative cooling
Shivering	Heating system

Some activities (e.g. eating and exercise) can generate an excessive amount of heat	Some activities (e.g. cooking and partying) can cause an excessive amount of cooling load
Active thermal transport by the cardiovascular system	Active thermal transport by the heating, ventilation and air conditioning (HVAC) system

However, there are also distinct differences between the heat balance of the human body and that of the building. Firstly, solar radiation plays a more significant role in the heat balance of the building than in that of the human body, clearly because buildings have transparent envelope components (e.g. windows, skylights and glazing doors) and the interior space of the building is also transparent to sunlight. Secondly, the internal space of the human body is filled with liquids, while that of the building is filled with air. Thirdly, the skin temperature of the human body has a great impact on the thermoregulation, while in most buildings the temperature of the envelope plays no part in the control of the HVAC system. Fourthly, the human body can adjust the heat exchange rate with the environment by means of vasoconstriction, vasodilatation, and adjusting clothing, while seldom can a building do the same (Arens & Zhang, 2006; Downey & Lemons, 1994).

These similarities and differences inspire us to think if we could apply the concept of thermoregulation to the control of the built environment. The similarities demonstrate that the same heat and mass transfer mechanisms apply to both the heat balance of the human body and that of the building. The differences, on the other hand, show the potential to improve the current control methods of the built environment by means of biomimetics, i.e., learning from the thermoregulation of the human body.

If we make an analogy between the human body and the building in terms of thermoregulation, the counterpart of the skin in the building is the envelope. However, the function of the skin in the thermoregulation is far more crucial and versatile than that of traditional building envelope. The traditional role of building envelope is to separate the indoor and outdoor environments. By doing so, the building envelope provides shelter and protection for the occupants from the outside and keeps the indoor environment insensitive to the variation of the outdoor environment (Loonen et al., 2013; Oral, Yener, & Bayazit, 2004; Sadineni, Madala, & Boehm, 2011). In the building codes of the UK and the US, increasingly stringent requirements are imposed on the thermal insulation of the building envelope with the release of each new version (Sadineni et al., 2011). In the practice of high-performance building design, high-insulation and airtightness are regarded as the key features of a high-performance building (D. H. W. Li, Yang, & Lam, 2013; Torcellini et al., 2006). The emphasis on insulation and airtightness reflects the ingrained notion of the building envelope's role as a static partition (Favoino, Overend, & Jin, 2015). In ECBCS Annex 44 (Heiselberg, 2012), this approach to the design of the building envelope is called the exclusive approach, while the approach which will be introduced below is called the selective approach. In the exclusive approach, all the temperature and humidity control tasks are left to the HVAC system, which is quite energy intensive. However, in the regulation of the human body, the skin not only serves as a partition of the internal and external environments but also is equipped with temperature receptors and thermoregulatory actuators. The signal from skin receptors serves as an early warning to the central nervous system of potential changes in the heat exchange rate with the environment so that appropriate physiological responses can be initiated to minimize the disturbance to the internal environment (Downey & Lemons, 1994). The responses of the skin to thermal stress include vasoconstriction, vasodilatation, and sweating (Arens &

Zhang, 2006). Although the adjustment of clothing is a conscious action of the person, here we will juxtapose it with the responses of the skin, because its function is basically the same as vasoconstriction and vasodilatation, namely, adjusting the heat exchange rate with the environment. In the regulation of the human body, the homeothermy is first realized by the responses of the skin. Only when the disturbance exceeds the control ability of these responses, are more intensive actions like shivering taken. From this point of view, it is better to control the temperature and humidity of the indoor environment first with the building envelope. Only when the thermal load exceeds the control ability of the building envelope, does the HVAC system come into play. Apparently, a traditional building envelope does not possess the capacity to do this.

1.2 The Definition of the Adaptive Building Envelope

Partially inspired by the skin, the concept of the adaptive building envelope (ABE) or the adaptive building façade (ABF) is proposed (Loonen et al., 2013). It is able to perform more functions of the skin than the traditional building envelope is. The concept of adaptive building components has been reflected in many other studies, in which different terms are used to convey the same concept as "adaptive". These terms are responsive, active, dynamic, intelligent, smart, interactive, switchable, and so on (Favoino et al., 2015; Heiselberg, 2012; Loonen et al., 2013). Before we begin the in-depth discussion of ABE, it is critical to give it a clear and precise definition. Some attempts to define ABE have been made in previous studies. In (Ferguson, Siddiqi, Lewis, & Weck, 2007), adaptability is defined as "a system's ability to adapt itself to deliver intended functionality under varying conditions through the design variables changing their physical values". According to (Loonen et al., 2013), ABE is defined as the building envelope that "has the ability to repeatedly and reversibly change some of its functions, features or behavior over time in response to changing performance requirements and boundary conditions, and does this with the aim of improving overall building performance". However, these definitions are given in an arbitrary rather than systematic way. It is hard for the readers to follow the researchers' path of developing these definitions. In addition, these definitions are not definitive enough, hence readers sometimes cannot determine whether a system belongs to ABE or not simply based on these definitions. For instance, according to the definition given by (Loonen et al., 2013), window air conditioners should probably be classified into ABE systems, but in most people's views HVAC systems do not belong to ABE. Therefore, a new concept system is needed to provide a systematic and unambiguous definition of ABE. The roadmap of developing the new definition of ABE is shown in Figure 1.

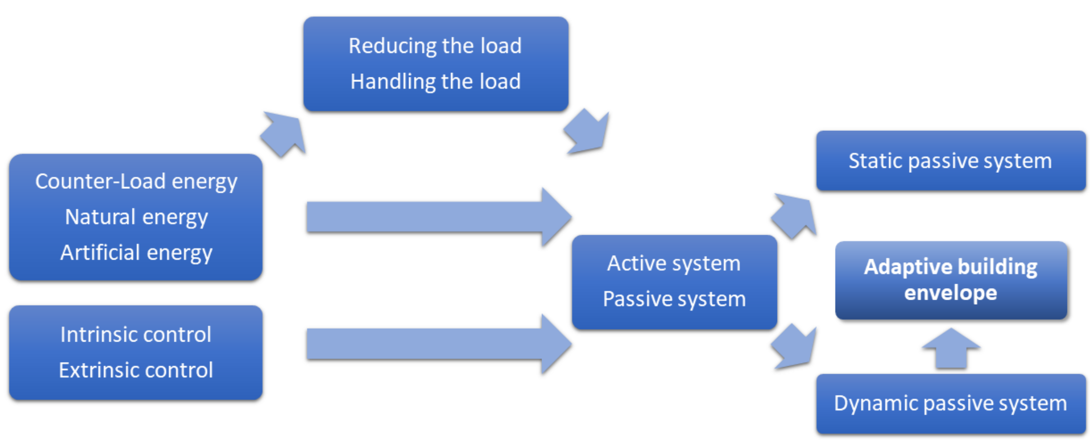

Figure 1 – The roadmap of developing the new definition of the ABE

1.2.1 Counter-Load Energy, Natural Energy, and Artificial Energy

First, we need to specify three types of energy: counter-load energy, natural energy, and artificial energy. The counter-load energy is the energy in the built environment that can balance the building load. It has the same form as the building load and can improve the quality of the built environment. The building load consists of heating load, cooling load, and lighting load. The heating/cooling load is the thermal energy that needs to be added to or removed from the built environment to keep the temperature and humidity within certain ranges. The lighting load is the light needed to maintain a comfortable lighting level. The natural energy is the energy that exists naturally in the outdoor environment and can be utilized directly. It includes thermal energy in the outdoor environment, solar energy, wind, etc. It can be transformed into the counter-load energy freely without resorting to mechanical or electrical systems. The artificial energy is the energy generated through human interference and at least one energy conversion. It includes electricity, thermal energy produced by burning fuel, cooling energy stored in chilled water, etc.

1.2.2 Intrinsic Control and Extrinsic Control

The control method of the building systems can be classified into two types: intrinsic control and extrinsic control (Loonen et al., 2013). If a building system changes its working status or properties by responding to environmental stimuli (temperature, light, relative humidity, etc.) directly, we call it intrinsically controlled. Intrinsic control is realized by the self-regulating mechanisms of the system. These mechanisms usually cannot be changed once the system is produced. Therefore, intrinsically controlled systems do not give users access to control. Conversely, if a building system changes its working status or properties by responding to the signal from an external control system, we call it extrinsically controlled. Extrinsic control is usually realized by a feedback loop consisting of sensors, processors, and actuators. Extrinsically controlled systems give users more freedom to change the control logic or to control them manually.

1.2.3 Two Functions of Building Systems

A building can be seen as a system. Its components or the collection of some components are its subsystems (Blanchard & Fabrycky, 2005). In a general sense, the function of all environment-related building systems is to provide a comfortable built environment for the occupants in an efficient way. There are two approaches to achieving this goal. The first is to make the best of the environmental conditions to reduce the building load. This approach requires the building systems to be selective, i.e., blocking the adverse factors in the outdoor environment while admitting the favorable ones. In this approach, all the counter-load energy is transformed from the natural energy. The artificial energy can only be used in the transport of the energy carrier or the control of the energy transformation and transport processes rather than the production of the counter-load energy. The transformation from the natural energy to the counter-load energy does not necessarily entail the change of energy form. For example, when the sunlight enters a room in need of heating though a window, it transforms naturally from the natural energy to the counter-load energy. The second approach is to improve the efficiency of the building systems that handle the load. It differs from the first approach in that these systems cannot change the quantity of the load. The improvement of the efficiency of these systems can only reduce the amount of artificial energy required. In this approach, the counter-load energy is at least partially transformed from or produced by the artificial energy. This process may either entail or not entail the change of energy form. For example, the conversion from electricity to light involves the change of energy form, while the transformation from the heat produced by burning natural gas to the thermal energy in the built environment does not involve the change of energy form.

1.2.4 Passive System and Active System

Since the concept of "Passive House" was first put forward by Wolfgang Feist and Bo Adamson in 1988 (iPHA, 2018), the term passive building or passive design have been widely used in high-performance building research and practice to express a sense of not costing traditional energy (Loonen et al., 2013; Sadineni et al., 2011). However, the meanings of passive building and its opposite, active building, in different documents are inconsistent and even contradictory. According to the Passive House Standard published by the International Passive House Association (iPHA), the Passive House features high insulation and high airtightness of the envelope, low space heating and cooling demand, and high thermal comfort (iPHA, 2018), but this standard is not widely adopted by other researchers. In (Loonen et al., 2013), active technologies are defined as those technologies that "aim at enhancing the level of sustainability in the built environment via the introduction of innovative technical devices. Such devices are used for decentralized generation and supply of energy from renewables, or for conversion of resources at higher overall efficiencies". While passive building is defined as those buildings "where the design of construction and shape of the building itself, as opposed to its servicing, play major roles in capturing, storing and distributing wind and solar energy, normally with the aim of displacing fossil fuels for space conditioning and lighting". In this definition, "active" is an attribute of devices, while "passive" is associated with the design of the construction and the shape of the building itself. In (Sadineni et al., 2011), active energy efficient strategies are defined as "improvements to heating, ventilation and air conditioning (HVAC) systems, electrical lighting, etc.". Passive energy efficient strategies, on the other hand, are defined as "improvements to building envelope elements". In this definition, the author equates active systems with HVAC and electrical lighting systems, which can be seen as energy-consuming systems, and equates passive systems with building envelope elements. Neither of these definitions delimit active system and passive system clearly or catch the essential characteristics that differentiate these two systems. In (Favoino, Fiorito, Cannavale, Ranzi, & Overend, 2016; Favoino et al., 2015; Kamalisarvestani, Saidur, Mekhilef, & Javadi, 2013; Ye, Meng, Long, & Xu, 2013), the passive system is defined as the system modulated by self-triggered adaptive mechanisms, while the active system is defined as the system modulated by external stimuli. This definition focuses on the difference in the control methods. In passive heating/cooling system studies (Balcomb, Hedstrom, & Mcfarland, 1977; H. Y. Chan, Riffat, & Zhu, 2010; Henze, Felsmann, & Knabe, 2004), the active system refers to a system with separate solar collectors and thermal storage devices that require mechanically driven thermal fluids to function, whereas the passive system does not have such features. This categorization is clear but needs to be generalized to other building systems. In order to maintain consistency within this thesis and pave the way for future studies, we will try to unify different ways of defining passive system and active system into one concept system.

Various ways of distinguishing between the passive system and the active system in the literature can be classified into three ways, which are from the aspects of function, energy source, and control method, respectively, as shown in Figure 2. In Figure 2, the blue cells denote passive systems and the orange cells denote active systems. In the first way, all building systems whose function is to reduce the building load are passive systems, which include building envelope, shading device, heat recovery system, etc. The building systems whose function is to handle the building load are active systems, which include HVAC system and electrical lighting system. The most fundamental difference between the passive system and the active system is where the counter-load energy is from. The passive system transforms the natural energy into the counter-load energy, while the active system transforms or converts the artificial energy into the counter-load energy. Some passive systems may consume artificial energy, but only for the transport of the energy carrier or the control of the energy transformation and transport process. Examples of such passive systems are active thermal storage system, heat recovery system, and liquid crystal-based switchable window.

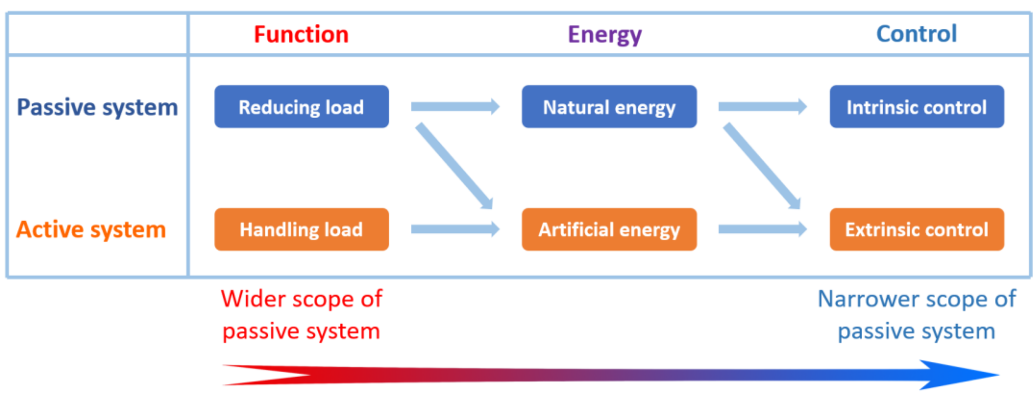

Figure 2 – The three ways of distinguishing between passive systems and active systems

The second way of distinguishing between the passive system and the active system is based on the energy sources that drive them. If a system is driven fully by natural energy, it is a passive system. If a system is at least partially driven by artificial energy, it is an active system. Natural energy can also be used to improve the efficiency of active systems. For example, the air conditioning system must be driven by electricity or high-temperature heat, but the economizer can be employed to improve the efficiency of the air conditioning system. All the active systems defined from the aspect of function are still active systems by this definition. However, the passive systems defined from the aspect of function can be divided into two groups: those consuming artificial energy and those not. The former are categorized as the active system by this definition while the latter are categorized as the passive system. For systems using artificial energy for control, if the system needs continuous artificial energy supply to maintain its working status, it should be categorized as the active system. Conversely, if the system only needs artificial energy input during the switching process, it should be categorized as the passive system. In this respect, liquid crystal-based switchable windows are active systems, while chromogenic windows are passive systems.

The third way of defining the passive system is from the aspect of control method. If a system is intrinsically controlled, it is a passive system, while an extrinsically controlled system is an active system. By this definition, all the active systems defined from the aspect of energy source are active systems. Some of the passive systems defined from the aspect of energy source are categorized into active systems and some are still passive systems. Examples of the building systems that do not consume the artificial energy but are extrinsically controlled are chromogenic windows and automatic natural ventilation windows.

As shown in Figure 2, from the first way to the third way of defining passive systems, the scope of passive systems is getting narrower. For brevity, these three definitions can be referred to as the function definition, energy definition, and control definition of the passive system, respectively. There are valid reasons for adopting any of them. In this study we will stick to the function definition of the passive system, because we want to cover as many passive systems as possible in the discussion of this thesis.

1.2.5 Static Passive System and Dynamic Passive System

The passive system can also be classified into static passive system and dynamic passive system. The dynamic passive system is the passive system that has movable components and more than one working status. By changing its working status, it can change the energy exchange process between the outdoor and indoor environments in a spatial or temporal manner. In a spatial manner, the dynamic passive system can enhance, temper, or redirect the energy exchange between the outdoor and indoor environments. In a temporal manner, it can collect and store the natural energy and release it when and where needed. Typical dynamic passive systems include dynamic shading devices, switchable windows, thermal storage systems, heat recovery systems, heat pipes, etc. Correspondingly, the static passive system is any passive system that is not a dynamic passive system. Most of the traditional building systems that we are familiar with are static passive systems, e.g., well-insulated walls, static shading devices, and Trombe walls. They may also change the energy exchange process between the outdoor and indoor environments in a spatial or temporal manner, but this process cannot be controlled. For example, light shelf can change the path of sunlight and Trombe wall can store solar energy in the day the release it in the night.

1.2.6 The Definition of ABE

Finally, with the definitions of the passive system and active system clarified, we can define ABE. The adaptive building envelope (ABE) is the building envelope that has dynamic passive components which are able to change their working statuses according to the varying outdoor and indoor conditions to exploit the potential of reducing the building load by blocking the adverse factors in the outdoor environment while admitting the favorable ones.

According to this definition, ABE is a dynamic passive system. The active systems that are integrated into the building envelope such as building-integrated photovoltaics (BIPV) (Norton et al., 2011) do not belong to ABE systems. Although these systems can be integrated into the building envelope, they can also be stand-alone systems without impairing any of their functions.

1.3 A Review of ABE Technologies

This section provides a comprehensive review of the ABE technologies. The scope of this review is determined by the definition of ABE given in Section 1.2.6.

1.3.1 Classification of ABE Technologies

The classification of ABE technologies is shown in Table 2.

Table 2 – The classification of different ABE technologies

Category	Family	Technology
Glazing technology	Dynamic shading device	
	Switchable window	Chromogenic window (Electrochromic window, gasochromic window, thermochromic window, photochromic window)

		Liquid crystal (LC)-based window
		Suspended particle device (SPD) window
	Double skin façade (DSF)	
	Movable insulation	
Opaque technology	Dynamic façade	Dynamic insulation
		Ventilated façade
		Breathing wall
	Radiative coating	Variable radiative coating
		Daytime radiative cooling (DRC) material
	Thermal storage	
Bridge technology	Thermodiode	
	Evaporative cooling	Direct evaporative cooling
		Indirect evaporative cooling
		Maisotsenko cycle

1.3.2 Glazing Technology

The adaptive technologies applied to the glazing part of the envelope mainly include dynamic shading, switchable window, double skin façade (DSF), and movable insulation.

1.3.2.1 <u>Dynamic Shading Device</u>

Shading devices are the devices that can block undesired sunlight while transmit or redirect desired sunlight. Shading devices can be installed on either the outside or the inside of the glazing system. The external shading device mainly includes overhang, fin, vertical panel, louver, and light shelf, while the internal shading device mainly includes venetian blinds and roller shade (Kirimtat, Koyunbaba, Chatzikonstantinou, & Sariyildiz, 2016; Konstantoglou & Tsangrassoulis, 2016). Dynamic shading devices are shading devices whose position, tilt angle, or transparency can be changed. They represent the earliest attempts of humans to regulate the indoor environment using ABE. Most existing external shading devices are static shading devices owing to the considerations of cost, accessibility, and durability. Deciduous trees can be regarded as a type of external dynamic shading device because of the seasonal variation of their canopy density (Berry, Livesley, & Aye, 2013; Huang, Akbari, Taha, & Rosenfeld, 1987). On the other hand, almost all internal shading devices are dynamic shading devices.

Dynamic shading devices have two major advantages. Firstly, it can achieve great cooling and heating energy savings with relatively low cost. When a designer is designing a static shading device, a balance has to be stricken between reducing the cooling need in the summer and increasing the heating need in the winter (Palmero-Marrero & Oliveira, 2010). With dynamic shading device, both cooling and heating energy savings can be assured. In certain cases dynamic shading device has similar energy performance to those significantly more expensive technologies, such as DSF (D. Kim, Cox, Cho, & Yoon, 2018). Secondly, dynamic shading device can adjust the amount of daylight that enters the building, which not only saves lighting electricity but also improves the visual comfort of the occupants (Hammad & Abu-Hijleh, 2010; Kirimtat et al., 2016; Konstantoglou & Tsangrassoulis, 2016; E. S. Lee, DiBartolomeo, & Selkowitz, 1998; Nielsen, Svendsen, & Jensen, 2011).

1.3.2.2 Switchable Window

Chromogenic windows are the windows that can change their optical properties upon receiving some external stimuli. Depending on the stimulus that triggers the change, chromogenic windows can be divided into electrochromic windows (responding to electricity), gasochromic windows (responding to gases), thermochromic windows (responding to heat), and photochromic windows (responding to light).

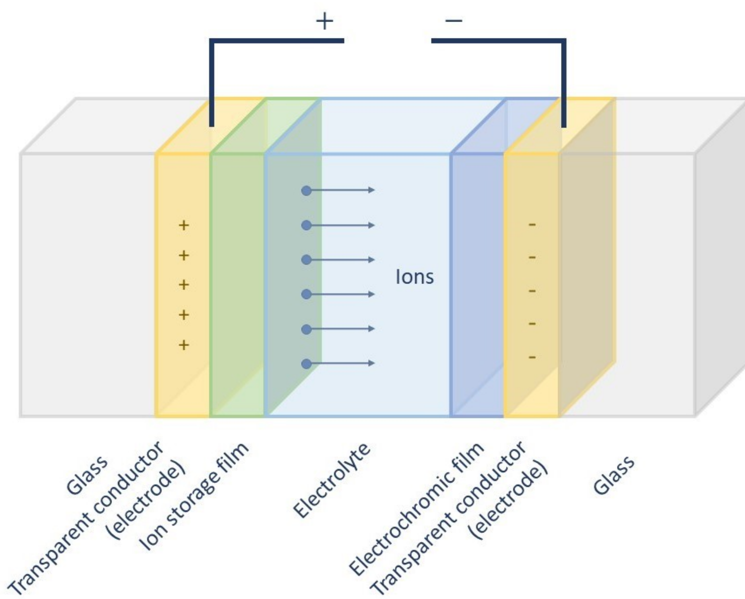

Figure 3 – The configuration of an electrochromic device

The **electrochromic window** can change its optical properties reversibly when an electrical potential is applied. It usually consists of five layers sandwiched between two substrates made of glass or plastic (Baetens, Jelle, & Gustavsen, 2010; Georg, Georg, Graf, & Wittwer, 2008; Granqvist, 2007; Y. Wang, Runnerstrom, & Milliron, 2016). As shown in Figure 3, from one side to the other, the five layers are transparent conductor (electrode), ion storage film, ion conductor (electrolyte), electrochromic film, and transparent conductor (electrode). Many metal oxides can be used as electrochromic materials, among which WO_3 is the most popular and promising one (Baetens et al., 2010; Georg et al., 2008; Granqvist, 2007; Sbar et al., 1999; Y. Wang et al., 2016). Besides metal oxides, some organic materials also show electrochromism, but most of them degrade when exposed to ultraviolet and thus cannot be used in windows (Baetens et al., 2010; Y. Wang et al., 2016). When an external electrical potential is applied to the electrochromic window, the electrons and ions in the ion storage film are inserted into the electrochromic film and the electrochromic material transforms to its coloured state which has low visible transmittance (Tr_{vis}) and solar transmittance (Tr_{sol}). When the electrical potential is reversed or the two electrodes are short-circuited, the electrochromic material returns to the bleached state which has high Tr_{vis} and Tr_{sol}. The transmittance curves of the coloured and bleached states of a typical WO_3-based electrochromic device is shown in Figure 4. The colouration can be halted at any intermediate level between the fully coloured and fully bleached states (Granqvist, 2007), which means the optical properties of an electrochromic window can be controlled continuously. If the external circuit is open, the coloured state can be maintained for extended hours (as long as 160 h) (Granqvist, 2007; Y. Wang et al., 2016). This feature is called open-circuit memory, which is highly desirable in terms of energy saving, as the power supply is only needed during adjustment. The applied electrical potential is a direct-current (DC) voltage of around 1–2 V, with higher voltages leading to a faster rate of reaction, a deeper colouration, and consequently a longer bleaching time (Georg et al., 2008; Sbar et al., 1999). This requires a specialized low-voltage DC power source with adjustable output, which is a disadvantage of electrochromic windows. Although the optical properties of electrochromic window can be changed, they have little impact on the U-factor of the window. The determinants of the U-factor of an electrochromic window are the same as a static window, i.e., number of glazing, type of filled gas, property of low-e coating, etc. The U-factor of most electrochromic window products right now is similar to that of low-e double-glazed window (Baetens et al., 2010; Papaefthimiou, Syrrakou, & Yianoulis, 2006; SageGlass®).

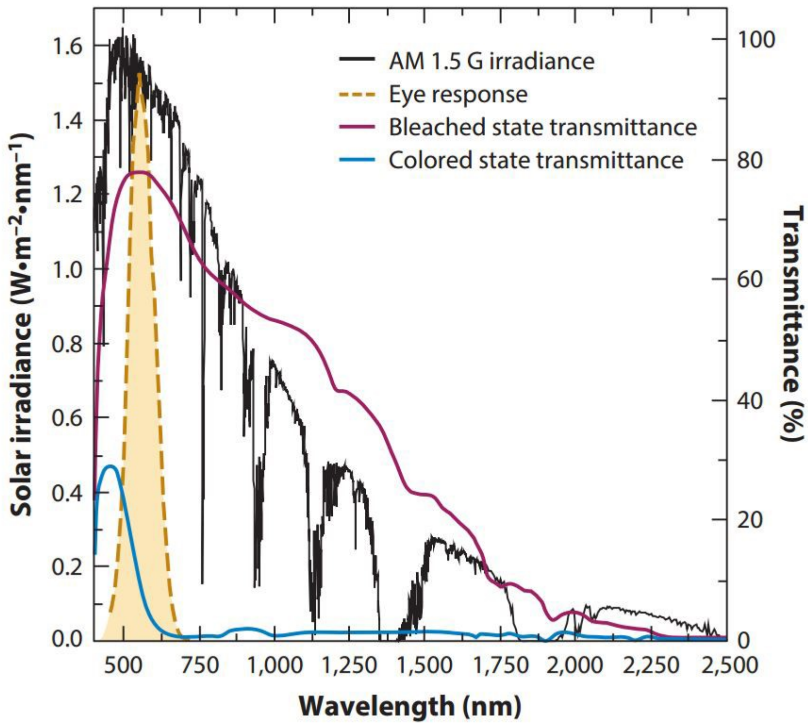

Figure 4 – The transmittance curves of a full WO_3-based electrochromic device (Y. Wang et al., 2016)

The most important properties of electrochromic windows concerned with their application are size, modulation range of transmittance, colouring/bleaching time, and durability. The size is important because it is technically difficult to keep the two electrodes isolated over a large area, avoiding the contact of electrons but providing a good contact for ions (Georg et al., 2008). Larger area also causes longer colouring/bleaching time (E. S. Lee & DiBartolomeo, 2002). The size of the electrochromic devices in the literature varies from a few square centimeters to over 2,000 square centimeters. Manufacturers like

SageGlass and EControl-Glas already have the ability to produce windows with a size of $1.6 \times 2.6\ m^2$ (Baetens et al., 2010).

The modulation range of Tr_{vis} and Tr_{sol} measures the ability of an electrochromic window to modulate the transmitted light. The larger the range, the stronger the ability. As shown in Figure 4, in the coloured state WO_3 has a wide absorption band centered in the near infrared, thus appearing blue. The coloured and bleached Tr_{vis} of the electrochromic devices in the literature are in the range of 0.02–0.38 and 0.58–0.81, respectively. The coloured and bleached Tr_{sol} are in the range of 0.08–0.45 and 0.53–0.74, respectively (Baetens et al., 2010). The product flyer of SageGlass shows that the coloured Tr_{vis} and Tr_{sol} of the products available on the market can already be lower than 0.01, while the bleached Tr_{vis} is in the range of 0.40–0.60 and the bleached Tr_{sol} is in the range of 0.18–0.33 (SageGlass®). The low Tr_{vis} and Tr_{sol} values indicate that the electrochromic windows currently available on the market may impede the exploitation of daylight and are not suitable for heating dominated climates.

The colouring/bleaching time is usually defined as the time required to reach 90% of the maximum coloured and bleached state (Baetens et al., 2010). Shorter colouring/bleaching time is desired because a fast reaction speed can increase visual comfort level. The normal colouring/bleaching time is in the order of a few minutes (Baetens et al., 2010; Georg et al., 2008; Granqvist, 2007; Sbar et al., 1999). However, in cold environment, this time can increase dramatically up to 85 min (E. S. Lee & DiBartolomeo, 2002; Eleanor S Lee et al., 2006).

Superior durability is a key characteristic for a product to succeed on the market. Customers are expecting warranties of 20 years for window products (Sbar et al., 1999). The general indicator of the durability of an electrochromic window is the number of cycles it can perform before losing its modulation range. The order of magnitude of typical number of cycles in the literature is 3 (Baetens et al., 2010; Granqvist, 2007). SageGlass reported that the electrochromic window it produced only lost 2% of its bleached state transmittance after 52,000 cycles in moderate conditions. In high-temperature and high-light intensity cycling conditions, the number of cycles significantly reduces to the range of 1,300 to 5,300 (Sbar et al., 1999). However, these values are usually obtained in the accelerated tests, which cannot reflect the long lifespan that these windows are expected to have. If we want to test the windows in real working conditions, direct exposure tests are required. However, the data for long periods (years) of direct exposure tests are scarce. Results of direct exposure tests of only 18 weeks are reported by SageGlass (Sbar et al., 1999). Both SAGE and EControl-Glas offer warranties of 10 years on their products (Baetens et al., 2010). In conclusion, the durability of electrochromic windows has reached an acceptable level but is still far from as competitive as static windows.

The benefits of adopting electrochromic windows are improved comfort level, lower energy consumption, and lower peak load. The most recognized benefit of electrochromic windows is the improvement of visual comfort and higher occupant satisfaction (Eleanor S Lee et al., 2006; E. S. Lee & Tavil, 2007). The improvement of visual comfort arises from not only the elimination of glare, but also the continuous access to view to the outside (Eleanor S Lee et al., 2006; Sbar et al., 1999). If the coloured Tr_{vis} of the electrochromic window is greater than 0.03, it should still be combined with blinds.

However, the electrochromic window can reduce the period of pulling down the blinds to only 2% of a year, compared to 62% for a static window with Tr_{vis} = 0.60 (Eleanor S Lee et al., 2006). Since its transmittance can be tuned continuously, the electrochromic window is the ideal window to be used in parallel with dimmable lights. The savings of lighting energy can be 44% compared to a reference case with no daylight control (Eleanor S Lee et al., 2006). Different from the great lighting savings, the electrochromic window can only provide marginal cooling load reduction, specifically, below 10% (Eleanor S Lee et al., 2006; E. S. Lee & Tavil, 2007; Papaefthimiou et al., 2006). If the reference window is well shaded, the cooling load of the electrochromic window is even 11% higher than the reference window (Eleanor S Lee et al., 2006). This is because although the transmittance of electrochromic windows is low, their absorptance is rather high. The absorption of solar radiation can raise the temperature of the glazing to more than 60°C in real situations (Sbar et al., 1999). Thus, the thermal radiation of the glazing to the indoor environment is strong. The electrochromic window can reduce the peak cooling load by 19% relative to a fully shaded case and 26% relative to an unshaded case (Eleanor S Lee et al., 2006). The peak electric demand can be reduced by 7–8% for medium windows and 14–16% for large windows (E. S. Lee & Tavil, 2007). The reduction of peak cooling load makes the selection of a smaller cooling equipment possible, and thus saves initial investment.

The main constraint on the application of electrochromic windows is without doubt its high cost. In 2005 and 2006, the price of electrochromic windows is around 10 times that of static solar controlled windows: 1080 €/m^2 vs. 80 €/m^2 (Syrrakou, Papaefthimiou, & Yianoulis, 2005) and \$100/ft^2 vs. \$10–15/ft^2 (Eleanor S Lee et al., 2006). Over the past decade, the price of electrochromic windows has been dropping significantly. In 2016, most of the smart windows (not necessarily electrochromic windows) cost between \$50/ft^2 and \$100/ft^2 (Home Ideas, 2016). In the news posted in 2018, electrochromic windows were said to cost 2 to 4 times as much as standard double-paned windows (Vance, 2018; Wesoff, 2018).

The advantages and disadvantages of electrochromic window is summarized as follows:

Advantages:

- Elimination of glare without blocking view to the outside;
- Continuous adjustment of the transmittance;
- Giving the occupants access to control;
- Power supply only needed during adjustment;
- Replacing conventional windows directly;
- Lighting energy savings when combined with dimmable lights;
- Reduction of peak cooling load.

Disadvantages:

- High cost;
- Requirement of specialized power source;
- Blue colour;
- Worse durability than static window;
- Low bleached Tr_{sol}.

The working mechanism of **gasochromic windows** is similar to that of electrochromic windows. In gasochromic windows, the electrons and ions are provided to the electrochromic material by means of hydrogen gas instead of an external electrical potential, which obviates the need for electrodes, electrolyte, and ion storage film (Baetens et al., 2010). High porosity of the electrochromic material is conducive to the gas exchange process and thus enhances the switching speed (Feng et al., 2016; Georg et al., 2008). With a much simpler configuration, the gasochromic window not only can have higher transmittance but also is less expensive than the electrochromic window. The bleached and coloured Tr_{vis}s of gasochromic windows in the literature are in the range of 0.67–0.77 and 0.06–0.12, respectively (Baetens et al., 2010; Georg et al., 2008). Diluted hydrogen (usually a mixture of 4% hydrogen and 96% argon) well below its combustion limit can be used to turn the gasochromic window into the coloured state, while diluted oxygen (usually a mixture of 4% oxygen and 96% argon) can be used to restore the gasochromic window back to the bleached state (Baetens et al., 2010; Feng et al., 2016; Georg et al., 2008). The hydrogen can be provided either by pressurized containers or electrolysers (Baetens et al., 2010; Georg et al., 2008). The pros and cons of gasochromic window are similar to those of electrochromic window. Other issues that hinder the application of gasochromic window are the complexity of the gas supply system and the difficulty in system assembly (Feng et al., 2016).

Thermochromic windows have a transition temperature, τ_c, below which the thermochromic material is semiconductor and has relatively high Tr_{sol} and above which the thermochromic material is metal and has relatively low Tr_{sol} (Babulanam, Eriksson, Niklasson, & Granqvist, 1987; Granqvist, 2007; Kamalisarvestani et al., 2013). The semiconducting state is also called the cold state and the metallic state is also called the hot state. The spectral reflectance and transmittance of a 0.05-μm-thick VO_2 film is shown in

Figure 5. As can be seen in Figure 5, the transition from the cold state to the hot state significantly reduces the infrared transmittance but has little impact on the visible transmittance (Babulanam et al., 1987; Kamalisarvestani et al., 2013; Saeli, Piccirillo, Parkin, Binions, & Ridley, 2010). Therefore, unlike electrochromic windows, thermochromic windows do not have the ability to adjust the indoor daylight level, which entails the use of blinds. The ideal transition temperature of a thermochromic window is around 20°C (Babulanam et al., 1987; Granqvist, 2007; Kamalisarvestani et al., 2013; Long & Ye, 2014; Saeli et al., 2010), which is between the cooling setpoint and heating setpoint. As the most widely used and most promising thermochromic material, the crystal of VO_2 has a transition of 68°C, which is far above the desired value (Granqvist, 2007; Kamalisarvestani et al., 2013). However, other metal oxides that show thermochromism have even higher τ_cs and therefore are less promising starting points for developing thermochromics with a τ_c in the comfort zone (Granqvist, 2007). Another obstacle to the application of the thermochromic window is its low transmittance (Granqvist, 2007; Kamalisarvestani et al., 2013). The cold state Tr_{vis} of most VO_2 specimens in the literature is in the range of 0.37–0.50 with only a few outliers of 0.65 and 0.78 (Kamalisarvestani et al., 2013). This low transmittance may lead to insufficient daylight. The brown and yellow colour of the VO_2 film may also be an undesirable feature for the occupants (Kamalisarvestani et al., 2013). There are various ways to solve these problems. Fluorine doping can increase the Tr_{vis} of VO_2 film remarkably and decrease the τ_c, but the colour remains brown and yellow. Tungsten doping, on the other hand, can efficiently reduce the τ_c to the comfort zone, increase the Tr_{vis} to a certain degree, and turn the colour to the more

attractive blue. Overlaying an anti-reflection coating, such as TiO_2 and ZrO_2, is also conducive to the improvement of Tr_{vis} (Granqvist, 2007; Kamalisarvestani et al., 2013).

In terms of energy saving, an ideal thermochromic window should have a transition temperature around 20°C, constant Tr_{vis} values in both the cold and hot states, and large infrared transmittance difference between the cold and hot states. In addition, it is preferable that the decrease of infrared transmittance is accompanied by the increase of infrared reflectance instead of the increase of infrared absorptance (Saeli et al., 2010). A thermochromic window is most appropriate for cooling dominated climates, where the window stays in the hot state almost all the time throughout a year (Saeli et al., 2010; Ye, Long, Zhang, & Gao, 2014). In such a climate, the annual load reduction by adopting the thermochromic window can be 44% relative to a clear glass window, and 9%–12.5% relative to a static low-e window (Hoffmann, Lee, & Clavero, 2014; Saeli et al., 2010). In places with hot summer and cold winter, the cooling energy savings by adopting the thermochromic window may be neutralized or even surpassed by the heating energy increase (Ye et al., 2014).

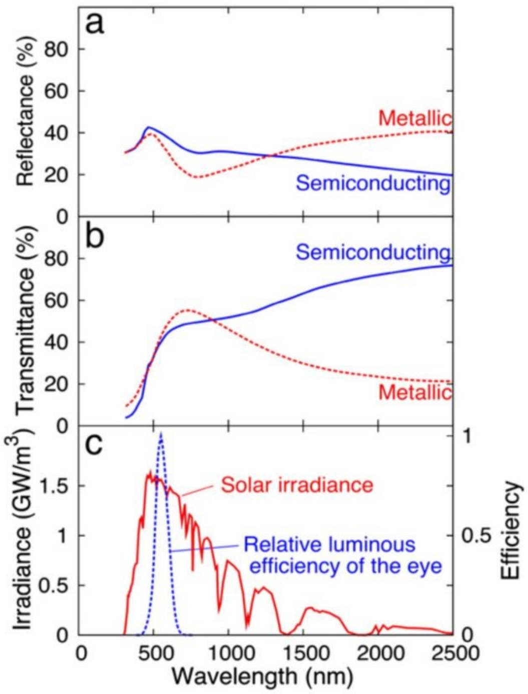

Figure 5 – Spectral reflectance (a) and transmittance (b) for a 0.05-µm-thick VO_2 film in semiconducting and metallic states (S. Y. Li, Niklasson, & Granqvist, 2012)

A photochromic material changes its optical properties when exposed to radiation. Photochromic materials include polymers and metal oxides (Y. Wang et al., 2016; Zhang, Zou, & Tian, 2013). Conventional photochromic materials have been used in eyewear, lens, data recording and storage, and many other areas, but there lacks the information of the application of photochromic materials in building windows (Teowee et al., 1999; Y. Wang et al., 2016; Zhang et al., 2013). This is probably because the transmittance of photochromic materials heavily relies on the incident radiation intensity and does not allow user control (Y. Wang et al., 2016).

There is also another type of "photochromic" window called the photoelectrochromic window. A photoelectrochromic window is the combination of an electrochromic window and a dye-sensitized film (e.g. TiO_2) (Bechinger, Ferrere, Zaban, Sprague, & Gregg, 1996; Teowee et al., 1999). It is basically an electrochromic window powered by a photovoltaic cell. By opening or connecting the external circuit, the occupants can control the state of the window. A photoelectrochromic window does not require an external power source, but the use of dye-sensitized films lowers the bleached state transmittance owing to the dye's absorption, which hinders its application in windows (Y. Wang et al., 2016).

The working mechanisms of **liquid crystal (LC)-based switchable windows** and **suspended particle device (SPD) windows** are similar. They are both originally developed for the display function and thus have fast switching speed (Baetens et al., 2010). In liquid crystal-based switchable windows, a liquid crystal layer is sandwiched between two transparent electrodes, which are further placed between two layers of glass. Polymer-dispersed liquid crystals (PDLC) and encapsulated liquid crystals (NCAP) are the most commonly used liquid crystal types (Baetens et al., 2010). In the off state, the liquid crystal molecules are randomly oriented and scatter the incident light, with the window appearing opaque. When an electrical potential is applied, all the liquid crystal molecules are aligned, allowing more light to pass through (Baetens et al., 2010; Kamalisarvestani et al., 2013). Due to the blocking of the liquid crystal molecules, in the bleached state, a liquid crystal window is still opaque when viewed at an angle (Xu, Liu, Legenski, Ning, & Taya, 2004). The Tr_{vis} in the bleached and coloured states is usually in the range of 0.012–0.061 and 0.505–0.62, respectively (Baetens et al., 2010; Hosseinzadeh Khaligh, Liew, Han, Abukhdeir, & Goldthorpe, 2015). Colouring and bleaching times are usually in the order of 2 and 0.5 min (Baetens et al., 2010). The applied voltage is usually between 65 and 230

V AC, which means mains electricity can be used directly (Baetens et al., 2010; Ghosh, Norton, & Duffy, 2015). Large-area LC-based switchable windows are already commercially available. Continuous power supply is needed to maintain the bleached state, resulting in a power consumption of 3.5 to 15.5 W/m^2 (Baetens et al., 2010). Therefore, liquid crystal-based switchable windows are commonly adopted for aesthetic or privacy purposes instead of energy saving (Baetens et al., 2010).

Similar to LC-based switchable windows, in SPD windows the needle-shaped or spherical particles suspend in an organic fluid or gel with random orientations in the off state, scattering the incident light. When a voltage of 20–220 V AC is applied, the suspended particles are aligned and the window is transformed to the transparent state (Baetens et al., 2010; Cupelli et al., 2009; Ghosh et al., 2015; Vergaz, Sánchez-Pena, Barrios, Vázquez, & Contreras-Lallana, 2008), causing a continuous power consumption of 1.9 to 16 W/m^2 (Baetens et al., 2010). The Tr_{vis} in the bleached and coloured states is usually in the range of 0.04–0.050 and 0.49–0.79, respectively (Baetens et al., 2010). A short switching time of 100–200 ms can be realized (Baetens et al., 2010; Cupelli et al., 2009; Ghosh et al., 2015).

Comparing with electrochromic window, the advantages of LC-based switchable windows and SPD windows are that they do not require a specialized power source and have fast switching speed. The disadvantage is very obvious, i.e., high energy consumption.

1.3.2.3 Double Skin Façade (DSF)

The DSF is the construction in which an external glazing skin is added to the outside of a building façade with an intermediate space (called the channel) between them (Ghaffarianhoseini et al., 2016; Shameri, Alghoul, Sopian, Zain, & Elayeb, 2011; Zhou & Chen, 2010). Typically, the exterior skin uses single-layer safety glass while the interior skin uses single- or double-pane glass. It is desired that both skins are operable. Controllable blinds are usually installed in the channel. In theory, DSF is the technology that can best reflect the concept of passive thermoregulation because of its versatility. It has the capability of passive cooling, passive heating, daylight control, solar heat gain control, thermal storage, enhanced natural ventilation, and acoustic insulation. They are discussed in detail below.

- Passive cooling and enhanced natural ventilation. With the openings in both skins controlled properly and the blinds lowered, the stack effect in the channel can enhance natural ventilation by extracting the hot air from the building (E. Lee, Selkowitz, Bazjanac, Inkarojrit, & Kohler, 2002).
- Passive heating and thermal storage. With the exterior window closed, DSF works similarly to a Trombe wall and stores solar heat in a thermal storage device. In some cases, opening the interior windows helps direct solar heat into the room (Gratia & De Herde, 2004).
- Daylight control. The daylight level can be controlled continuously by changing the slat angle or the position of the blinds (D. Kim et al., 2018; Shameri et al., 2011).
- Solar heat gain control. The amount of solar heat gain entering the room can be controlled by changing the state of the blinds and the openings in both skins (D. Kim et al., 2018; Shameri et al., 2011).

- Acoustic insulation. Field studies have shown that DSF can reduce the indoor noise level significantly due to the acoustic insulation capability of a second skin. This is especially effective for building located in loud places such as airports and high-traffic urban areas (E. Lee et al., 2002; Pasquay, 2004).

Despite its various functions, there are two main obstacles to the widespread application of DSF. The first one is the suboptimal design and operation of DSF due to the large number of degrees of freedom in both design and operation. For a DSF to realize its full potential, two rounds of optimization are required. Firstly, the design of a DSF should be optimized. The variables that should be optimized include the window size of the interior and exterior skins, the window type of the interior and exterior skins, the depth of the channel, and the configuration of the blinds (Joe, Choi, Kwak, & Huh, 2014). These variables should be optimized for each location and each building type. Then, the operation of a DSF should be optimized. The optimization variables include the state of the blinds and the state of each window (Gratia & De Herde, 2004; Park, Augenbroe, Sadegh, Thitisawat, & Messadi, 2004). These variables should be optimized not only for each location and each building type, but also for each moment of the operation. The objective function of the optimization may also be changed during the operation due to the change of room function or occupant preference. This makes the optimization of the operation of DSF a formidable task. As a result of uneven design and control quality, the reported energy savings by adopting DSF range widely from negative to 50% (Ghaffarianhoseini et al., 2016; Stribling & Stigge, 2009).

The second obstacle is the exorbitant cost of DSF. Different sources report the cost of DSF at \$135–360/m^2, €500/m^2, \$585/m^2, \$680/m^2, and even \$900–1,800/m^2, respectively (E. Lee et al., 2002; Pasquay, 2004; Roth, Lawrence, & Brodrick, 2007). The pay-back period of DSF was also estimated by different studies to be 30–200 years and 81 years (A. L. S. Chan, Chow, Fong, & Lin, 2009; Stribling & Stigge, 2009). Therefore, DSF is mostly used in landmark projects in which cost is not a primary concern (Roth et al., 2007).

1.3.2.4 Movable Insulation

Movable insulation is an opaque insulation layer that can be either attached to or removed from the window according to the need. The moving mechanism can be sliding, folding, or rolling, and the installation position can be either the inside or the outside of the glazing. Movable insulation can change not only the SHGC but also the U-factor of the window. Numerous movable insulation application examples have been summarized in books by Langdon and Shurcliff, respectively (Langdon, 1980; Shurcliff, 1980). Figure 6 shows the configuration of a sliding movable insulation system. The main difference between movable insulation and dynamic louvers is that the use of dynamic louvers emphasizes on the control of the SHGC alone, the associated U-factor change being unintended and uncontrolled. Therefore, automatically controlled louvers are mostly applied to office buildings only to reduce solar heat gain (Hammad & Abu-Hijleh, 2010). In contrast, movable insulation controls both the U-factor and SHGC of the window, and it is mainly applied to residential buildings to reduce both cooling and heating loads.

Hashemi and Gage investigated the risk of condensation and heating energy savings of movable insulation through simulation and experiment (Hashemi & Gage, 2012). They placed a test cell with a double-glazed window inside a climate chamber and measured the heating load of the test cell with or without the thermal shutter in typical static heating conditions. A heating load reduction of around 40% was observed in all cases.

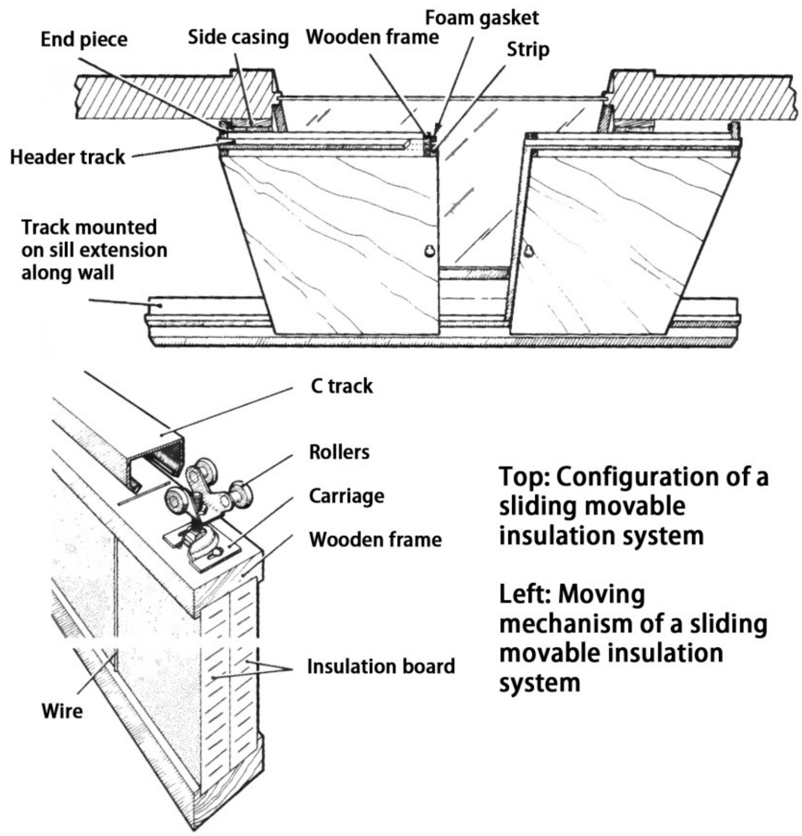

Figure 6 – The configuration of a sliding movable insulation system (Langdon, 1980)

1.3.3 Opaque Technology

Opaque technology refers to those adaptive technologies applied to the opaque parts of the envelope. It includes dynamic façade, radiative coating, and thermal storage. Dynamic façade performs its function through the variation of the U-factor and the airflow through the façade. Radiative coating has the capability to vary the solar absorptance and thermal emittance of the exterior surface of the envelope. Thermal storage is able to change the energy exchange process between the outdoor and indoor environments in a temporal manner. It is an efficient way to mitigate the diurnal or seasonal fluctuation of the ambient temperature.

1.3.3.1 Dynamic Façade

Dynamic façade is the façade whose equivalent U-factor can be changed by rearranging the volume, position, or flow of the air inside the façade. It is referred to as smart insulation (Kimber, Clark, & Schaefer, 2014), dynamic insulation (Imbabi, 2012; Koenders, Loonen, & Hensen, 2018; Taylor, Cawthorne, & Imbabi, 1996; Taylor & Imbabi, 1998), ventilated façade (Balocco, 2002; Ciampi, Leccese, & Tuoni, 2003; de Gracia, Navarro, Castell, Ruiz-Pardo, Alvárez, et al., 2013; de Gracia, Navarro, Castell, Ruiz-Pardo, Álvarez, et al., 2013; López, Jensen, Heiselberg, & Ruiz de Adana Santiago, 2012), and breathing wall (Wong, Glasser, & Imbabi, 2007) in different papers. To avoid confusion, dynamic façade is used to denote the entire category of façades with variable U-factor. Dynamic insulation façade is used to denote those façades that do not involve the mass exchange between the façade and the environment. In these façades, the air is sealed within the cavity of the façade at steady state. Ventilated façade is used to denote those façades in which the air is naturally or mechanically ventilated through some channels. In these façades, there is a clear boundary between the air channel and the solid construction. At last, breathing wall is used to denote those façades that are permeable to air and moisture. The porous structure of these façades is filled with air and allows air and moisture to pass through.

The U-factor variation mechanism of most **dynamic insulation façades** is based on the fact that the thermal conductivity of stagnant air is very low (0.0263 W/(m·K) at

26°C) (Kimber et al., 2014). Once the air starts moving, its convective heat transfer rate is prominently higher than the conductive heat transfer rate. One way to prevent the air from moving is to divide the air into thin layers with polymer membranes. The high insulation state is realized by multiple thin air layers divided by polymer membranes with low thermal emittance. To transition to the low insulation state, all the polymer membranes are lumped together to form a single layer and all air is expelled from the façade. For a typical design based on this concept, the thermal resistance of the high insulation state and the low insulation state is 3.70 and 0.118 $m^2 \cdot K/W$, respectively (Kimber et al., 2014). Another way to change the U-factor of a façade is to change the air flow speed inside the air ducts with fans, as shown in Figure 7. When the fans are off, the air inside the air ducts serves as a good insulation material. When the fans are on, the flowing air can transfer heat from one side of the façade to the other effectively. The U-factor of the high insulation state and the low insulation state of a façade using this mechanism is 0.185 and 1.657 $W/m^2 \cdot K$, respectively (Koenders et al., 2018). Other methods of modulating the U-factor of a dynamic insulation façade include changing the position of an insulation panel (Pflug et al., 2015), changing the type of fluid filling the cavity inside the façade (Al-Nimr, Asfar, & Abbadi, 2009), and changing the pressure of the gas filling the cavity inside the façade (Benson, Potter, & Tracy, 1994; Berge, Hagentoft, Wahlgren, & Adl-Zarrabi, 2015). The development of dynamic insulation facades is still at the conceptual stage.

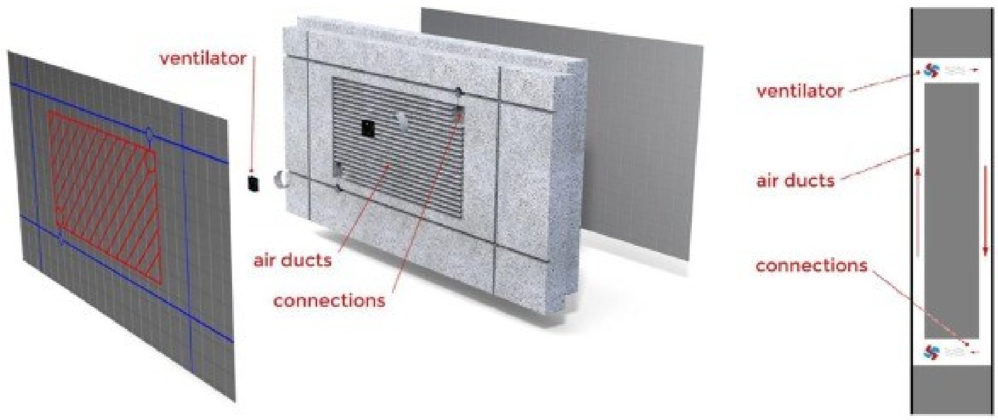

Figure 7 – Exploded view and section of a type of dynamic insulation façade (Koenders et al., 2018)

Unlike the dynamic insulation façade, there may be air flowing into and out of a **ventilated façade** at steady state. Based on the airflow direction, the operation modes of the ventilated façade can be categorized into no flow, external to external (E-E), external to internal (E-I), internal to external (I-E), and internal to internal (I-I). Some ventilated façades only have one operation mode, while others have several operation modes. Each operation mode is suitable for certain scenarios. No flow mode applies to the solar heat collection phase of ventilated façades with thermal storage in the winter (de Gracia, Navarro, Castell, Ruiz-Pardo, Alvárez, et al., 2013). E-E mode is appropriate for cooling the thermal mass during summer nights or taking away the solar heat absorbed by a façade during summer days (Ciampi et al., 2003; de Gracia, Navarro, Castell, Ruiz-Pardo, Álvarez, et al., 2013). Both E-I mode and I-E mode can be used to recover part of the thermal energy lost through the façade and at the same time perform part of the ventilation function (Imbabi, 2012). E-I mode can also be used for free cooling during summer nights (de Gracia, Navarro, Castell, Ruiz-Pardo, Álvarez, et al., 2013). I-I mode is suitable for releasing the thermal energy stored in the thermal storage material to the inside (de Gracia, Navarro, Castell, Ruiz-Pardo, Alvárez, et al., 2013; de Gracia, Navarro, Castell, Ruiz-Pardo, Álvarez, et al., 2013; El Mankibi, Zhai, Al-Saadi, & Zoubir, 2015). The airflow through the air channel can be either mechanical ventilation or natural ventilation. In most cases, natural ventilation is more energy efficient than mechanical ventilation (de Gracia, Navarro, Castell, Ruiz-Pardo, Álvarez, et al., 2013; Imbabi, 2012).

As shown in Figure 8, different from the ventilated façade, in which the airflow direction is perpendicular to the heat conduction direction, in a **breathing wall** the airflow direction is parallel with the heat conduction direction. Porous materials are used to allow air to pass through (Wong et al., 2007). Breathing wall works best with materials that are inherently good insulators when there is no airflow (Taylor & Imbabi, 1998). If the airflow is in the same direction as the heat conduction (called pro-flux flow), the U-factor of the breathing wall is increased. If the airflow is in the opposite direction of the heat conduction (called contra-flux flow), the U-factor of the breathing wall is reduced. For example, for a wall with a static thermal resistance of 6.434 $m^2 \cdot K/W$, if the air flows in the opposite direction of the heat conduction at a speed of 1 $m^3/m^2 \cdot h$, the heat flux reduces to approximately one fourth that of no airflow. If the air flows in the same direction as the heat conduction at a speed of 1 $m^3/m^2 \cdot h$, the heat loss increases to approximately 2.5 times that of no airflow (Taylor et al., 1996).

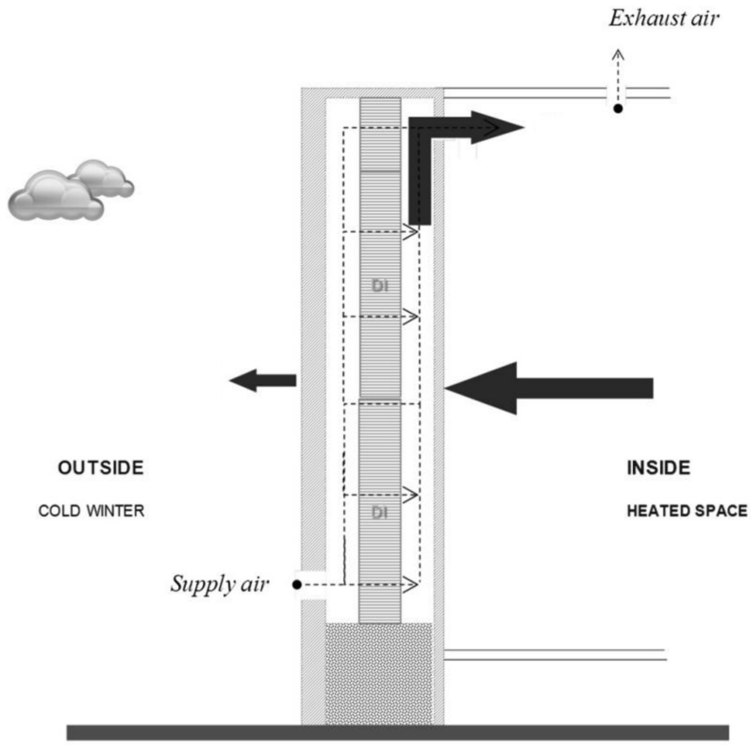

Figure 8 – The configuration and working mechanism of the breathing wall in the winter (Imbabi, 2012)

1.3.3.2 Radiative Coating

Radiative coating can change the solar absorptance and thermal emittance of the exterior surface of the envelope. Solar absorptance determines the proportion of incident solar radiation absorbed by the envelope. Thermal emittance determines the intensity of the heat loss of the envelope through radiative heat exchange mainly with the sky. For winter application high solar absorptance and low thermal emittance are desired, while for summer application the opposite is desired.

In order to meet the different requirements of winter application and summer application, **variable radiative coatings** are developed. Most variable radiative coatings change their radiative properties at different temperatures. Some of them have binary states (Yiping Ma, Li, & Zhu, 2012; Yiping Ma, Zhu, & Wu, 2000; Zheng, Xu, Shen, & Yang, 2015). Below the transition temperature, these coatings have high solar absorptance and low thermal emittance. Above the transition temperature, the solar absorptance becomes lower and the thermal emittance becomes higher. The transition temperature is usually between 17°C and 26°C. Others have radiative properties that change continuously with the change of temperature. For example, the solar absorptance of a material called G17S decreases almost linearly from 0.81 at 0°C to 0.5 at 40°C (Yiping Ma et al., 2012). Besides coatings whose properties depend on temperature, there are some devices whose properties can be controlled by an external electrical voltage. For instance, the solar absorptance of a device can be modulated between 0.55 and 0.83 with an external electrical voltage. The thermal emittance of another device can be modulated between 0.43 and 0.73. Both devices require a power input < 30 mW/in^2 that lasts for 1–2 min to change their properties (Bergeron, White, Boehme, Gelb, & Joshi, 2008).

The **daytime radiative cooling (DRC) material** is another category of radiative coating material that can cool close to or even below the ambient temperature in direct sunlight. Due to the existence of greenhouse gases (e.g. carbon dioxide, water vapor, and methane), the atmosphere can absorb most of the long-wave infrared radiation emitted by the objects near sea level. However, there are some wavebands within which the absorption of the atmosphere is very weak. These wavebands are called the atmosphere’s transparency windows. One of the atmosphere’s transparency windows is between 8 and 13 μm, which coincides with the peak of the radiation curve of the objects at ambient temperature (Zhu, Raman, & Fan, 2013). If the solar absorptance of a material is very low while its emittance between 8 and 13 μm is very high, this material can reflect most of the incident sunlight and lose heat to the cold outer space effectively through radiation. Since the first DRC material that is able to cool down below ambient temperature under sunlight was created in 2014 (Raman, Anoma, Zhu, Rephaeli, & Fan, 2014), several other DRC materials have been created, each with better performance and lower cost (Mandal et al., 2018; Zhai et al., 2017). A paint-like material recently created has a solar reflectance as high as 0.96 ± 0.03 and a long-wave infrared emittance as high as 0.97 ± 0.02. Under direct sunlight, its cooling power can reach 96 W/m^2 (Mandal et al., 2018).

Despite a promising future for the application of DRC in buildings, there are some issues that need to be solved first. Since the cooling ability of a DRC material depends on the radiative heat exchange with the outer space through the atmosphere's transparency window, it is heavily influenced by the geometry of the building, surroundings of the building, and weather conditions. The total cooling power of a surface with the DRC material depends on the total surface area that participates in the heat exchange. For high-rise buildings whose roof area to floor area ratio is very small, the cooling potential of using DRC materials is marginal. Furthermore, in order to realize efficient radiative heat exchange between the DRC material and the sky there should not be any obstructions between them, which makes buildings shaded by trees or surrounded by tall buildings inappropriate for using DRC. The weather conditions also play a critical role because high moisture content of the ambient air, high cloud cover of the sky, and poor air quality will enhance the absorption of long-wave infrared by the atmosphere. Therefore, DRC materials are appropriate for arid regions.

Besides the issues that impact the efficiency of the radiative heat transfer, another problem to be solved is the negative effect of DRC materials on the heating load. The arid regions like Arizona and New Mexico usually have large diurnal temperature fluctuations. The favourable cooling effect during the day may become a burden during the night. In the winter, this problem is even more prominent. Some methods to alter the radiative properties of a surface using mechanical systems have been proposed by (Oh, Chun, Han, Kim, & Chen, 2008). For example, we can cover the DRC material with a flexible shield with high solar absorptance and low thermal emittance when heating is required. During the cooling season, this flexible shield can be scrolled up with a roller.

1.3.3.3 Thermal Storage

Thermal mass is the capability of a material to absorb and release heat (Hoes, Trcka, Hensen, & Hoekstra Bonnema, 2011). By controlling the absorption and release of heat, thermal storage systems can mitigate the diurnal or seasonal fluctuation of the ambient temperature and thus reduce the cooling and heating loads. Thermal storage systems can be divided into active systems and passive systems. Different from the definitions of passive system and active system presented in Section 1.2.4, in the context of thermal storage systems the passive system usually refers to the system in which the thermal mass is confined to a certain place where heat absorption, storage, and release take place. In the active system, heat absorption, storage, and release usually take place in different places that are connected by a fluid loop (Henze et al., 2004).

Thermal mass integrated into building envelope belongs to the passive thermal storage system. Thermal mass can be solid, liquid, or the phase change material (PCM).

For a building, the optimal amount of thermal mass is different for different seasons. In general, high thermal mass is desired in the summer and the contrary in the winter (Hoes et al., 2011; Loonen, 2018). As for the location of the thermal mass in the façade, placing the thermal mass close to the inside leads to better energy performance than placing the thermal mass elsewhere (El Mankibi et al., 2015; Koenders et al., 2018). For thermal mass materials, PCMs with a phase change temperature close to the indoor heating/cooling setpoint are preferred over sensible thermal storage materials (El Mankibi et al., 2015; Zeng, Wang, Di, Jiang, & Zhang, 2011). There are two main reasons. Firstly, since the specific latent heat of PCMs is significantly larger than the specific heat capacity of sensible thermal storage materials, the required mass and occupied space of PCMs will be much smaller, which leads to a lower building construction cost. For example, the specific heat capacity of concrete is only 653 J/(kg·K) (American Society of Heating Refrigerating and Air-Conditioning Engineers, 2013), while the specific latent heats of common PCMs are all larger than 140 kJ/kg (Khudhair & Farid, 2004). Secondly, PCMs are at a constant temperature when releasing or absorbing heat, which results in less heating/cooling demand than using sensible thermal storage materials. In theory, the optimal phase change temperature of a PCM is the heating setpoint in order to reduce the heating demand or the cooling setpoint in order to reduce the cooling demand. However, a temperature difference is needed for a heat transfer process to continue. Therefore, in practice the optimal melting temperature should be a little lower than the cooling setpoint and the optimal solidification temperature should be a little higher than the heating setpoint. When the phase change temperature of a PCM is on the upper bound of the temperature control dead band, any environmental temperature lower than this value can be utilized to store cold energy in the

PCM. The same is true for the heating case, thus maximizing the potential of utilizing environmental factors. Moreover, the heat transfer rate is proportional to the temperature difference, so maintaining the indoor temperature at the upper and lower bounds of the dead band can minimize the cooling and heating demand, respectively. A phase change temperature close to the upper/lower bound of the dead band is conducive to keeping the indoor temperature on the upper/lower bound of the dead band for the maximum amount of time.

Some PCMs may show a hysteresis in the phase change temperature, i.e., the melting temperature is higher than the solidification temperature. The solidification process of a PCM may also be affected by subcooling, which means the solidification process will not initiate until the temperature reaches a certain point below the solidification temperature (de Gracia, Navarro, Castell, Ruiz-Pardo, Alvárez, et al., 2013; de Gracia, Navarro, Castell, Ruiz-Pardo, Álvarez, et al., 2013).

1.3.4 Bridge Technology

Bridge technology refers to the systems that function by directly connecting the indoor and outdoor environments. This connection can take place in the form of heat transfer as well as mass transfer.

1.3.4.1 Thermodiode

A diode is a two-terminal electronic component that conducts electrical current in one direction, while blocks it in the opposite direction. Similarly, a thermodiode is a device that transfers heat efficiently in one direction, while blocks the heat transfer in the opposite direction. The function of thermodiodes relies upon the gravity force. Due to the existence of gravity force, hot fluids with low density will rise, while cold fluids with high density will fall. If a high-temperature heat source is at a lower altitude than a low-temperature heat sink, the working fluid will absorb heat at the heat source, expand or evaporate, rise to the heat sink, release heat, contract or condense, then return to the heat source. However, if the heat source is at a higher altitude than the heat sink, the heat transfer can only take place through conduction which is far less efficient than convection. Based on the state of the working fluid, thermodiodes can be divided into single-phase thermodiodes and multi-phase thermodiodes. The latter has higher heat transfer rate, but requires good sealing and strong construction (Chun & Chen, 2002; Chun, Chen, & Kim, 2002; Oh et al., 2008). Heat pipe is a type of multi-phase thermodiode (Maydanik, 2005; Noie, 2005). Based on the heat transfer direction, thermodiodes can be divided into uni-directional thermodiodes and bi-directional thermodiodes. The reversal of heat transfer direction is realized by changing the relative altitudes of the two heat sources using some mechanical methods. The working mechanism of a bi-directional thermodiode is shown in Figure 9.

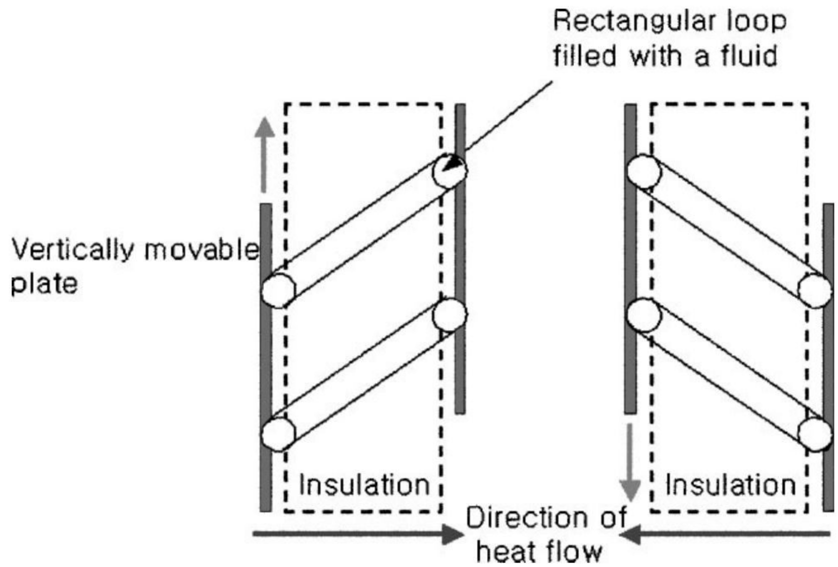

Figure 9 – The working mechanism of a bi-directional thermodiode (Chun et al., 2002)

The effective heat conductivity of a two-phase thermodiode can exceed that of copper 200–500 times (Noie, 2005). Due to its high efficiency and not requiring power input, thermodiodes have been widely used for heat recovery and solar energy utilization (Chun & Chen, 2002; Chun et al., 2002; Noie, 2005). However, there are few examples of using thermodiodes to directly enhance the heat exchange between the indoor space and the outdoor environment. This is probably due to their high production cost.

1.3.4.2 Evaporative Cooling

When water evaporates, it absorbs heat from the surrounding substances. Thus, we can cool the air by increasing its water content. This method of cooling the air is called evaporative cooling. Evaporative cooling can be divided into direct evaporative cooling (DEC) and indirect evaporative cooling (IEC). The principle as well as psychrometric representation of DEC and IEC is shown in Figure 10 (a) and Figure 10 (b), respectively.

One measurement of the efficiency of an evaporative cooling system is called the wet-bulb effectiveness (Cuce & Riffat, 2016). It is defined as follows:

$$\eta_{wb} = \frac{T_{o,db} - T_{p,o}}{T_{o,db} - T_{o,wb}} \tag{1}$$

where $T_{o,db}$ is the outdoor dry-bulb temperature, °C; $T_{p,o}$ is the temperature of the product stream at the outlet, °C; $T_{o,wb}$ is the outdoor wet-bulb temperature, °C;. Since the evaporation of water inside the wet channel can be seen as an adiabatic process, the $T_{p.o}$ of DEC is close to $T_{o,wb}$. Thus, the wet-bulb effectiveness of a DEC system is in the range of 80%–95% (Rogdakis & Tertipis, 2015; Zhao, Liu, & Riffat, 2008). However, the relative humidity of the product stream of a DEC system is usually too high to be acceptable. In contrast, since the product stream of an IEC system is cooled by sensible heat transfer with the working stream, the humidity ratio of the product stream is kept constant. Due to the extra heat transfer resistance (Zhao et al., 2008), the wet-bulb effectiveness of an IEC system is only around 55% (Cuce & Riffat, 2016; Rogdakis & Tertipis, 2015).

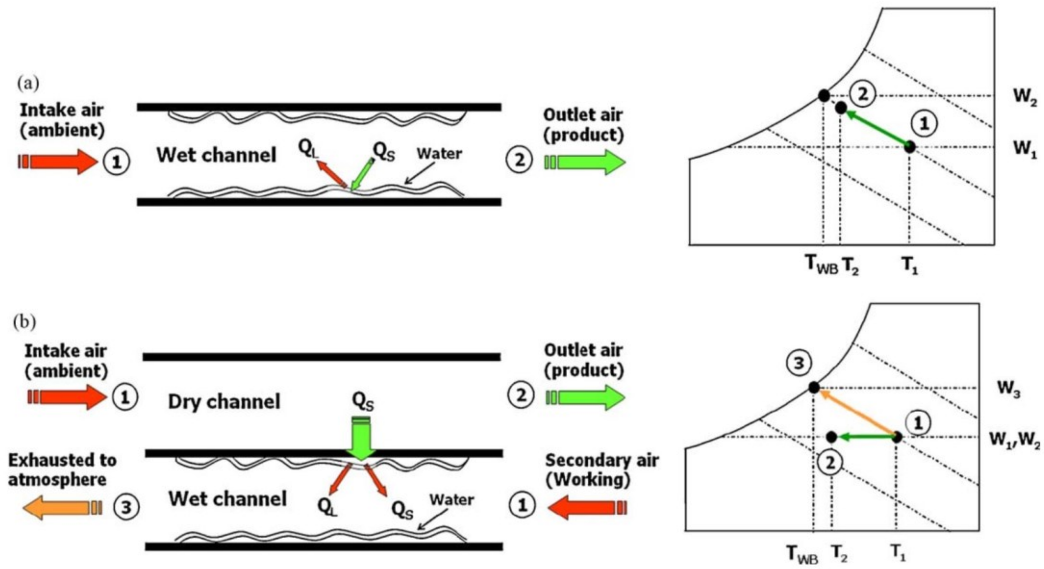

Figure 10 – (a) Direct evaporative cooling and (b) indirect evaporative cooling (Riangvilaikul & Kumar, 2010)

In order to improve the wet-bulb effectiveness of IEC, a novel IEC cycle called the Maisotsenko cycle (M-cycle) was proposed. The principle and psychrometric representation of the M-cycle is shown in Figure 11. After entering the dry working channel, the working stream is pre-cooled by sensible heat transfer with the wet working channel. As it moves along the dry working channel, part of the working stream enters the wet working channel through the perforations between the two channels. In the wet working channel, the water evaporates and absorbs heat from the working stream in the wet working channel, the wall between the wet working channel and the dry working channel, and the wall between the wet working channel and the product channel. Since the working stream is precooled, it has the potential to cool the product stream down to the dew point (Mahmood, Sultan, Miyazaki, Koyama, & Maisotsenko, 2016; Riangvilaikul & Kumar, 2010; Rogdakis & Tertipis, 2015). Hence, an evaporative cooling system based on the M-cycle is also called a dew point evaporative cooling system. The wet-bulb effectiveness of an M-cycle system is usually between 90% and 125% (Riangvilaikul & Kumar, 2010; Rogdakis & Tertipis, 2015). In conclusion, the M-cycle is able to cool the air close to the dew point without increasing its humidity ratio. Thus, its application in buildings has a promising future.

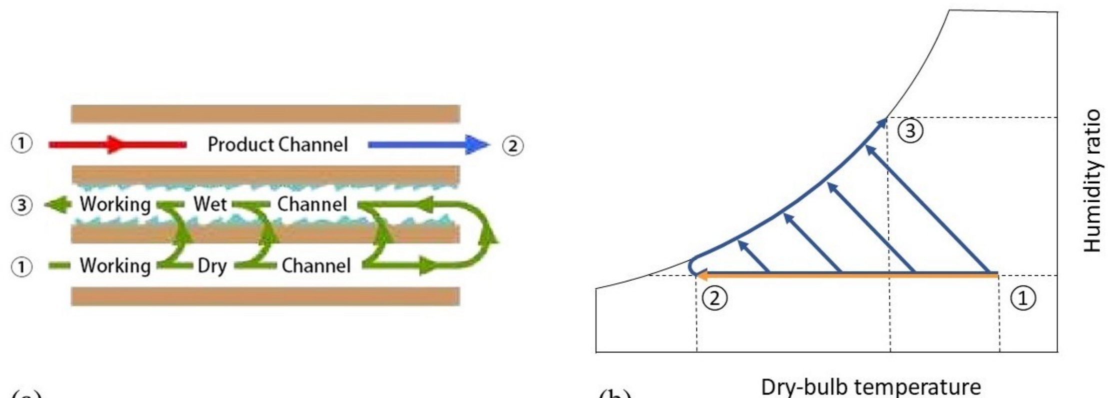

(a) (b)

Figure 11 – (a) The principle of the M-cycle (Wani, Ghodke, & Shrivastava, 2012) and (b) the psychrometric representation of the M-cycle

The only electricity consumption of an evaporative cooling system comes from the fans and pumps than drive the air and the water. Although the electricity consumption of the evaporative cooling system is significantly lower than the vapor-compression cooling system, the consumption of water should also be taken into account. The specific water consumption of an evaporative cooling system is defined as the amount of water consumed to produce 1 kWh of cooling energy. For the system tested in (Rogdakis & Tertipis, 2015), this value is between 2.5 kg/kWh and 3.0 kg/kWh. There are also strict requirements on the purity of water used in the evaporative cooling system to avoid deposition and congestion in the heat and mass exchanger, an example of which is shown in Figure 12. In order to achieve high wet-bulb effectiveness, the size of the heat and mass exchanger should be sufficiently large, which increases the initial investment. The weather conditions also have a significant impact on the performance of the evaporative cooling system (Cuce & Riffat, 2016; Riangvilaikul & Kumar, 2010; Rogdakis & Tertipis, 2015). The evaporative cooling system achieves the best cooling effect when the ambient air has high temperature and low humidity ratio. However, the regions with hot and arid climates usually lack fresh water.

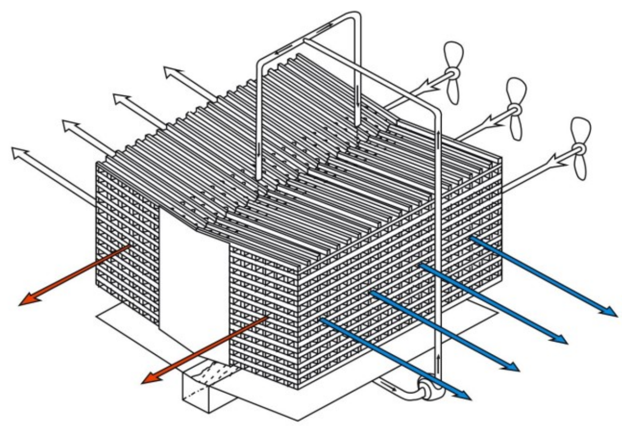

Figure 12 – The configuration of an M-cycle cooler (Rogdakis & Tertipis, 2015)

1.3.5 A Finite-Difference Model of ABE Technologies

As shown in Figure 13, a finite-difference model was developed with the intention of being representative of all the ABE technologies summarized in Table 2. Explicit Euler method is used to solve the equation set. In this model, **A**, **B**, and **D** are the coefficient matrices; **C** and **E** are the source vectors; **T** is the temperature vector; A denotes the surface area, m^2; h denotes the heat transfer coefficient, W/(m^2·K); k denotes the thermal conductivity, W/(m·K); T denotes the temperature, °C; Q denotes the heat transfer rate, W, or the temperature, °C; Δt denotes a time step, s; c denotes the specific heat, J/(kg·K); $\dot{m}$ denotes the mass flow rate, kg/s. A single node, 7, is used to represent the indoor temperature, because for buildings without radiant systems the indoor air temperature is close to the indoor mean radiant temperature. For buildings with radiant systems, node 7 should be split into a radiant temperature node and an air temperature node. The variables in blue are constants for a particular ABE system while those in red can be varied in the operation of the ABE system.

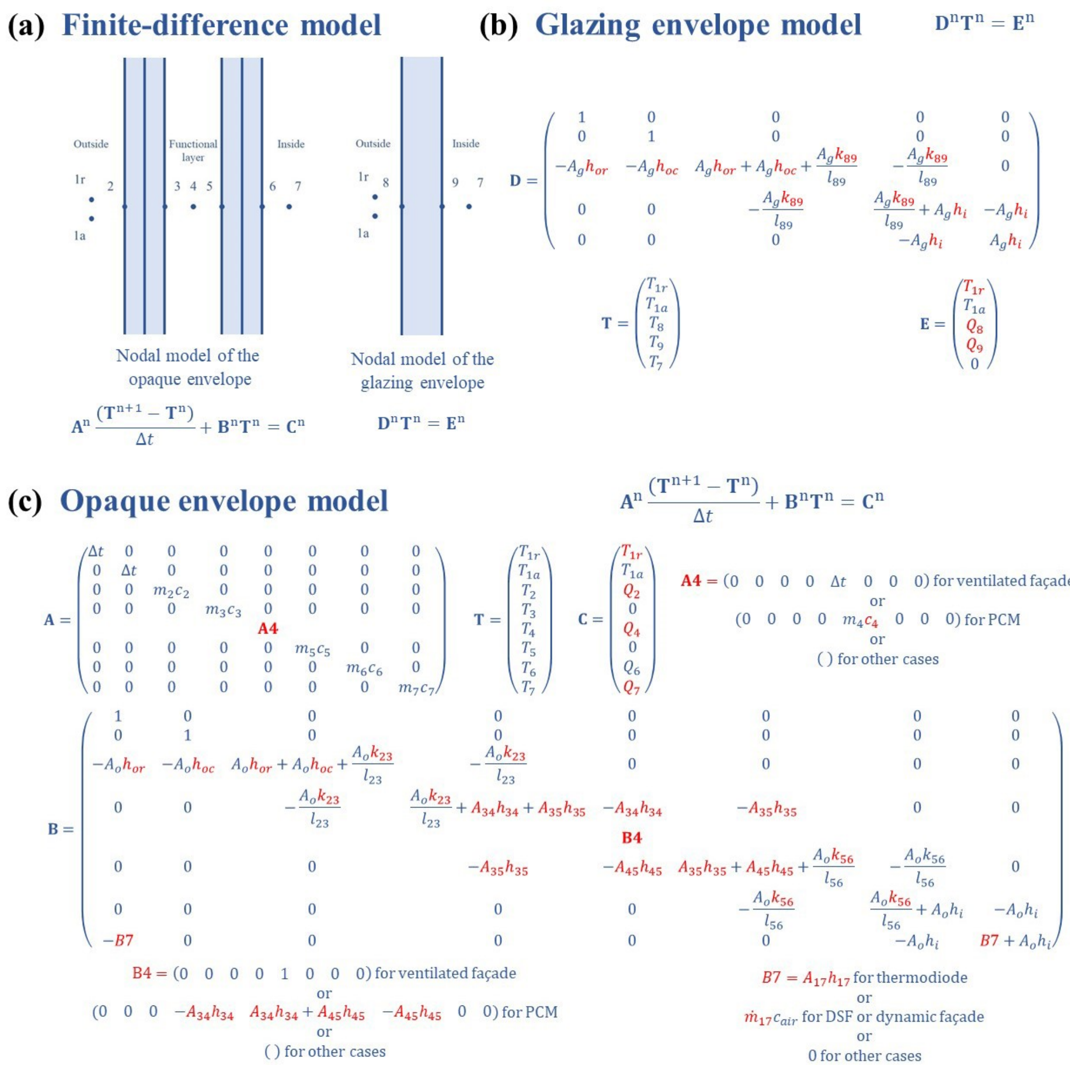

Figure 13 – (a) The nodal representation of the finite-difference model; (b) the matrix representation of the glazing envelope model; and (c) the matrix representation of the opaque envelope model

Table 3 shows the variables associated with each family of ABE technology. The variables are associated with each family instead of each particular technology because although the technologies in the same family may have different configurations, they perform their functions by changing the same group of variables. As will be shown later, this level of abstraction corresponds to the quasi-forward approach to optimization, which offers methodological rigor and soundness as well as a certain degree of generality.

Table 3 – The variables associated with each family of ABE technology

ABE Technology		Associated Variables
Glazing technology	Dynamic shading device	h_{oc}, T_{1r}, Q_8, Q_9, h_i
	Switchable window	h_{or}, Q_8, Q_9
	Double skin façade (DSF)	h_{oc}, T_{1r}, Q_8, Q_9, $\dot{m}_{17}$
	Movable insulation	h_{or}, k_{89}, Q_8, Q_9, h_i
Opaque technology	Dynamic façade	k_{23}, k_{56}, h_{34}, h_{35}, h_{45}, A_{34}, A_{35}, A_{45}, Q_4, $\dot{m}_{17}$
	Radiative coating	h_{or}, Q_2
	Thermal Storage	c_4, h_{34}, h_{35}, h_{45}, A_{34}, A_{35}, A_{45}
Bridge technology	Thermodiode	A_{17}, h_{17}
	Evaporative cooling	Q_7

1.4 Research Questions

The research questions of this thesis are presented below. There are three primary research questions and under each primary research question there are several secondary research questions. After each question, the section that answers the question are presented.

1. How to determine the energy saving potential of ABE? – CHAPTER 2

    1.1 What are the weather variables that determine the energy saving potential of ABE? – Section 2.1

    1.2 How to calculate the energy saving potential of ABE systems associated with each weather variable? – Section 2.2

2. How to model and simulate ABE technologies in building energy modelling (BEM) programs? – CHAPTER 3

3. How to guide the formulation of ABE optimization problems with a generic framework? – CHAPTER 4 and CHAPTER 5

3.1 What is the content of this framework? – Sections 4.2–4.5

3.2 How to select the appropriate ABE technologies for a building? – Section 4.4.1

3.2 How can this framework guide the formulation of a building design problem? – Section 5.1

3.3 How can this framework guide the formulation of a product development problem? – Section 5.2

3.4 How can this framework guide the formulation of a building operation problem? – Section 5.3

1.5 The Structure of This Thesis

Figure 14 shows how each section of thesis is related to one another.

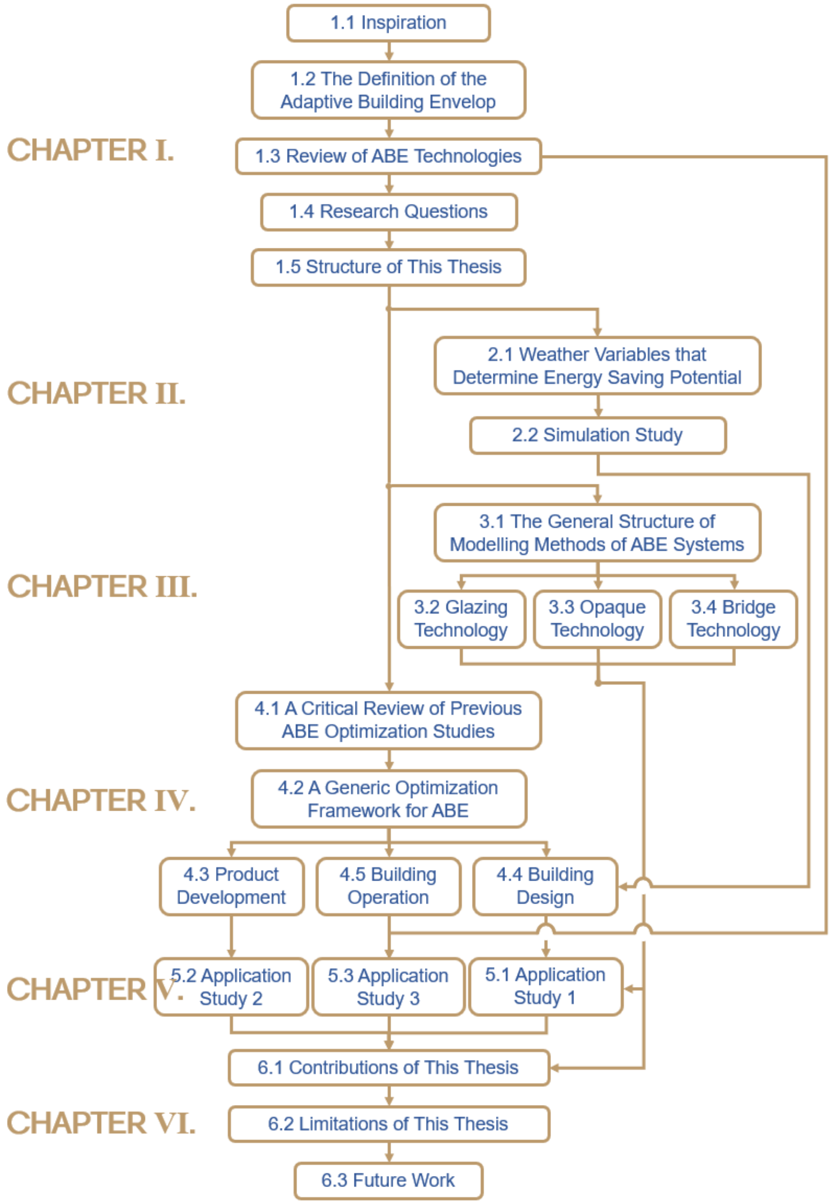

Figure 14 – The structure of this thesis

CHAPTER 2. ENERGY SAVING POTENTIAL OF ABE

The energy saving potential of an ABE system is defined as its maximum capability to reduce the load of a building. From the definition of ABE, we can see that its energy saving potential stems from two sources, i.e. blocking the adverse factors in the outdoor environment and admitting the favorable ones. The way of exploiting the first source is to increase the insulation and airtightness of the building envelope as much as possible, which has been widely adopted in the design of static passive buildings. Of more interest is the second source, which relies upon the building envelope's ability to actively "embrace" the factors in the outdoor environment that are conducive to reducing the load. These factors are called weather variables. In this chapter four such weather variables are identified and the calculation method of the energy saving potential of ABE systems associated with each weather variable is presented.

2.1 Weather Variables that Determine Energy Saving Potential

According to the definition of ABE, all the counter-load energy provided by ABE systems to the indoor environment is transformed from the natural energy. The artificial energy can only be used in the transport of the energy carrier or the control of the energy transformation and transport processes rather than the production of the counter-load energy. Therefore, the limit to which ABE systems can reduce the building load hinges on the weather variables that are the sources of natural energy. There are four such variables, which are the outdoor dry-bulb temperature, outdoor wet-bulb temperature, sky temperature, and solar radiation. The first three are related to the reduction of cooling load, while the last one is related to the reduction of heating load. As shown in Table 4, each weather variable is associated with some ABE technologies, which means it is the determinant of the energy saving potential of these technologies. For instance, double skin façade, movable insulation, dynamic insulation, ventilated façade, breathing wall, and thermodiode are all associated with the outdoor dry-bulb temperature. Movable insulation, dynamic insulation, and thermodiode can change the heat transfer rate between the indoor and outdoor environments. DSF, ventilated façade, and breathing wall can change the mass transfer rate between the indoor and outdoor environments. If we assume that these systems have unlimited capability, i.e., unlimited heat transfer rate and mass transfer rate, the lowest temperature they are able to cool the indoor air down to is the outdoor dry-bulb temperature.

Table 4 - The weather variables and the ABE technologies associated with them

Weather variable	ABE technology
Outdoor dry-bulb temperature	Double skin façade, movable insulation, dynamic insulation, ventilated façade, breathing wall, thermodiode
Outdoor wet-bulb temperature	Direct evaporative cooling, indirect evaporative cooling, Maisotsenko cycle
Sky temperature	Dynamic shading device, movable insulation, dynamic insulation, ventilated façade, breathing wall, variable radiative coating, DRC material, thermodiode
Solar radiation	Dynamic shading device, chromogenic window, LC-based window, SPD window, DSF, movable insulation, dynamic insulation, ventilated façade, breathing wall, variable radiative coating, DRC material, thermodiode

There are two advantages in associating the energy saving potential with weather variables instead of defining it by means of a reference system. The first is that universal calculation methods can be developed. In Table 2, more than sixteen ABE technologies are listed and more new ABE technologies are being developed at this moment. Even for the same type of ABE technology, different systems may have different functions. Therefore, it is impossible to specify a reference system for each single ABE system. In contrast, by associating the energy saving potential with weather variables, universal calculation methods can be developed for all ABE systems. The second is that the energy saving potential associated with weather variables is the theoretical limit, which is not dependent on changing technology and can better show the maximal capability of ABE systems to reduce the building load.

It should be noted that the energy saving potential of a weather variable is only the theoretical maximal capability of ABE systems associated with this weather variable to reduce the building load. In practice, to approach this limit may not always be possible. In order to cool the indoor environment to the outdoor dry-bulb temperature, the heat or mass transfer rate between the indoor and outdoor environments has to be sufficiently large. This can be realized by (1) using a dynamic façade whose modulation range is sufficiently wide, (2) using a thermodiode with a sufficiently large size, or (3) using a ventilation system with a sufficiently large mass flow rate. In order to cool the indoor environment to the outdoor wet-bulb temperature, a sufficiently large M-cycle evaporative cooling system is required, and the supply of water and electricity should be adequate. In order to utilize all the available solar radiation, we can either use a building envelope whose solar transmittance is close to 1 and U-factor is equivalent to that of the original building envelope or use a sufficiently large active solar heating system. In order to utilize all the available radiative heat loss to the sky, we can either use a coating whose long-wave infrared emissivity is 1 and solar reflectance is 1or use a sufficiently large active radiative cooling system.

There are three purposes of investigating the energy saving potential of weather variables. The first is to identify the promising weather variables and select suitable ABE technologies accordingly. For different locations, the energy saving potential of each weather variable is different. For example, for a place with dry climate the cooling load reduction potential of the outdoor wet-bulb temperature and the sky temperature is significant. Thus, technologies associated with these weather variables like evaporative cooling and DRC are likely to be appropriate for buildings located in this place.

The second purpose is to find the limit to which each weather variable can reduce the building load. This limit can be compared with the energy saving target to see if a technology is suitable for the building. For example, if the outdoor dry-bulb temperature has the potential to remove 30% of the cooling load, but the target is to reduce the cooling load by 50%, technologies like evaporative cooling should be adopted instead of or in addition to the technologies associated with the outdoor dry-bulb temperature.

The third purpose is to calculate the degree of perfection (DOP) of an ABE system. In mechanical engineering, the DOP or the Second-Law Efficiency of a refrigeration system is defined as follows (American Society of Heating Refrigerating and Air-Conditioning Engineers, 2014):

$$\mathrm{DOP} = \frac{\mathrm{COP}}{\eta_c} \tag{2}$$

where COP is the coefficient of performance of a refrigeration system; η_c is the Carnot efficiency between the two temperatures at which the refrigeration system operates. The COP of a refrigeration system is defined as follows:

$$\mathrm{COP} = \frac{Q_c}{P_e} \tag{3}$$

where Q_c is the cooling power output of the refrigeration system, W; P_e is the electric power input of the refrigeration system, W. Carnot efficiency is the upper limit of the COP of a refrigeration system operating between two temperatures according to the Second Law of Thermodynamics. It is calculated as follows:

$$\eta_c = \frac{T_L}{T_H - T_L} \tag{4}$$

where T_L is the temperature of the low-temperature heat reservoir, K; T_H is the temperature of the high-temperature heat reservoir, K.

Similar to the DOP of a refrigeration system, we can define the DOP of an ABE system. In this definition, the COP is replaced by the proportion of cooling or heating need removed by using the ABE system compared to the reference building and the Carnot efficiency is replaced by the energy saving potential of a weather variable for the reference building. There is a critical difference between the DOP of a refrigeration system and that of an ABE system. For a refrigeration system the Carnot efficiency only depends on the two temperatures. Thus, it is an abstract and universal concept. In contrast, the energy saving potential is related to a specific weather variable and a particular building with given boundary conditions. The joint effect of ABE systems associated with the same weather variable can be measured by a single DOP, while the effects of ABE systems associated with different weather variables should be measured by different DOPs.

2.2 Methods of Calculating the Energy Saving Potential

In this section, the methods of calculating the energy saving potential associated with each weather variable are developed. Although EnergyPlus (U.S. Department of Energy, 2016b) is used to simulate the building in this study, these methods apply to other BEM programs as well.

2.2.1 Building Model

In this study, the small office building of the Commercial Prototype Building Models developed by Pacific Northwest National Laboratory (PNNL) is adopted (Pacific Northwest National Laboratory, 2018). As shown in Figure 15, the building is a one-story building with a floor area of 5,500 ft^2 (511 m^2). The building is divided into six thermal zones—four perimeter zones, one core zone, and one unconditioned attic between the five conditioned zones and the roof. Details of the model and the EnergyPlus idf file can be found in (Pacific Northwest National Laboratory, 2018). Since this study is only concerned with the thermal load of the building, all the HVAC systems in the model are removed and the Ideal Loads Air System is used instead. TMY3 weather data are used as input. Since TMY3 only provides hourly weather data, EnergyPlus employs linear interpolation to calculate sub-hourly weather data if the time step is smaller than one hour.

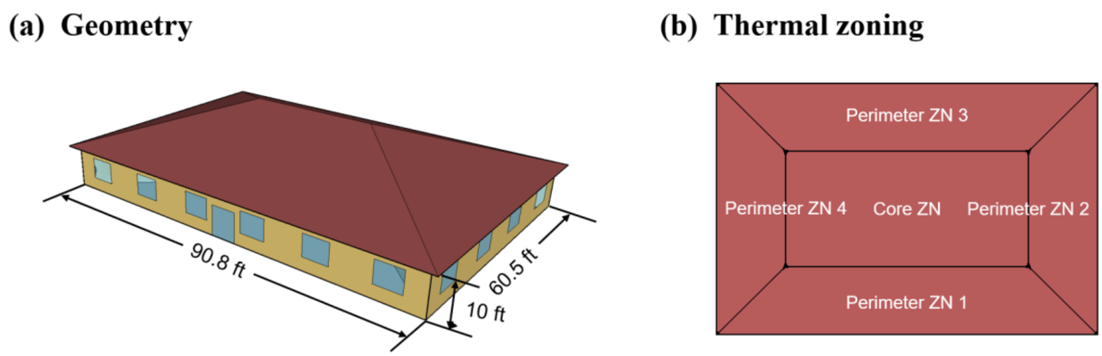

- WWR: 24.4% for South and 19.8% for the other three orientations (Window Dimensions: 6.0 ft x 5.0 ft punch windows for all façades)
- Perimeter zone depth: 16.4 ft (Percentages of floor area: perimeter 70%, core 30%)
- Glazing sill height: 3 ft (top of the window is 8 ft high with 5 ft high glass)
- Exterior wall/Roof/Window U-factor: Requirements in codes or standards
- Roof tilts: Hipped roof: 10.76 ft attic ridge height, 2 ft overhang-soffit

Figure 15 – (a) Geometry and (b) thermal zoning of the small office building model

2.2.2 Outdoor Dry-bulb Temperature

To calculate the cooling load that can be removed by cooling the indoor air down to the outdoor dry-bulb temperature, we need to set the cooling setpoint to the maximum of the original cooling setpoint and the outdoor dry-bulb temperature, as shown in Equation 5. For each time step

$$T_{cl,n} = \max\left(T_{cl,o}, T_{o,db}\right) \tag{5}$$

where $T_{cl,n}$ is the new cooling setpoint, °C; $T_{cl,o}$ is the original cooling setpoint, °C; and $T_{o,db}$ is the outdoor dry-bulb temperature, °C. This setting can be understood in this way: When the outdoor dry-bulb temperature is lower than the original cooling setpoint, the cooling load can be removed completely by letting in sufficient outdoor air. When the outdoor dry-bulb temperature is higher than the original cooling setpoint, the indoor air can be first cooled down to the outdoor dry-bulb temperature. Then, the indoor air is further cooled by the active cooling system to the cooling setpoint.

Three cities are selected as examples, as shown in Table 5. The cooling season is from March to October. The simulated results are shown in Figure 16. The proportion of the cooling need removed for the whole year is 0.502, 0.293, and 0.342 for Atlanta, Tucson, and Tampa, respectively. It can be seen that Atlanta has the highest potential of utilizing the outdoor dry-bulb temperature for cooling, followed by Tampa and Tucson.

Table 5 – Cities chosen as examples for the outdoor dry-bulb temperature case

City	Tampa, FL	Tucson, AZ	Atlanta, GA
Climate zone	2A	2B	3A

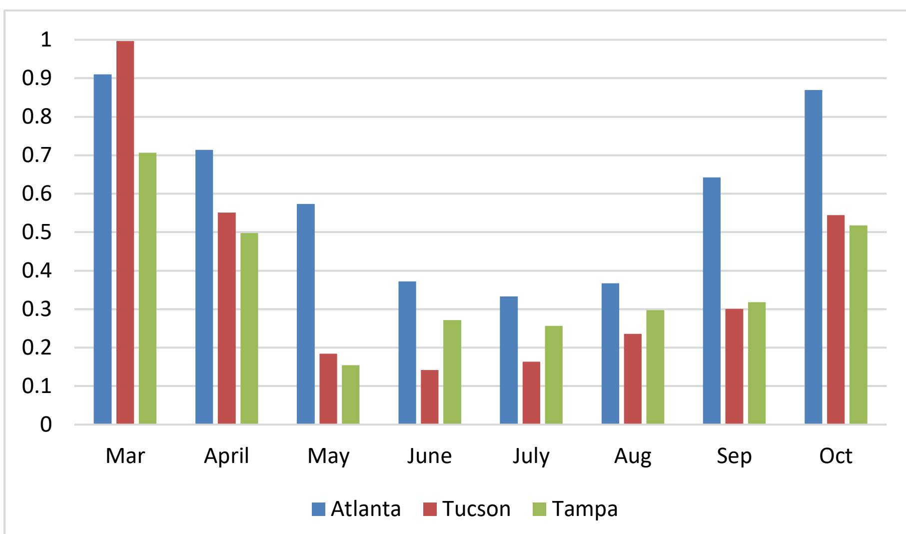

Figure 16 – Proportion of the cooling need removed by cooling the indoor air down to the outdoor dry-bulb temperature

2.2.3 Outdoor Wet-bulb Temperature

Using evaporative cooling systems, the indoor air can be cooled down to the outdoor wet-bulb temperature. As introduced in Section 1.3.4.2, evaporative cooling systems can be classified into DEC systems, IEC systems, and M-cycle systems. DEC systems are able to cool the outdoor air down to the wet-bulb temperature through an isenthalpic process. However, the product stream of this process is saturated air, which is unacceptable from a comfort perspective. IEC systems have two channels. The working stream goes through an evaporation process in the working channel and absorbs the sensible heat from the product stream in the product channel. Due to the heat transfer resistance of the channel wall, the wet-bulb effectiveness of an indirect evaporative cooling is only around 55% (Cuce & Riffat, 2016; Rogdakis & Tertipis, 2015). An improved IEC cycle called the M-cycle combines the advantages of both DEC and IEC. Its product stream has the potential of being cooled down to the dewpoint while its humidity ratio is unchanged. The wet-bulb effectiveness of an M-cycle system is usually between 90% and 125% (Riangvilaikul & Kumar, 2010; Rogdakis & Tertipis, 2015). High wet-bulb effectiveness requires a large size of the heat and mass exchanger and a high water consumption rate. In order to be representative of most cases, this study assume an M-cycle system is adopted and the wet-bulb effectiveness is 100%.

Similar to the outdoor dry-bulb temperature case, to calculate the cooling load that can be removed by cooling the indoor air down to the outdoor wet-bulb temperature, we need to set the cooling setpoint to the maximum of the original cooling setpoint and the outdoor wet-bulb temperature, as shown in Equation 6. For each time step

$$T_{cl,n} = \max\left(T_{cl,o},\, T_{o,wb}\right) \tag{6}$$

where $T_{cl,n}$ is the new cooling setpoint, °C; $T_{cl,o}$ is the original cooling setpoint, °C; and $T_{o,wb}$ is the outdoor wet-bulb temperature, °C. The cities chosen as examples are the same as those in the outdoor dry-bulb case. The simulated results are shown in Figure 17. In this figure we can see that in Atlanta and Tucson, evaporative cooling has the potential to completely remove the cooling load of the building. Even for one of the most hot and humid cities in the U.S., Tampa, around 90% of the cooling load can be potentially removed by evaporative cooling. However, although the potential of utilizing the outdoor wet-bulb temperature for cooling is high in Tampa, evaporative cooling systems are seldom used there. This is because to realize this potential an extremely large evaporative cooling system is required, and the fan power of the system will be very high.

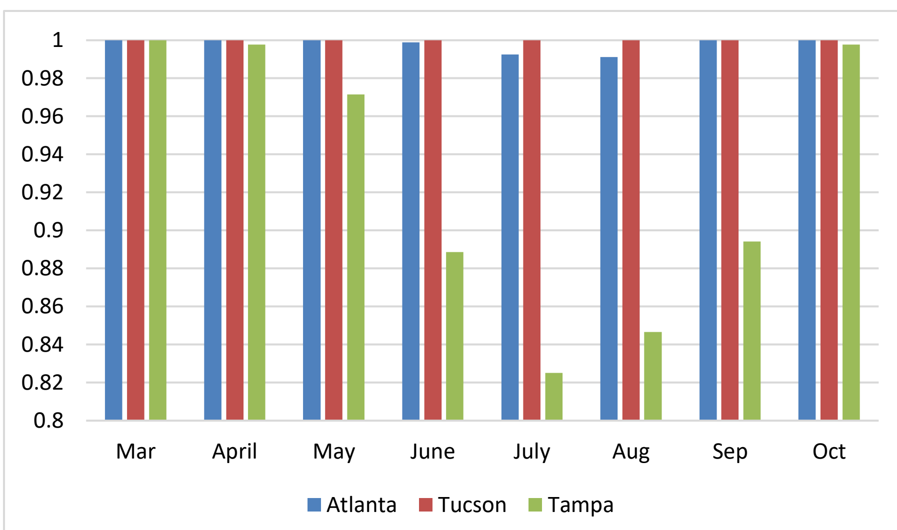

Figure 17 – Proportion of the cooling need removed by cooling the indoor air down to the outdoor wet-bulb temperature

2.2.4 Sky Temperature

The sky temperature is an equivalent value used in the modelling of the radiative heat exchange between the building and the sky. Its calculation can be found in (U.S. Department of Energy, 2016b). It is a good source of cooling energy especially on clear nights in arid regions. The cooling energy available from the sky temperature for a building can be seen as the additional radiative heat loss of a building to the sky by adopting ABE technologies. It equals the total radiative heat loss from all building surfaces to the sky minus the portion of heat loss from the inside. The reason for subtracting the portion of heat loss from the inside is that the cooling need reduction potential of the sky temperature is expressed as a proportion of the cooling need of the baseline model and the heat loss from the inside has already been accounted for in the cooling need calculation of the baseline model. The calculation of the heat loss from the inside is based on the method provided by ISO 13790-2008 as shown below (International Organization for Standardization, 2008):

$$\Phi_r = R_{se} \times U_c \times A_c \times h_{or} \times \Delta\theta_{er} \tag{7}$$

where R_{se} is the external surface heat resistance of the building envelope element considered, m^2·K/W; U_c is the thermal transmittance of the element, W/(m^2·K); A_c is the projected area of the element, m^2; h_{or} is the external radiative heat transfer coefficient, W/(m^2·K); $\Delta\theta_{er}$ is the average difference between the external air temperature and the apparent sky temperature, °C.

Four scenarios are considered in this study, as shown in Table 6. The cities chosen as examples are the same as those in the outdoor dry-bulb temperature case. When the strategy of whole day radiative cooling is used, the cooling load can be removed almost completely in all three cities regardless of whether there is a thermal storage system. In the night-time radiative cooling only scenario, the proportion of the cooling need removed in all cities are nearly 0%, because the radiative cooling availability schedule totally mismatches the operation schedule of the office. Night-time radiative cooling plus thermal storage is the only scenario in which there are some differences between the three cities. The result of this scenario is shown in Figure 18. It can be seen that in all three cities the proportion of cooling need removed by using the strategy of night-time radiative cooling plus thermal storage is around 90%. The results show that the potential of sky radiative cooling is enormous. There are two approaches to completely replacing active cooling with radiative cooling. The first is to use a sufficiently large thermal storage system in combination with traditional radiative cooling materials. This approach has no technical difficulties but requires a large amount of investment. The second approach is to further improve the performance of DRC materials.

Table 6 – The four scenarios of utilizing the sky temperature for cooling

Scenario	Note
Whole day radiative cooling	In this scenario, perfect DRC materials are used to provide radiative cooling even in direct sunlight. The assumption is that the perfect DRC materials can reflect solar radiation completely and its emissivity between 8–12 nm is 1.
Night-time radiative cooling only	In this scenario, perfect traditional radiative cooling materials whose thermal emissivity is 1 are used. Therefore, there is no radiative cooling effect in the daytime.

Whole day radiative cooling + thermal storage	In this scenario, perfect DRC materials and thermal storage systems are used. The assumption is that the cooling energy collected on the previous day can be used on this day.
Night-time radiative cooling + thermal storage	In this scenario, perfect traditional radiative cooling materials and thermal storage systems are used. The assumption is that the cooling energy collected on the previous night can be used on this day.

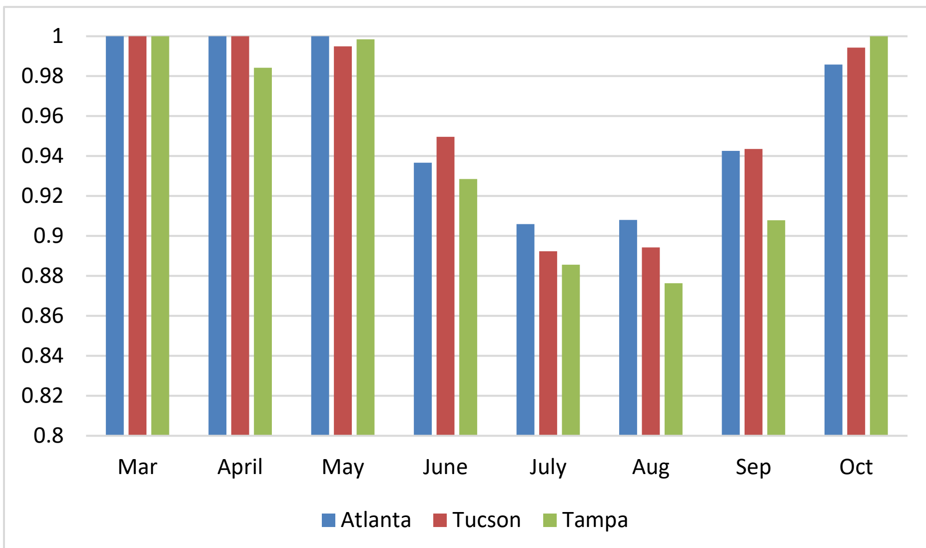

Figure 18 – The proportion of cooling need removed by using nighttime radiative cooling + thermal storage

2.2.5 Solar Radiation

Solar radiation is the only weather variable that is associated with heating. The solar energy available for a building can be seen as the additional solar energy a building can utilize by adopting ABE technologies. It equals the total solar energy incident on all the building surfaces minus the solar energy transferred to the inside. The reason for subtracting the solar energy transferred to the inside is that the heating need reduction potential of solar radiation is expressed as a proportion of the heating need of the baseline model and the solar energy transferred to the inside has already been accounted for in the heating need calculation of the baseline model. The calculation of the solar energy transferred to the inside is based on the method provided by ISO 13790-2008 as shown below (International Organization for Standardization, 2008):

$$\Phi_{sol,k} = F_{sh,ob,k} \times A_{sol,k} I_{sol,k} - F_{r,k} \Phi_{r,k} \tag{8}$$

where $F_{sh,ob,k}$ is the shading reduction factor for external obstacles for the solar effective collecting area of surface k; $A_{sol,k}$ is the effective collecting area of surface k with a given orientation and tilt angle, in the considered zone or space, m^2; $I_{sol,k}$ is the solar irradiance, the mean energy of the solar irradiation over the time step of the calculation, per square meter of collecting area of surface k, with a given orientation and tilt angle, W/m^2; $F_{r,k}$ is the form factor between the building element and the sky; $\Phi_{r,k}$ is the extra heat flow due to thermal radiation to the sky from building element k, W.

Two scenarios are considered in this study, one with thermal storage, the other without. Without thermal storage, the solar energy can only be used to remove the heating need at that time. With thermal storage, the solar energy collected on the previous day can be used on this day. Three cities are chosen as examples, as shown in Table 7. The heating season is from October to March of the next year.

Table 7 – Cities chosen as examples for the solar radiation case

City	Atlanta, GA	Rochester, MN	Fairbanks, AK
Climate zone	3A	6A	8

In Atlanta and Rochester, heating load can be removed completed when thermal storage is adopted. In Fairbanks, the proportion of heat need removed when thermal storage is adopted for October, November, December, January, February, and March is 100%, 98%, 51%, 82%, 100%, and 100%, respectively. When there is no thermal storage, the result is shown in Figure 19. It can be seen that even in Fairbanks, there is a substantial amount of solar energy available for heating. However, to fully exploit this potential is not easy. There are two essentials for exploiting the energy saving potential of solar radiation. The first one is to have a sufficient surface area to collect solar energy. The surface can be either the surface of a solar collector or a glazing surface of the building facing the sun. The second is to have highly insulated building envelope. The ideal case is to have a building envelope that is transparent to sunlight, opaque to long-wave infrared, and at the same time well-insulated.

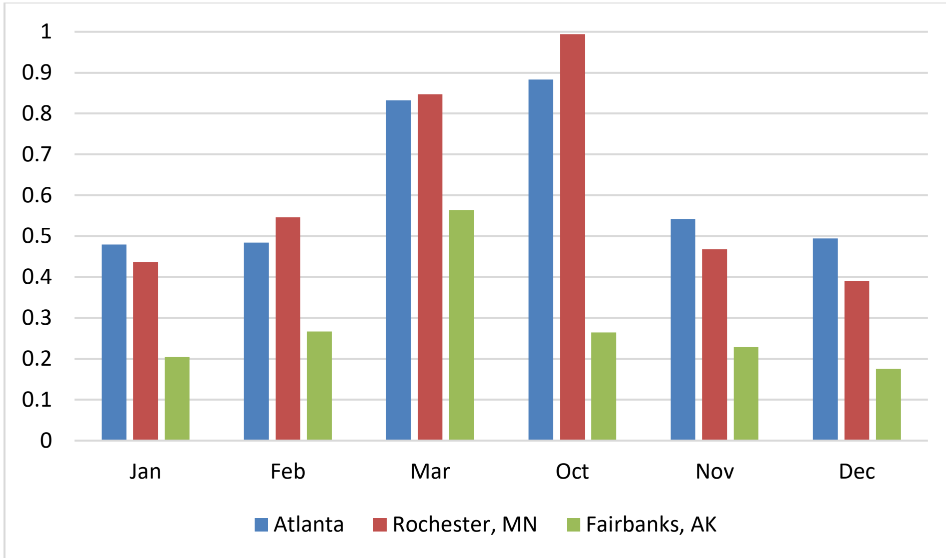

Figure 19 – The proportion of heating need removed with solar energy

CHAPTER 3. MODELLING METHODS OF ABE SYSTEMS

Since building models are created to simulate the behavior of actual building systems, the development of ABE modules in commercial BEM programs inevitably lags behind the invention or first application of corresponding ABE systems (Brahme, O'Neill, Sisson, & Otto, 2009; Loonen, 2018; Loonen, Favoino, Hensen, & Overend, 2017; Loonen, Singaravel, Trčka, Cóstola, & Hensen, 2014). Although EnergyPlus is one of the most versatile BEM programs in terms of modelling ABE systems (Loonen et al., 2017), the variables that can be controlled during the simulation process are still very limited. In this chapter, modelling methods of ABE systems based on EnergyPlus will be presented. Some ABE systems, such as electrochromic windows, dynamic louvers/blinds, and PCM systems, can be modelled by existing modules in EnergyPlus. Others have to be modelled with some workarounds developed by the author.

3.1 The General Structure of Modelling Methods of ABE Systems

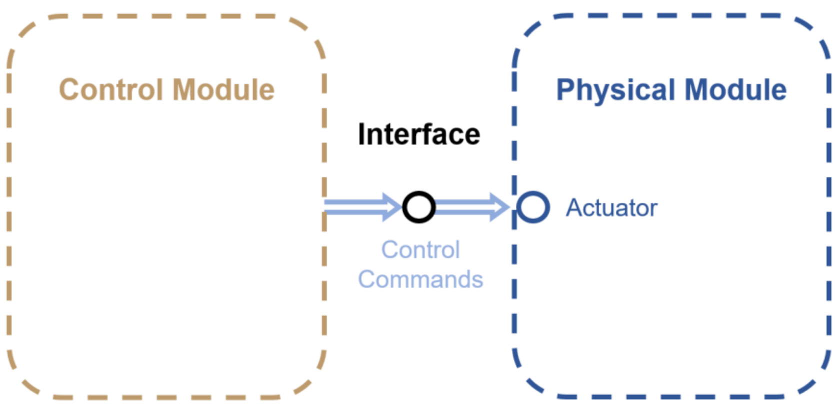

Figure 20 – The general structure of modelling methods of ABE systems

As shown in Figure 20, in general the modelling method of an ABE system consists of a control module, a physical module, and an interface. The control module is composed of a set of control functions or schedule files that generate the control commands. The control functions are built-in modules of EnergyPlus or external programs whose outputs are used as control commands. The input variables of the control functions are called sensors, such as outdoor dry-bulb temperature, indoor temperature, presence of occupants, etc. The term, sensor, used here has a different meaning from that used in Section 1.2.2. In Section 1.2.2, sensors are physical components of an extrinsic control system. Intrinsic control systems do not have sensors. Here, sensors are an integral part of control functions. The self-regulating mechanisms of intrinsically controlled systems are also represented by functions with sensors. When schedule files are used in the control module, time can be seen as a sensor. The sources of sensors include BEM programs, physical sensors, the internet, or user-defined input files. Schedule files usually cannot be changed during the simulation process of EnergyPlus. They can be used in the control module because TMY3 weather data are commonly adopted for building simulation. Since weather data of all the time steps are available, the control commands of all the time steps can be calculated in advance and then stored in schedule files.

The control commands generated by the control module are passed to the physical module by the interface. If the control functions are built-in modules of EnergyPlus, the interface is the Energy Management System: Program Calling Manager object from the Energy Management System (EMS) group of EnergyPlus (U.S. Department of Energy, 2016a). If the control functions are external programs, the interface is the Building Controls

Virtual Test Bed (BCVTB) + the External Interface object from the External Interface group of EnergyPlus (U.S. Department of Energy, 2016c).

The physical module is the physical model of ABE systems in EnergyPlus. Within the physical module, the actuator is of paramount importance. The actuator here is the variable in the physical model that can be controlled during the simulation process, which is different from that used in Section 1.2.2. The type of actuators provided by EnergyPlus determines what ABE systems can be modelled. Besides standard actuators that are variables of building systems, there is an actuator called Schedule Value. Using this actuator, all the schedules in EnergyPlus can be changed at each time step. Since the actuators provided by EnergyPlus are limited, some ABE systems have to be modelled with some workarounds. A main drawback of using workarounds is that they usually involve lots of approximations and simplifications that may impair the accuracy of the model (Loonen et al., 2017).

3.1.1 Control Module and Interface

3.1.1.1 Energy Management System (EMS)

EMS is an advanced feature of EnergyPlus that provides high-level, supervisory control to override selected aspects of EnergyPlus modelling (U.S. Department of Energy, 2016a). The necessary objects for an EMS application include:

- Energy Management System: Sensor,
- Energy Management System: Actuator,
- Energy Management System: Program Calling Manager, and
- Energy Management System: Program,

among which Energy Management System: Sensor and Energy Management System: Program belong to the control module, Energy Management System: Program Calling Manager is the interface, and Energy Management System: Actuator is part of the physical module.

The Energy Management System: Sensor object is used to declare input variables of the control program. Any output variable or meter of EnergyPlus can be used as a sensor. An example of this object is shown below. The Name field contains the user-defined name of the sensor that will be referenced by the control program. The Output:Variable or Output:Meter Index Key Name field contains the key reference for the specified output variable. In this case, it is the name of the zone whose zone mean air temperature is an input of the control program. The Output:Variable or Output:Meter Name field contains the name of the output variable or meter of EnergyPlus (U.S. Department of Energy, 2016d). In this case, it is the zone mean air temperature.

```
EnergyManagementSystem:Sensor,
    TIN,                         !- Name
    living_unit1,                !- Output:Variable or Output:Meter Index Key Name
    Zone Mean Air Temperature ;  !- Output:Variable or Output:Meter Name
```

The Energy Management System: Program object is the central processor of the EMS where the control program is written. The control program should be written in EnergyPlus Runtime Language (Erl), a programming language specially developed for defining EMS control. The output of the control program is the values assigned to the actuators. Only rule-based control can be realized by the control program. If MPC is selected, external control modules should be used. More details of Erl can be found in (U.S. Department of Energy, 2016a).

The Energy Management System: Program Calling Manager object specifies which control program should be run at what time. There are various calling points at each stage of the working process of EnergyPlus (U.S. Department of Energy, 2016a). The selection of calling points depends on the characteristics of the control system and the ABE system. An example of this object is shown below. The Name field contains the user-defined name of the program calling manager. The EnergyPlus Model Calling Point field describes when the control programs managed under this object are called during an EnergyPlus simulation (U.S. Department of Energy, 2016d). In this case, Begin Timestep Before Predictor is selected. This calling point occurs near the beginning of each time step but before the zone's thermal loads are calculated, which is suitable for building systems that affect the thermal loads (U.S. Department of Energy, 2016a). Since the function of ABE is to reduce the building load, Begin Timestep Before Predictor should be used for most ABE systems. The Program Name 1 field contains the name of the control program that will be the first to run for the calling point. More control programs can be specified in the Program Name 2, 3, …, N fields, which will be called in sequence (U.S. Department of Energy, 2016d).

```
EnergyManagementSystem:ProgramCallingManager,
    PCM1,                    !- Name
    BeginTimestepBeforePredictor,  !- EnergyPlus Model Calling Point
    P1;                      !- Program Name 1
```

3.1.1.2 Schedule

There are two ways of using schedules in the control module. The first is to choose Schedule Value in the Actuated Component Control Type field of the Energy Management System: Actuator object or declare an External Interface: Schedule object. In this case, the schedule value is given by the corresponding control program at each time step, which is the same as other actuators. The second way is to use the Schedule: File object in the Schedules group. An example of this object is shown below. The File Name field contains the name of the file that contains the data for the schedule. If the file is not in the same directory as the EnergyPlus idf file, this field should include the full path to the file. The pre-calculated control commands of all the time steps should be stored in this file.

```
Schedule:File,
    S1,                         !- Name
    ,                           !- Schedule Type Limits Name
    Dry.csv,                    !- File Name
    2,                          !- Column Number
    1,                          !- Rows to Skip at Top
    8760,                       !- Number of Hours of Data
    Comma,                      !- Column Separator
    No;                         !- Interpolate to Timestep
```

3.1.1.3 Matlab + BCVTB

The programs that can be linked to EnergyPlus via BCVTB for co-simulation include Matlab, Modelica, Radiance, etc. Matlab is a programming platform for solving engineering and scientific problems (MathWorks, 2019). It is selected as the primary external program of the control module in this section. Matlab is able to not only generate the control commands but also simulate some ABE systems that cannot be simulated directly in EnergyPlus.

The data exchange between Matlab and EnergyPlus is realized by BCVTB. The Building Controls Virtual Test Bed (BCVTB) is a software environment developed by Lawrence Berkeley National Laboratory (LBNL) that allows users to couple different simulation programs for co-simulation, and to couple simulation programs with actual hardware (Wetter, 2016). A simple configuration of BCVTB is shown in Figure 21. In this configuration, BCVTB serves as the bridges between different programs. It passes the sensor values from EnergyPlus to Matlab and passes the control commands from Matlab to EnergyPlus. Due to the data exchange between the two programs, the action of the actuator lags two time steps behind the measurement of sensor values. This lag will not be a severe problem for the control of ABE systems when the time step is smaller than half an hour, because as will be shown later the switching intervals of ABE systems are usually several hours.

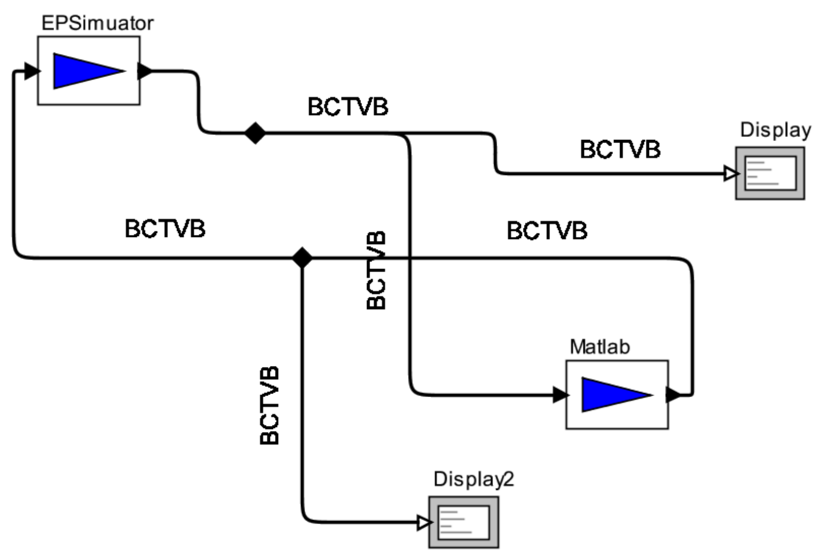

Figure 21 – A simple configuration of BCVTB that connects Matlab and EnergyPlus

BCVTB should be linked to the External Interface of EnergyPlus. The Name of External Interface field of the External Interface object should be set as Ptolemy Server. The External Interface: Schedule object and the External Interface: Actuator object are the same as the Energy Management System: Actuator object, except that they are controlled by external programs.

3.1.2 Actuator

Actuators are variables in the physical module that can be controlled during the simulation process. In EnergyPlus, the actuators available depend on the building model. One can set the Output: Energy Management System object as shown below to let EnergyPlus report all the actuators available to the users. The report can be opened by clicking the button "EDD" in EP-Launch.

```
Output:EnergyManagementSystem,
    Verbose,                 !- Actuator Availability Dictionary Reporting
    Verbose,                     !- Internal Variable Availability Dictionary
Reporting
    None;                    !- EMS Runtime Language Debug Output Level
```

There are two ways of declaring actuators. If EMS is chosen as the control module, the Energy Management System: Actuator object should be used. If external program is chosen as the control module, the External Interface: Schedule object or the External Interface: Actuator object should be used. The settings of these objects are similar. An example of the External Interface: Actuator object is shown below. The Name field contains the user-defined name of the actuator that will be referenced in the control program.

```
ExternalInterface:Actuator,
    ConIndexS,               !- Name
    SUB SURFACE 2,           !- Actuated Component Unique Name
    Surface,                 !- Actuated Component Type
    Construction State,      !- Actuated Component Control Type
    29;                      !- Optional Initial Value
```

Note that the meaning of actuator here is a little bit different from that used in EnergyPlus. In EnergyPlus terminology, an actuator refers to the name specified in the Actuated Component Type field, which can be understood as a class of actuators applying to the same building component. In the terminology of this thesis, an actuator refers to a specific variable specified in the Actuated Component Control Type field in EnergyPlus. The usage of actuators will be discussed in detail according to the classification of ABE systems in the following sections.

3.2 Glazing Technology

3.2.1 Dynamic Shading Device

3.2.1.1 Overhang with Variable Tilt Angle

There is an EnergyPlus object called Shading: Overhang that is the most commonly used object to define an overhang. However, an overhang defined by this object cannot be controlled during the simulation process. Instead, the Shading: Building: Detailed object or the Shading: Zone: Detailed object should be used. The author has not found any significant difference between these two objects yet. In these objects, the same overhang at different tilt angles should be specified as different ones, as shown in Figure 22. The rendering of the same overhang at different tilt angles is shown in Figure 23. The transmittance of these objects is determined by their respective transmittance schedule. At any time step, only one transmittance schedule should be set as 0, and the other two should be set as 1. For example, when the overhang is perpendicular to the wall, the transmittance of Shading Surface 1 should be set as 0, and the transmittance of the other two shading surfaces should be set as 1. Note that the sum of reflectance and transmittance of a surface should be less than or equal to 1. Therefore, in the Shading Property: Reflectance object, the diffuse solar reflectance and diffuse visible reflectance of these shading surfaces should all be set as 0 in order to avoid errors.

Field	Units	Obj1	Obj2	Obj3
Name		Shading Surface 1	Shading Surface 2	Shading Surface 3
Transmittance Schedule Name		Schedule1	Schedule1	Schedule3
Number of Vertices				
Vertex 1 X-coordinate	m	20	20	20
Vertex 1 Y-coordinate	m	10.56	10.485	10.28
Vertex 1 Z-coordinate	m	2.9	2.62	2.415
Vertex 2 X-coordinate	m	20	20	20
Vertex 2 Y-coordinate	m	10	10	10
Vertex 2 Z-coordinate	m	2.9	2.9	2.9
Vertex 3 X-coordinate	m	0	0	0
Vertex 3 Y-coordinate	m	10	10	10
Vertex 3 Z-coordinate	m	2.9	2.9	2.9
Vertex 4 X-coordinate	m	0	0	0
Vertex 4 Y-coordinate	m	10.56	10.485	10.28
Vertex 4 Z-coordinate	m	2.9	2.62	2.415

Figure 22 – Specifying overhangs with different tilt angles in the Shading: Building: Detailed object

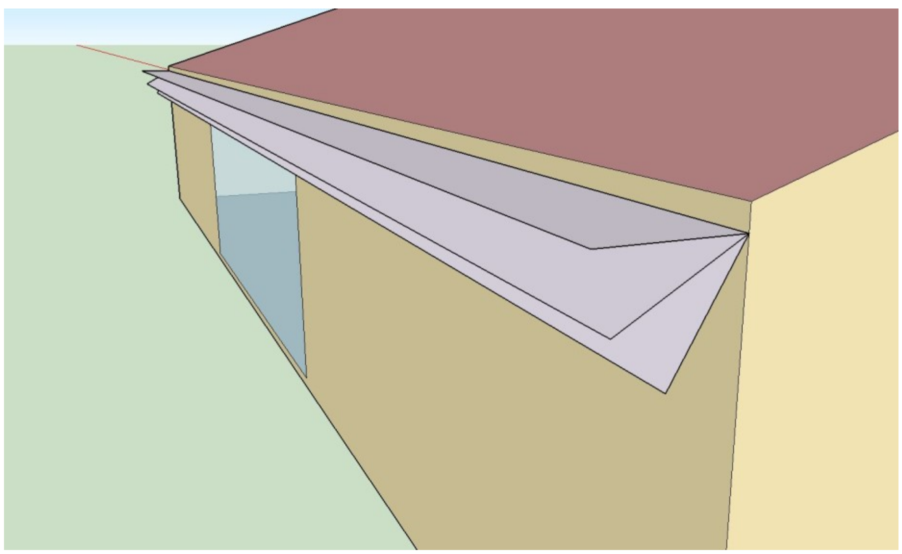

Figure 23 – The rendering of the overhang at different tilt angles

3.2.1.2 Shade, Blind, and Screen

In EnergyPlus, there are three types of window shading material objects: Window Material: Shade, Window Material: Blind, and Window Material: Screen. Window

Material: Shade should be used for diffusing materials such as drapery and translucent roller shades. For slat-type shading devices, such as Venetian blinds, that have a strong angular dependence of transmission, absorption and reflection, Window Material: Blind is recommended. Window Material: Screen is suitable for modelling wire mesh insect screens where the solar and visible transmission and reflection properties vary with the angle of incidence of solar radiation (U.S. Department of Energy, 2016d). There are EnergyPlus Reference Data Sets that contain properties of generic shading devices. These data sets can be found in the installation directory of EnergyPlus. There are two ways of modelling the control of these shading devices. The first way is as follows:

- Define the construction of the window without the shade, the so-called "bare" construction.
- Reference the bare construction in the Fenestration Surface: Detailed for the window.
- Define the shading device (Window Material: Shade, Window Material: Blind, or Window Material: Screen).
- Define a Window Property: Shading Control for the window in which you (1) specify that this shading device is the window's shading device and (2) specify how the shading device is controlled (U.S. Department of Energy, 2016d).

The second way is as follows:

- Define the Construction of the window without the shade, the so-called "bare" construction.
- Reference the bare construction in the Fenestration Surface: Detailed for the window.

- Define the shading device (Window Material: Shade, Window Material: Blind, or Window Material: Screen).
- Define another Construction, called the "shaded construction", that includes the shading device.
- Define a Window Property: Shading Control for the window in which you (a) reference the shaded construction and (b) specify how the shading device is controlled (U.S. Department of Energy, 2016d).

The Window Property: Shading Control object is where the shading device type, shading device location (interior, exterior, and between-glass), and shading device control are specified. The Name field of this object will be referenced in the Fenestration Surface: Detailed object. The Shading Type field specifies the type and location of the shading device (e.g. Interior Shade). The user can specify the specific shading device in either the Name of Construction with Shading field or the Material Name of the Shading Device field. The Construction or the Window Material object referenced in either of these fields must accord with the Shading Type field. The Shading Control Type field specifies how the shading device is controlled. The shading device only has two states, on and off. "On" means the shading device covers all of the window except its frame, while "off" means the shading device is fully retracted. There are several simple control criteria provided by EnergyPlus, such as diffuse solar radiation incident on the window, outdoor air temperature, etc. When the measured variable exceeds the setpoint, the shading device is turned on.

If the user wants to use more complicated control logic, the shading device should be controlled by a schedule or an actuator. If the shading device is controlled by a schedule, the Shading Control Type field should be set as On If Schedule Allows, and the Shading Control Is Scheduled field should be set as Yes. If the actuator is used, an actuator should be created as shown below. The Name field contains the user-defined name of the actuator that will be used as a variable in the control program, where it is assigned an integer value from -1 to 9. Each integer value represents a different state of the shading device. For example, -1 represents no shading device, 0 represents shading device is off, and 1 represents interior shade is on (U.S. Department of Energy, 2016a). The Actuated Component Unique Name field contains the name of the window to be controlled. When Window Material: Blind is used, the slat angle can also be controlled by a schedule. The slat angle value is continuous between 0 and 180.

```
EnergyManagementSystem:Actuator,
    SA1,                      !- Name
    sub surface 2,            !- Actuated Component Unique Name
    Window Shading Control,  !- Actuated Component Type
    Control Status;           !- Actuated Component Control Type
```

3.2.2 *Switchable Window*

In practice, only electrochromic windows and thermochromic window are kind of widely used in buildings. Therefore, this section will only present the modelling methods of these two types of windows.

3.2.2.1 Electrochromic Window

There are two ways of modelling electrochromic windows. The first way is to use the Window Property: Shading Control object. In the Shading Type field, there is an option called Switchable Glazing. With this option, the fully bleached state is specified by the Construction object referenced by the Fenestration Surface: Detailed object and the fully coloured state is specified by the Construction object referenced by the Window Property: Shading Control object. With this method, the state of the window is either fully bleached or fully coloured for all Shading Control Types except Meet Daylight Illuminance Setpoint. When this control type is selected, the transmittance of the glazing is adjusted to just meet the daylight illuminance set point at the first daylighting reference point (U.S. Department of Energy, 2016d).

If the user wants to control the electrochromic window at more intermediate states, the actuator Construction State should be used. With this method, several Construction objects representing different states of the electrochromic window should be created. Then, the actuator Construction State is used to switch between these Construction objects. An example of this object is shown below. The Name field contains the user-defined name of the actuator that will be used as a variable in the control program, where it is assigned the indices of different Construction objects in different situations. The Actuated Component Unique Name field contains the name of the electrochromic window to be controlled.

```
EnergyManagementSystem:Actuator,
    A1,                         !- Name
    sub surface 5,              !- Actuated Component Unique Name
    Surface,                    !- Actuated Component Type
    Construction State;         !- Actuated Component Control Type
```

3.2.2.2 Thermochromic Window

Thermochromic windows can be modelled by an EnergyPlus object called Window Material: Glazing Group: Thermochromic. An example of this object is shown below. The Optical Data Temperature <N> fields specify a series of temperatures, and the Window Material Glazing Name <N> fields specify the name of Window Material: Glazing objects corresponding to each temperature. Note that the Window Material: Glazing Group: Thermochromic object only represents a single glazing layer with thermochromism. To form a complete window construction, this object and other window objects, like Window Material: Glazing and Window Material: Gas, should be referenced by a Construction object. There is an example file named ThermochromicWindow.idf in the installation directory of EnergyPlus.

```
WindowMaterial:GlazingGroup:Thermochromic,
    TCGlazings,               !- Name
    25,                       !- Optical Data Temperature 1 {C}
    WO18RT25,                 !- Window Material Glazing Name 1
    27,                       !- Optical Data Temperature 2 {C}
    WO18RT27,                 !- Window Material Glazing Name 2
    29,                       !- Optical Data Temperature 3 {C}
    WO18RT29,                 !- Window Material Glazing Name 3
    31,                       !- Optical Data Temperature 4 {C}
    WO18RT31,                 !- Window Material Glazing Name 4
    33,                       !- Optical Data Temperature 5 {C}
    WO18RT33,                 !- Window Material Glazing Name 5
    35,                       !- Optical Data Temperature 6 {C}
    WO18RT35,                 !- Window Material Glazing Name 6
    37,                       !- Optical Data Temperature 7 {C}
    WO18RT37,                 !- Window Material Glazing Name 7
    39,                       !- Optical Data Temperature 8 {C}
    WO18RT39,                 !- Window Material Glazing Name 8
    41,                       !- Optical Data Temperature 9 {C}
    WO18RT41,                 !- Window Material Glazing Name 9
    43,                       !- Optical Data Temperature 10 {C}
    WO18RT43,                 !- Window Material Glazing Name 10
    45,                       !- Optical Data Temperature 11 {C}
    WO18RT45,                 !- Window Material Glazing Name 11
    50,                       !- Optical Data Temperature 12 {C}
    WO18RT50,                 !- Window Material Glazing Name 12
    55,                       !- Optical Data Temperature 13 {C}
    WO18RT55,                 !- Window Material Glazing Name 13
    60,                       !- Optical Data Temperature 14 {C}
    WO18RT60,                 !- Window Material Glazing Name 14
    65,                       !- Optical Data Temperature 15 {C}
    WO18RT65,                 !- Window Material Glazing Name 15
    70,                       !- Optical Data Temperature 16 {C}
    WO18RT70,                 !- Window Material Glazing Name 16
    75,                       !- Optical Data Temperature 17 {C}
    WO18RT75,                 !- Window Material Glazing Name 17
    80,                       !- Optical Data Temperature 18 {C}
    WO18RT80,                 !- Window Material Glazing Name 18
    85,                       !- Optical Data Temperature 19 {C}
    WO18RT85;                 !- Window Material Glazing Name 19
```

3.2.3 Double Skin Façade (DSF)

In EnergyPlus there is no single existing module that can model DSF. Therefore, the user has to build the DSF model from basic elements like thermal zones, windows, and shading devices. In this section, the method proposed by Kim et al. is adopted because it is in great detail and validated (D. Kim et al., 2018).

Since there is no air circulation or air temperature stratification within a thermal zone in EnergyPlus models, the DSF model created by Kim et al. is composed of four stacked thermal zones with shading devices, as shown in Figure 24. An airflow network model is created among these zones and the zones representing rooms to simulate airflows driven by buoyancy and wind pressure. The Airflow Network: MultiZone: Surface: Component: Simple Opening object in EnergyPlus is used to define vertical openings, and the Airflow Network: MultiZone: Component: Horizontal Opening object is used to define horizontal openings. Vertical openings on the exterior surface of the stacked thermal zones are used to represent the operable openings of DSF. Horizontal openings between the stacked thermal zones are used to form the DSF channel. Discharge coefficient is set as 0.65 and 0.2 for vertical and horizontal openings, respectively. The Airflow Network: MultiZone: Surface: Effective Leakage Area object is used to simulate the infiltration through building surfaces (D. Kim et al., 2018).

In (D. Kim et al., 2018), a physical DSF model identical to the one modelled is constructed. The surface temperature of the two skins are measured in two periods. The first one is from May 20th to May 28th. In this period the openings are always on. The second one is from July 28th to August 5th. In this period the openings are always off. The Effective Leakage Area (ELA) values of the Airflow Network: MultiZone: Surface:

Effective Leakage Area objects are manually tuned until the difference between the measured and simulated surface temperatures is within an acceptable range.

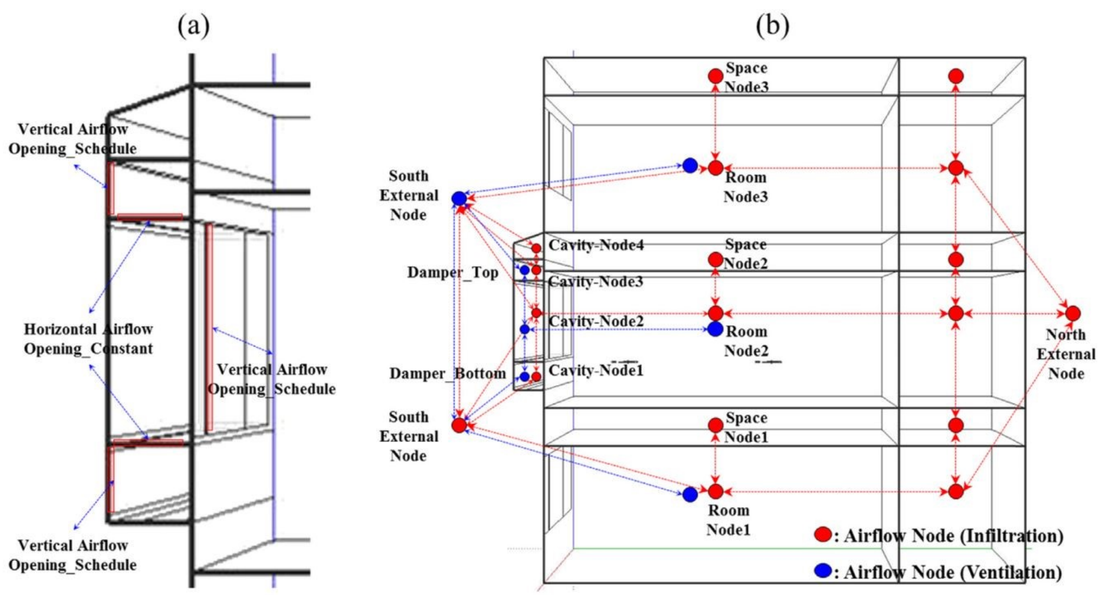

Figure 24 – (a) Double skin façade system opening conditions and (b) air nodes in EnergyPlus (D. Kim et al., 2018)

The user can use this method to model DSF. The more the stacked thermal zones, the more accurate the airflow simulation. Besides, in EnergyPlus glazed surfaces, called sub-surfaces, can only be created on the surfaces of a thermal zone, which means if the DSF is divided into many small thermal zones, the window also has to be divided into many small windows. This may affect the accuracy of the model. Due to the complexity of DSF, it is recommended to always calibrate a DSF model before using it.

3.2.4 Movable Insulation

EnergyPlus has an object called Surface Control: Movable Insulation. However, this object only applies to regular surfaces (e.g. walls, floors, roofs. etc.) rather than sub-surfaces. To model movable insulation on windows, the user should use the actuator Construction State. The settings are similar to those shown in Section 3.2.2.1. Two Construction objects should be created for the window. The first one is the bare window. The second one is the window with movable insulation, which has a much lower U-factor, a SHGC close to 0, and a Tr_{vis} equal to 0. The Construction object can be defined in a standard way which consists of several layers or in a simplified way where the Window Material: Simple Glazing System object is used. If the simplified way is used, the U-factor of the window with movable insulation can be calculated using the method given by (International Organization for Standardization, 2006).

3.3 Opaque Technology

3.3.1 Dynamic Façade

3.3.1.1 Dynamic Insulation Façade

In the dynamic insulation façades discussed in this section, there are no working mechanical parts (e.g. fans and pumps) at steady state. The type of dynamic insulation façade that employs a fan to circulate the air within the cavity (Hoes et al., 2011) will be discussed in Section 3.3.1.2 along with ventilated façades. There are two ways of modelling dynamic insulation systems. The first is using the Surface Control: Movable Insulation object. With this object, an extra layer of insulation can be added to the inside or the outside of the surface according to a schedule. An example of this object is shown below. The Insulation Type field determines whether the movable insulation is applied to the inside or the outside of the surface. The Surface Name field refers the movable insulation back to a particular surface via its user assigned name. The Material Name field refers to a material layer (e.g., Material, Material: No Mass, or Window Material: Glazing) via its user assigned name. Note that transparent layers can only be applied to the outside of a surface. The Schedule Name field specifies a schedule that controls movable insulation, whose values should be between 0 and 1. The actual thermal resistance of the movable insulation is equal to the resistance of the material layer times the value in the movable insulation schedule (U.S. Department of Energy, 2016d).

```
SurfaceControl:MovableInsulation,
    Outside,                 !- Insulation Type
    Surface 3,               !- Surface Name
    Insulation_panel,        !- Material Name
    MI_SCH;                  !- Schedule Name
```

The second way is also using the actuator Construction State. In this case, several Construction objects representing different states of the dynamic insulation system should be created.

3.3.1.2 Ventilated Façade

Ventilated façades can be either naturally ventilated or mechanically ventilated. Naturally ventilated façades should be modelled using the same method as DSF, as explained in Section 3.2.3. For mechanically ventilated façades, an EnergyPlus object called Zone HVAC: Ventilated Slab should be used. This modelling method is developed by Chae and Strand (Chae & Strand, 2013). The diagram of the ventilated slab model is shown in Figure 25. The original model contains a cooling coil and a heating coil, which should be omitted in the ventilated façade model.

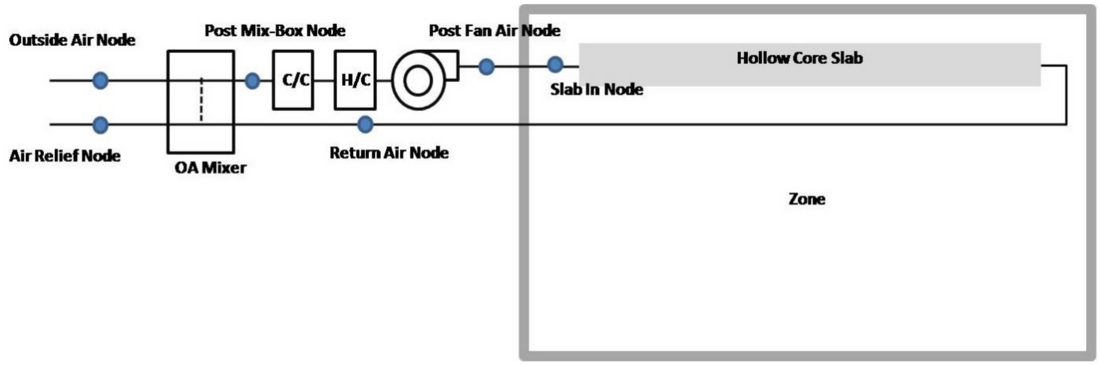

Figure 25 – The diagram of the ventilated slab model

An example of the Zone HVAC: Ventilated Slab object is shown below. The Zone Name field contains the name of the zone in which the ventilated slab system is principally located and intended to affect. A system that is between two zones will still act upon each zone. However, the zone name referenced here should be the zone that controls the system response. The Surface Name or Radiant Surface Group Name field contains the name of the surface or surface list in which the hollow cores are embedded. The Outdoor Air Control Type object has three options: Variable Percent, Fixed Temperature, and Fixed Amount. The variable percent control will vary the amount of outdoor air between some minimum and maximum schedules of fractions to minimize the current heating or cooling load. The fixed temperature control will vary the amount of outdoor air between the minimum schedule and 100% available outdoor air to obtain a desired mixed air temperature. The fixed amount control will set the outdoor air flow rate as minimum outdoor air flow rate. In this case, the maximum outdoor air flow rate and maximum outdoor air fraction will be ignored. The System Configuration Type field specifies how the air is circulated. The options are Slab Only, Slab And Zone, and Series Slabs. If Slab Only is selected, the outdoor air is sent to the slab only and does not enter the zone. With the Slab And Zone option, the air first enters the slab and then is delivered to the zone before returning to the system. If Series Slabs is selected, the air flows through a series of slabs specified by the user without entering any zone. The Temperature Control Type field specifies which temperature will be used as a sensor. The Coil Option Type field specifies whether there is a cooling coil and/or a heating coil in the system to modulate the mixed air's temperature (U.S. Department of Energy, 2016d). In our case, since ventilated façades are passive systems, this field should select None.

```
ZoneHVAC:VentilatedSlab,
    Zone1VentSlab,            !- Name
    VentSlabAvailability,     !- Availability Schedule Name
    SPACE1-1,                 !- Zone Name
    C1-1,                     !- Surface Name or Radiant Surface Group Name
    0.84,                     !- Maximum Air Flow Rate {m3/s}
    VariablePercent,          !- Outdoor Air Control Type
    0.168,                    !- Minimum Outdoor Air Flow Rate {m3/s}
    U2MinOASched,             !- Minimum Outdoor Air Schedule Name
    0.84,                     !- Maximum Outdoor Air Flow Rate {m3/s}
    VentSlabMaxOA,             !- Maximum Outdoor Air Fraction or Temperature
Schedule Name
    SlabOnly,                 !- System Configuration Type
    0.050,                    !- Hollow Core Inside Diameter {m}
    30.0,                     !- Hollow Core Length {m}
    50.0,                     !- Number of Cores
    MeanAirTemperature,       !- Temperature Control Type
    VentSlabHotHighAir,       !- Heating High Air Temperature Schedule Name
    VentSlabHotLowAir,        !- Heating Low Air Temperature Schedule Name
    VentSlabHotHighControl,   !- Heating High Control Temperature Schedule Name
    VentSlabHotLowControl,    !- Heating Low Control Temperature Schedule Name
    VentSlabCoolHighAir,      !- Cooling High Air Temperature Schedule Name
    VentSlabCoolLowAir,       !- Cooling Low Air Temperature Schedule Name
    VentSlabCoolHighControl,  !- Cooling High Control Temperature Schedule Name
    VentSlabCoolLowControl,   !- Cooling Low Control Temperature Schedule Name
    Zone1VentSlabReturnAirNode,  !- Return Air Node Name
    Zone1VentslabSlabInNode,  !- Slab In Node Name
    ,                         !- Zone Supply Air Node Name
    Zone1VentSlabOAInNode,    !- Outdoor Air Node Name
    Zone1VentSlabExhNode,     !- Relief Air Node Name
    Zone1VentSlabOAMixerOutletNode,  !- Outdoor Air Mixer Outlet Node Name
    Zone1VentSlabFanOutletNode,  !- Fan Outlet Node Name
    Zone1VentSlabFan,         !- Fan Name
    None,                     !- Coil Option Type
    ,                         !- Heating Coil Object Type
    ,                         !- Heating Coil Name
    ,                         !- Hot Water or Steam Inlet Node Name
    ,                         !- Cooling Coil Object Type
    ,                         !- Cooling Coil Name
    ;                         !- Cold Water Inlet Node Name
```

The settings of the nodes are quite complicated. The user is referred to an example file VentilatedSlab.idf in the installation directory of EnergyPlus. One drawback of this modelling method is that once the system is specified, the air can only flow in one direction (E-E, E-I, I-E, or I-I).

In (Koenders et al., 2018), the authors adapted the ventilated slab model to the closed-loop dynamic insulation system shown in Figure 7. The modification steps are shown in Figure 26. Firstly, the closed-loop dynamic insulation system is divided into two parts: an indoor side and an outdoor side. Then, the two parts are modelled as two separate slabs that are connected in series. Finally, the heating and cooling coils and outdoor air mixer are removed, as this system does not use conditioned outside air, resulting in a closed system with two ventilated slabs in series and a supply fan to control air circulation. Only one ventilated slab can be assigned to a surface. To implement the closed-loop dynamic insulation system with the ventilated slab model, the system needs to be modelled as two separate surfaces. The first surface is equipped with the indoor side of the system and the second surface with the outdoor side of the system. The zone that is created between the two surfaces is modelled as a cavity with stagnant air, with the remaining surfaces modelled with a massless high thermal resistance insulation material to ensure minimal losses in this zone.

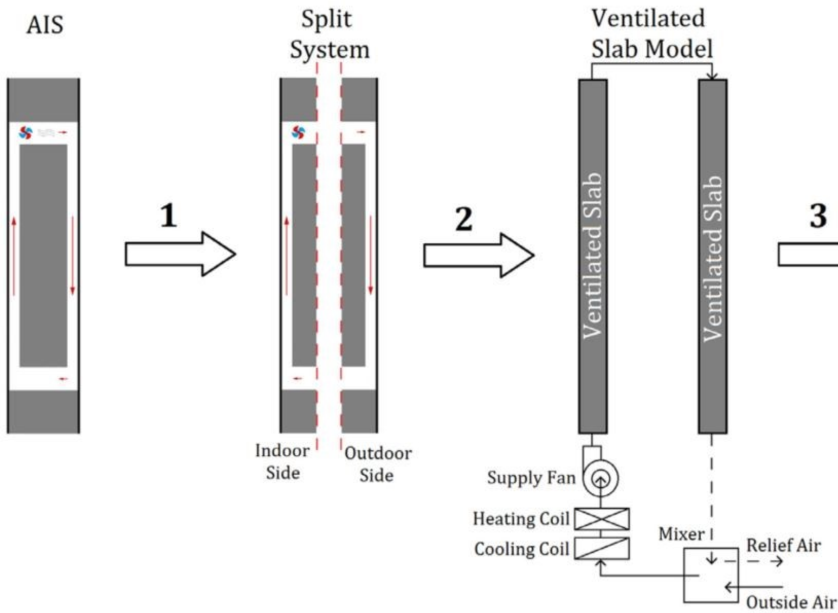

Figure 26 – Schematic process of adapting the ventilated slab model to a closed-loop dynamic insulation system (Koenders et al., 2018)

3.3.1.3 Breathing Wall

EnergyPlus has no built-in module that can model the porous structure of a breathing wall. Therefore, some workarounds have to be used. A breathing wall has two impacts on the building's energy calculation. Firstly, it changes the airflow rate into or out of the building through the façade. Secondly, it changes the equivalent U-factor of the façade. The user has to handle these two parts separately. The airflow and the convective heat exchange when the air is flowing through the façade can be modelled by the Ventilated Slab object described in Section 3.3.1.2. Since the contact area between the air and the façade is extremely large in a porous structure, the surface area of the hollow cores in the Ventilated Slab needs to be set as very large as well. The only problem is that the airflow direction in the ventilated slab model cannot be reversed. The variation of the U-factor can be modelled by the Surface Control: Movable Insulation object. The Material: No Mass object can be used for the extra thermal insulation. The schedule value of 0 (no extra thermal insulation) corresponds to the pro-flux flow state (U-factor is enhanced), while the schedule value of 1 (full extra thermal insulation) corresponds to the contra-flux flow state (U-factor is reduced). The no flow state should be modelled with a schedule value between 0 and 1.

3.3.2 Radiative Coating

3.3.2.1 <u>Variable Radiative Coating</u>

There are three actuators in EnergyPlus that can change the surface properties of the material placed in the outermost or innermost layer of a façade: Surface Property Solar Absorptance, Surface Property Thermal Absorptance, and Surface Property Visible Absorptance. Solar absorptance represents the fraction of incident solar radiation (0.3 to 2.537 microns) absorbed by the material. Thermal absorptance represents the fraction of incident long wavelength (>2.5 microns) radiation absorbed by the material. For long-wave radiative heat exchange, thermal emittance is equal to thermal absorptance. Visible absorptance represents the fraction of incident visible wavelength radiation (0.37 to 0.78 microns weighted by photopic response) absorbed by the material (U.S. Department of Energy, 2016d).

```
EnergyManagementSystem:Actuator,
    A1,                         !- Name
    Var_Material,               !- Actuated Component Unique Name
    Material,                   !- Actuated Component Type
    Surface Property Solar Absorptance;  !- Actuated Component Control Type
```

3.3.2.2 <u>Daytime Radiative Cooling (DRC) Material</u>

If the DRC device is not switchable, the Thermal Absorptance, Solar Absorptance, and Visible Absorptance fields in the Material object should be used to specify the properties of the DRC material. If the DRC device is switchable, the three actuators described in Section 3.3.2.1 should be used. However, this radiative heat exchange model is quite rough for DRC materials. Water vapor content, particulate concentration, cloud cover, and many other meteorological parameters all have a great impact on the performance of a DRC device. Besides, the surface conditions of a DRC device also play an important role in the radiative heat exchange. To take these parameters into account, a more complex radiative heat exchange model needs to be developed.

3.3.3 Thermal Storage

This section explains how to model thermal storage building envelope with PCMs. The heat transfer in a PCM can be described by a particular class of partial differential equation (PDE) problems called Stefan problems. Stefan problems feature a material with two phases and a moving boundary between them. There are several methods for formulating the PDEs of a Stefan problem, including the enthalpy method, heat capacity method, temperature transforming model, and heat source method (Al-Saadi & Zhai, 2013). The PCM models used in BEM vary in complexity, ranging from zero-dimensional RC model to three-dimensional model. In general, more complex models have higher accuracy but are more computationally expensive.

EnergyPlus uses a one-dimensional enthalpy method to model PCMs. To model PCMs, the Heat Balance Algorithm in EnergyPlus should be set as Conduction Finite Difference. For version 7 or higher of EnergyPlus, a fully implicit scheme is used as default to solve the PDEs. The user can manually switch to the semi-implicit Crank-Nicholson scheme which was adopted by EnergyPlus versions prior to 7. The implicit scheme is first-order in time but has unconditional stability, while the Crank-Nicholson scheme is second-order in time. The time step should be set as 20 time steps per hour or greater (U.S. Department of Energy, 2016b).

The Material Property: Phase Change object in EnergyPlus is used to specify PCMs. An example of this object is shown below. The Name field should be a regular material name specifying the material with which this additional temperature dependent property information will be associated. The Temperature Coefficient for Thermal Conductivity field is used to enter the temperature dependent coefficient for thermal conductivity of the material. The thermal conductivity is calculated by:

$$k = k_0 + k_1(T_i - 20) \tag{9}$$

where k_0 is the thermal conductivity at 20°C, W/(m·K); k_1 is the change in conductivity per degree temperature difference from 20°C (the input of this field), W/(m·K^2). The Temperature-Enthalpy field set specifies a two-column tabular temperature-enthalpy function for the basic material.

```
Material,
    E1 - 3 / 4 IN PLASTER OR GYP BOARD,  !- Name
    Smooth,                  !- Roughness
    1.9050000E-02,           !- Thickness {m}
    0.7264224,               !- Conductivity {W/m-K}
    1601.846,                !- Density {kg/m3}
    836.8000,                !- Specific Heat {J/kg-K}
    0.9000000,               !- Thermal Absorptance
    0.9200000,               !- Solar Absorptance
    0.9200000;               !- Visible Absorptance

MaterialProperty:PhaseChange,
```

```
    E1 - 3 / 4 IN PLASTER OR GYP BOARD,  !- Name
    0.0,                  !- Temperature coefficient ,thermal conductivity(W/m
K2)
    -20.,                    !- Temperature 1, C
    0.01,                    !- Enthalpy 1 at -20C, (J/kg)
    20.,                     !- Temperature 2, C
    33400,                   !- Enthalpy 2, (J/kg)
    20.5,                    !- temperature 3, C
    70000,                   !- Enthalpy 3, (J/kg)
    100.,                    !- Temperature 4, C
    137000;                  !- Enthalpy 4, (J/kg)
```

3.4 Bridge Technology

3.4.1 Thermodiode

Thermodiode systems can provide free heating or cooling energy for a building. The heating or cooling energy delivered without consuming any fuel can be modelled by the Other Equipment object in EnergyPlus. An example of this object is shown below. The Fuel Type field specifies what kind of fuel is used to generate the heating or cooling energy. For the modelling of thermodiode this field should select None. The Zone or ZoneList Name field contains the name of the thermal zone that this thermodiode system serves. The actual energy input of the thermodiode system equals the product of the value of the Design Level field and the value of the schedule specified by the Schedule Name field (U.S. Department of Energy, 2016d). The Design Level Calculation Method field should select Equipment Level.

```
OtherEquipment,
    Thermodiode1,            !- Name
    None,                    !- Fuel Type
    living_unit1,            !- Zone or ZoneList Name
    Sch_Thermo,              !- Schedule Name
    EquipmentLevel,          !- Design Level Calculation Method
    1,                       !- Design Level {W}
    ,                        !- Power per Zone Floor Area {W/m2}
    ,                        !- Power per Person {W/Person}
    ,                        !- Fraction Latent
    ,                        !- Fraction Radiant
    ,                        !- Fraction Lost
    ,                        !- Carbon Dioxide Generation Rate {m3/s-W}
```

```
    General;                 !- End-Use Subcategory
```

There are two ways of changing the value of this object that is actually added to the heat balance of a thermal zone. The first way is to create two Other Equipment objects. One has a Design Level value of 1, the other has a Design Level value of –1. Then, we use the schedule value (always positive) to determine the amount of heating or cooling energy delivered to the thermal zone separately. A positive Design Level value denotes heat gain while a negative one denotes heat loss. Since the Design Level value is 1 or –1, the schedule value should be the number of watts of the thermal energy added to or removed from the thermal zone. The second way is to use an actuator (This actuator is the actuator in EnergyPlus terminology.) called Other Equipment. The control type is Power Level (in W). The value of this actuator is positive if heating energy is delivered and negative if cooling energy is delivered.

The calculation of the heat transfer rate of a thermodiode system can use a nodal model similar to the one presented in Section 1.3.5, as shown in Figure 27. In this model, $T_{o,r}$, $T_{o,db}$, T_{op}, T_{ip}, and T_i are outdoor mean radiant temperature, outdoor dry-bulb temperature, outdoor panel temperature, indoor panel temperature, and indoor temperature, respectively, °C; h_{eq} is the equivalent heat transfer coefficient of a thermodiode whose value hinges on T_{op} and T_{ip}, W/(m^2·K). The h_{eq} function of T_{op} and T_{ip} should be obtained through measurement or provided by the manufacturer of the thermodiode. The equation set is formulated in the same way as that in Section 1.3.5. Since the value of h_{eq} hinges on T_{op} and T_{ip}, an iterative approach should be used to solve the equation set. Therefore, it is recommended to use Matlab to calculate the heat transfer rate.

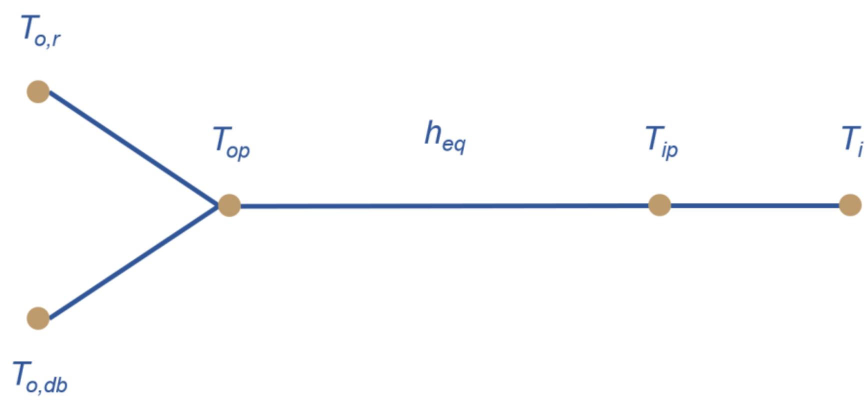

Figure 27 – The nodal model of thermodiode

3.4.2 Evaporative Cooling

There are a group of five objects in EnergyPlus that are used to model evaporative cooling systems, called Evaporative Cooler: Direct: CelDekPad, Evaporative Cooler: Direct: Research Special, Evaporative Cooler: Indirect: CelDekPad, Evaporative Cooler: Indirect: Wet Coil, and Evaporative Cooler: Indirect: Research Special, respectively. The first two are used to model DEC systems and the rest are used to model IEC systems. The additional functions of objects with Research Special in their names are that they allow the user to specify performance curves for cooler effectiveness, fan power, and pump power, and that the cooler's operating range can be controlled depending on the entering air dry-bulb and wet-bulb temperatures. The difference between the Indirect: CelDekPad object and the Indirect: WetCoil object is that the secondary air of the former first goes through an adiabatic evaporation process, then cools the supply air, while the secondary air of the latter evaporates and cools the supply air at the same time.

An example of the Evaporative Cooler: Indirect: Wet Coil object is shown below. Other objects can be set similarly. The Availability Schedule Name field contains the name of a schedule which defines when the evaporative cooler is available. A schedule value of 0 indicates that the evaporative cooler is off in the time step. A schedule value greater than 0 indicates that the evaporative cooler can operate in the time step. The Coil Maximum Efficiency field specifies the maximum efficiency of the cooler that is a combination of the efficiency due to the simultaneous heat and mass transfer on the outside of the tube and the efficiency of the heat exchanger. The Coil Flow Ratio is determined from performance data. The Coil Flow Ratio tells how quickly the efficiency of the stage would decrease with a mismatch of the supply and secondary flows.

```
EvaporativeCooler:Indirect:WetCoil,
    IndirectEvapCooler1,     !- Name
    Sch_1,                   !- Availability Schedule Name
    0.8,                     !- Coil Maximum Efficiency
    0.16,                    !- Coil Flow Ratio
    225,                     !- Recirculating Water Pump Power Consumption {W}
    1,                       !- Secondary Air Fan Flow Rate {m3/s}
    0.7,                     !- Secondary Air Fan Total Efficiency
    200,                     !- Secondary Air Fan Delta Pressure {Pa}
    EvapCoolerInletAirNode,  !- Primary Air Inlet Node Name
    EvapCoolerOutletAirNode,  !- Primary Air Outlet Node Name
    ,                        !- Control Type
    ,                        !- Water Supply Storage Tank Name
    ;                        !- Secondary Air Inlet Node Name
```

The M-cycle system cannot be modelled by a single object in EnergyPlus. The solution is to create three indirect evaporative coolers and one direct evaporative cooler and connect them in a way as shown in Figure 28. The wet-bulb effectiveness of this combined cooler can be greater than 1.

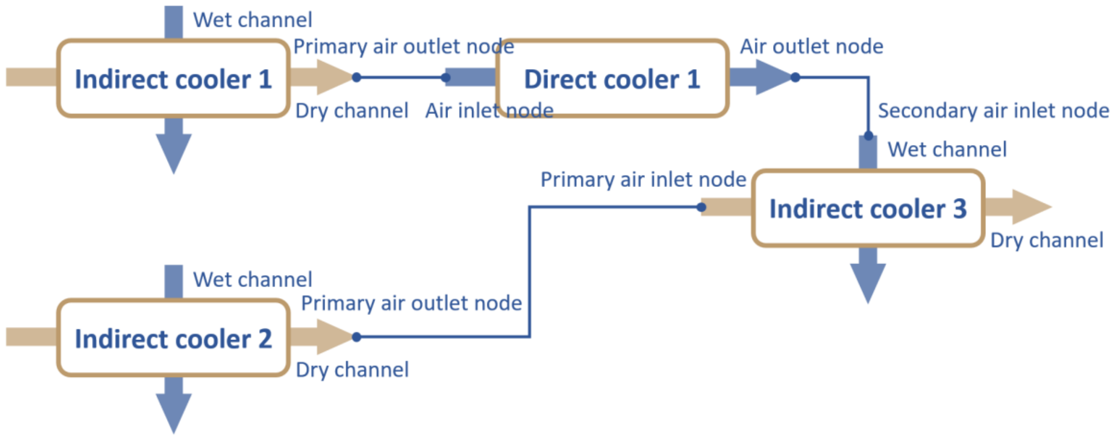

Figure 28 – The connection of three indirect evaporative coolers and one direct evaporative cooler to model an M-cycle system

CHAPTER 4. THE OPTIMIZATION OF ABE

This chapter answers research questions 4 and 5. In contrast to the design of a conventional exclusive building envelope that features high thermal insulation and airtightness, optimization is a critical step in the design of ABE to ensure that it realizes its full potential. This is because there are so many variables both in the design and operation stages of an ABE project that dictate the performance of the envelope. An ABE system usually consists of different parts with different functions and each part needs to be controlled with its own strategy. What makes the situation even more complicated is that the design parameters and operational parameters are sometimes coupled. Changing any design parameter will require the operational parameters to be changed as well in order to achieve the optimal performance, and vice versa. Instead of focusing on the optimization algorithm or the development of the toolchain, this chapter focuses on the formulation of the optimization problem, which has not been discussed systematically in the literature.

4.1 A Critical Review of Previous ABE Optimization Studies

4.1.1 Categorization of Previous ABE Optimization Studies

Numerous studies have been conducted in this field. Generally speaking, there are two approaches to the optimization of ABE, namely, the forward approach and the backward approach. In the forward approach, an ABE system is specified first in sufficient detail. Then optimization is performed for this system. In the backward approach, a group of properties of ABE are optimized first based on the boundary conditions and the requirements. Then a search for the specific ABE technology that best matches the optimized properties is performed. The transition from the forward approach to the backward approach is continuous. Between these two approaches, there are two intermediate approaches, the quasi-forward approach and the quasi-backward approach. The former is similar to the forward approach except for a certain level of abstraction in the specification of the ABE system, while the latter is similar to the backward approach except for some technological constraints on the variation of properties. The fundamental difference between them is that in the quasi-forward approach the abstraction does not go beyond the scope of a certain family of technology, while in the quasi-backward approach the constraints are not strong enough to specify the technology. These four approaches are explained in detail in Table 8 and Figure 29.

Table 8 – Explanation of the four approaches to the optimization of ABE

Approach	Description	Feasible region	Corresponding research
Forward	An ABE system is specified first in sufficient detail. Then optimization is performed for this system.	For design optimization, the feasible region is the set of all the available products. For operation optimization, the feasible region should be specified according to the operation characteristics of the system.	(Favoino et al., 2016; Gratia & De Herde, 2004; Hammad & Abu-Hijleh, 2010; Henze et al., 2004; Joe et al., 2014; Y.-J. Kim & Park, 2017; Ozel, 2011; Park et al., 2004)
Quasi-forward	This approach is similar to the forward approach except for a certain level of abstraction in the specification of the ABE system. The abstraction can only be made when several ABE systems have some characteristics or functions in common and there is no significant difference in selecting which of them.	For design optimization, the feasible region is bounded by the limit of existing technologies. For operation optimization, the feasible region should be specified according to the operation characteristics of the abstract system.	(Favoino, Jin, & Overend, 2017; Jin, Favoino, & Overend, 2017)
Quasi-backward	This approach is similar to the backward approach except for some technological constraints	The feasible region is bounded by the theoretical limit of technology. Similar to the backward approach,	(El Mankibi et al., 2015; Evins, 2015; Favoino et al., 2015; Hoffmann et al., 2014; Loonen et al., 2014; Saeli et

	on the optimization problem. The constraints are imposed in order to make the optimized properties more feasible and increase the possibility of finding the suitable technology.	there is no clear boundary between the design parameters and the operational parameters.	al., 2010; Ye et al., 2013; Zeng et al., 2011)
Backward	A group of properties of ABE are optimized first based on the boundary conditions and the requirements. Then, a search for the specific ABE technology that best matches the optimized properties is performed.	The feasible region is bounded by the physical laws. Since each design variable can be varied independently, there is no clear boundary between the design parameters and the operational parameters.	(Grynning, Gustavsen, Time, & Jelle, 2013; Kasinalis, Loonen, Cóstola, & Hensen, 2014; Long & Ye, 2014; Loonen, 2018; Mahdavi & Mahattanatawe, 2003; J. Wright & Mourshed, 2009; J. A. Wright, Brownlee, Mourshed, & Wang, 2014)

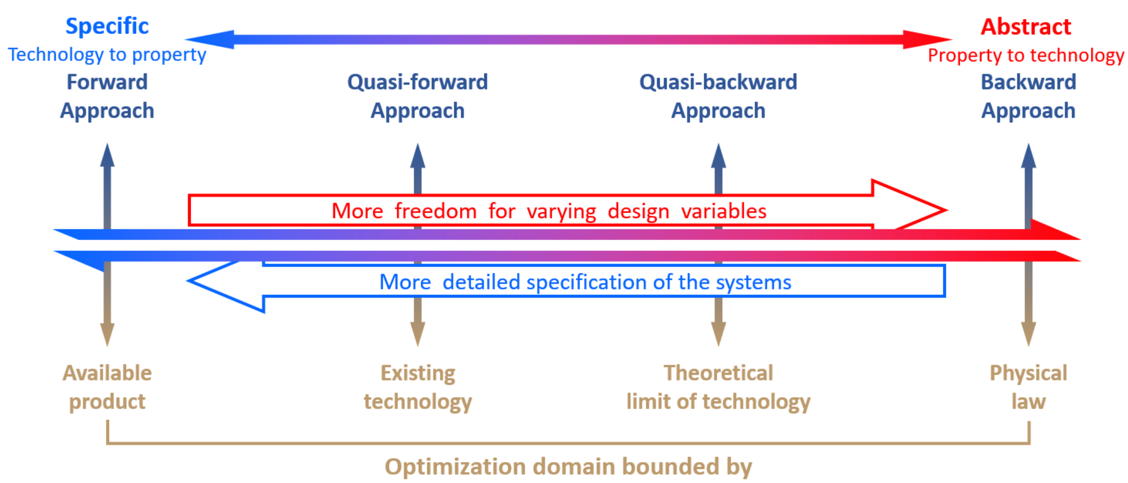

Figure 29 – The relationship between the four approaches to the optimization of ABE

As shown in Table 3, each family of ABE technologies is associated with a group of variables. These variables represent the properties that can be changed in the design and operation of an ABE system. However, the freedom of changing these variables in the optimization process depends on which optimization approach is adopted. The differences between different optimization approaches are explicated in Table 9.

Table 9 – The differences of the freedom of changing the design variables between different optimization approaches

Approach	Constraint	Example
Forward	The variation of variables associated with a particular system is constrained by the characteristics of the system or the available products on the market.	The U-factor, SHGC, and visible transmittance of windows are all tied to particular window options. Only a limited number of combinations of these properties exist.
Quasi-forward	The variation of variables associated with a family of technologies is constrained by the common characteristics of the family.	All dynamic insulation façades can be represented by a variable U-factor (Favoino et al., 2017).
Quasi-backward	The variation of variables is constrained by some technological features that are not strong enough to specify the type of technology.	When the visible transmittance and SHGC of a window are changed independently, the luminous efficacy (the ratio of visible transmittance to SHGC) is constrained by the proportion of energy contained in the visible spectrum to the total energy in the solar spectrum (41.5%) (Favoino et al., 2015).
Backward	All variables can be varied independently, and their variation is constrained by physical laws.	A façade is subdivided into a number of smaller elements. The solar transmittance and U-factor of each element are varied independently per hour over a period of time (Loonen, 2018).

4.1.2 Comments on Previous ABE Optimization Studies

As shown in Table 8, most ABE optimization studies adopted either forward approach or backward approach. The studies using forward approach are usually practical studies with the aim of optimizing a particular ABE system. There are no methodological flaws in this approach. However, this approach can only be used on a case-by-case basis—a particular optimization problem needs to be formulated and solved for each case—which is time-consuming and labor-intensive. In addition, the quality of the result heavily depends on the researcher's skill of specifying the ABE system and performing optimization. Thus, the conclusions of these studies usually lack generality and wholeness.

Using the backward approach, on the other hand, the result of a single study applies to a number of ABE technologies. Replacing the specific technologies with abstract properties of the building envelope has three advantages. Firstly, the conclusion drawn from such a study may apply to a large number of scenarios, making this method cost-effective in terms of input-output ratio. Secondly, this method makes it possible to perform optimization across different ABE technologies. The results of such studies can be seen as more global optima than those of studies using forward approach. Thirdly, this method can be used to analyze the performance that existing technologies are yet unable to achieve, thus guiding the development of new materials and systems.

Nevertheless, there are some methodological flaws in the backward approach. Since the backward approach assumes that each building envelope property can be varied independently and sometimes continuously, it is highly likely that there is no existing technology that can match the optimized properties. These studies may serve as good guidance for the conceptual design or operation of ABE, but they are of little use in practical scenarios. For example, in (Loonen, 2018) a façade was subdivided into a number of smaller elements. The solar transmittance and U-factor of each element were optimized independently per hour over a period of time. In practice no façade with such features can be constructed at present or in the near future. In (Grynning et al., 2013), an optimized window has a U-factor of 0.2 $W/(m^2 \cdot K)$ and an SHGC of 0.6. In theory, it is possible to create a window with such properties, but the required technological level far exceeds what is available at present. In (Zeng et al., 2011), the author optimized the specific heat of the thermal mass of a room in different temperature intervals. It was fortunate for the author to find that the optimal specific heat distribution was lumped into a narrow temperature interval that is similar to the characteristic of a PCM. If the optimal specific heat distribution has a peculiar form, the author will have a hard time trying to find the corresponding thermal storage materials. Furthermore, the assumption that the properties can be changed continuously is also questionable, as many practical systems, such as movable insulation, thermochromic window, and thermodiode, only have two status. Therefore, there is a clear gap between the results of these studies and the practical needs.

Besides the studies mentioned above, there is another class of studies that focus on the development of the toolchain that integrates different building performance simulation programs and the optimization program (Corbin, Henze, & May-Ostendorp, 2013; El Mankibi et al., 2015; Favoino et al., 2017; Favoino et al., 2015; E. C. Kerrigan, Bemporad, Mignone, Morari, & Maciejowski, 2000; Loonen, 2018; W. Wang, Rivard, & Zmeureanu, 2005). These implemental studies make it possible to solve complex optimization problems with multiple design variables, as a brute-force algorithm is too computation-intensive to solve these problems. Once an optimization toolchain is developed, it can be used universally, but the optimization problem still needs to be specially formulated in each particular case. Without correctly formulating the optimization problem, the optimized results are basically useless no matter which toolchain is used. However, there are few studies that focus on the formulation of optimization problems. This chapter is intended to fill this gap by developing a generic optimization framework for ABE.

4.2 A Generic Optimization Framework for ABE

As shown in Figure 30, this generic optimization framework for ABE has three levels. The first level is the application scenario. There are four application scenarios identified, which are product development, building design, building operation, and theoretical research. For each application scenario, there is a different series of implementation steps, which is shown in the second level. Among these steps, some are critical and have not been thoroughly discussed before. They will be the focus of this chapter and are highlighted by blue boxes in Figure 30. Others are either less important or have already been intensively discussed in previous studies and thus will not be the focus of this chapter. The third level is the implementation details of the implementation steps in the second level.

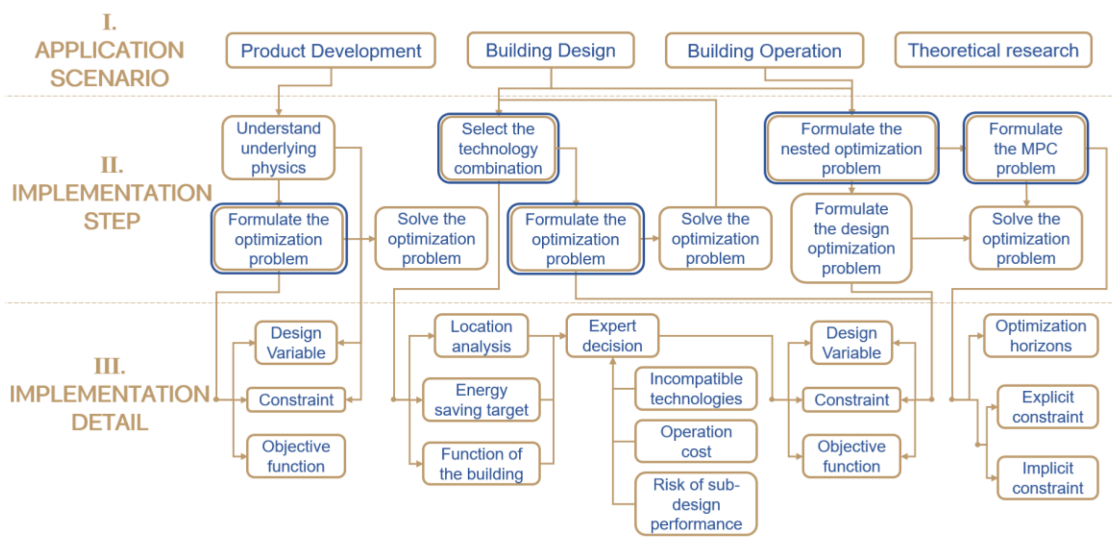

Figure 30 – A generic optimization framework for ABE (The focus of this chapter is highlighted by blue boxes.)

In the product development scenario, optimization is used to search for the optimal properties for a product that can be set as the target. In the building design scenario, one needs to select a set of ABE technologies and then optimize the design parameters of the building. In the building operation scenario, the control of ABE systems is optimized. In the theoretical research scenario, optimization research is performed to provide guidance for building conceptual design and show the right direction for future product development.

In the theoretical research scenario, since the studies are not intended to solve particular practical problems, their values cannot be measured from a practical point of view. The aforementioned weaknesses of the backward approach are not a concern in this case, while its advantages, such as generality and forward-looking power, can be exploited. Therefore, it is recommended to use the backward or quasi-backward approach. This scenario will not be the focus of this chapter.

A general optimization problem can be expressed in the following form (Snyman, 2005):

$$
\begin{aligned}
&\min_{\mathbf{x}} F(\mathbf{x}) \\
&\text{subject to} \\
&g_i(\mathbf{x}) \leq 0, \quad i = 1, 2, \ldots, n \\
&h_j(\mathbf{x}) \leq 0, \quad j = 1, 2, \ldots, m
\end{aligned}
\tag{10}
$$

where $F(\mathbf{x})$ is the objective function; $\mathbf{x}$ is the vector of design variables; $g_i(\mathbf{x})$ is the ith inequality constraint; $h_j(\mathbf{x})$ is the jth equality constraint.

4.3 Product Development

Optimization can be used to facilitate the development of new ABE products. The ABE products here refer to intrinsically controlled ABE systems and those extrinsically controlled ABE systems that are controlled with predetermined rule-based algorithms. These systems are ready to be used once they leave factory—all design and optimization processes are completed before the production process—whereas other ABE systems need to be designed and optimized along with the design of the building on a case-by-case basis.

Since no particular technology is specified before performing optimization and fewer constraints are imposed on the optimization problem, the backward approach has the ability to assess the performance of visionary and hypothetical products with properties that cannot yet be realized (Loonen et al., 2014). A number of studies using backward approach and quasi-backward approach claim that they can guide the development of new products (Hoffmann et al., 2014; Kasinalis et al., 2014; Long & Ye, 2014; Loonen, 2018; Saeli et al., 2010; Ye et al., 2013; Zeng et al., 2011). However, there are some weaknesses in these studies and the extent to which the backward approach can facilitate the development of new products should be carefully evaluated.

Firstly, the results of backward approach only tell us the goal that the developers should strive to achieve but give little information about how to achieve this goal. In most cases, it is far easier to set a target than to reach a target. Taking the development of a thermochromic window as an example, various simulation studies have shown that the optimal transition temperature is in the comfort zone (El Mankibi et al., 2015; Hoffmann et al., 2014; Long & Ye, 2014). How to effectively lower the transition temperature of VO_2 from 68°C to a temperature within the comfort zone is the key problem to be solved (S. Y. Li et al., 2012).

Secondly, there is a clear gap between the product developers and the building modelers. The specialties of product developers are usually manufacturing engineering, mechanical engineering, and material science, while those of building modelers are usually building construction, architecture, and thermal science. The research papers of ABE optimization are usually written and organized in a way that is easy for building modelers but difficult for product developers to understand. It is challenging for product developers to actively seek guidance from ABE optimization papers.

Thirdly, in some cases, such as those shown in Section 4.1.2, the optimized properties far exceed the capability of current technologies. It is impossible to actually create products with these properties at present or in the near future. This may not be a problem for theoretical research, but it is a serious problem for product development with a time limit. All companies develop new products in order to gain profit. Setting unrealistic goals for product development will lengthen the development cycle and increase the development cost significantly.

The National Aeronautics and Space Administration (NASA) introduced the concept of “technology readiness levels” (TRLs) and divided the whole development process of a novel technology into nine levels (Mankins, 2009), as shown in Figure 31. Different optimization approaches should be adopted for different TRLs. At an early research and development phase (TRL 1–5) (Loonen, 2018), the backward or quasi-backward approach is more helpful than the other two approaches, because these two approaches have fewer constraints and can provide insightful information on what an ideal product should look like. The optimization problems at this stage belong to the theoretical research scenario instead of the product development scenario. For product development at high TRLs (TRL 6–9), the backward and quasi-backward approaches have some weaknesses as discussed above. Thus, the forward or quasi-forward approach is more appropriate.

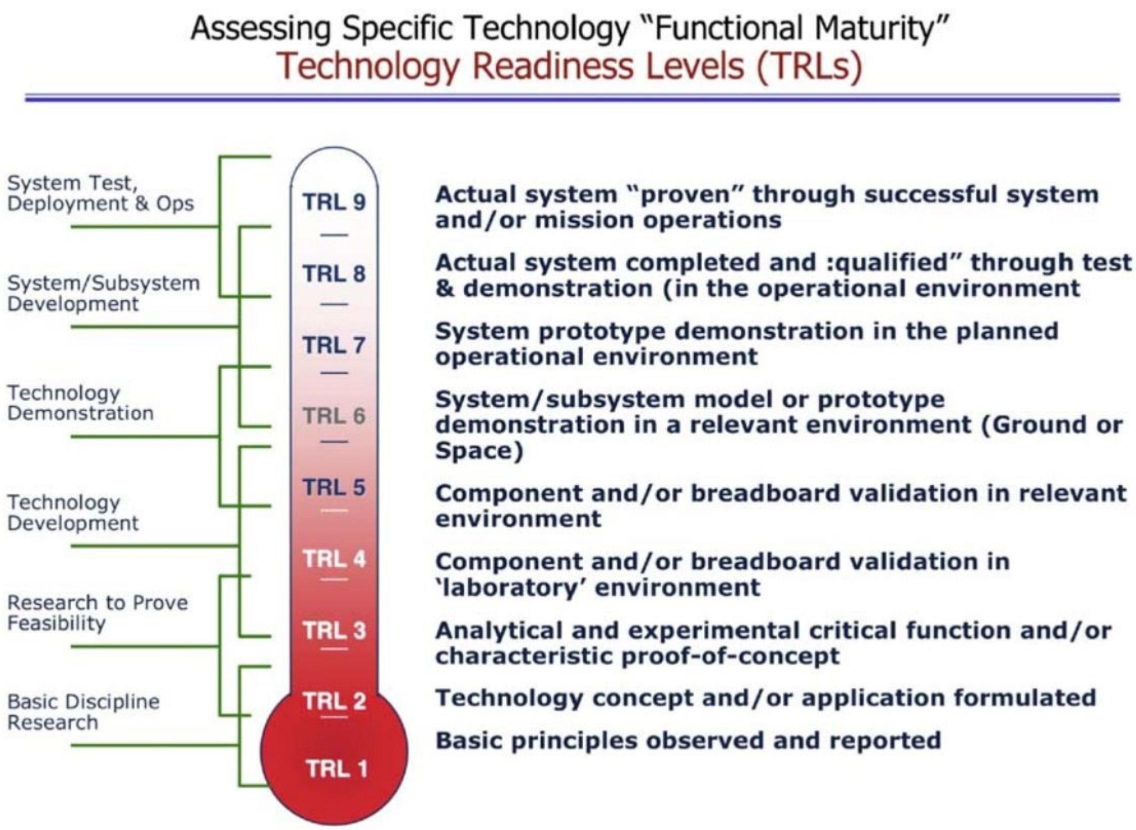

Figure 31 – Overview of the technology readiness level scale (Mankins, 2009)

This section presents a framework for the formulation of optimization problems at high TRLs. In this framework, the first step is to have a deep understanding of the underlying physics of the product. Researchers may either acquire the knowledge by themselves or collaborate with experts in the field. The importance of a deep understanding of the underlying physics will be seen in every part of this framework. The second step is to formulate the optimization problem correctly, which will be explained in detail later. The third step is to solve the optimization problem using an appropriate toolchain.

One of the critical differences between product development and building design is that the result of the former is usually supposed to accommodate a variety of situations, while the result of the latter usually only applies to one project. Therefore, the building model (including building type, building construction, schedule, climatic conditions, energy price, etc.) selected to evaluate the performance of the product needs to be representative of the target market.

4.3.1 Design Variable

Selecting the appropriate design variables is a key step to a successful optimization study. There are two types of design variables for product development, i.e., physical parameters and system properties. Physical parameters refer to those fundamental parameters in product design that can determine the properties of a product. Still using the example of the development of a thermochromic window, the physical parameters include the type of high-refractive-index dielectric coatings, state of VO_2 (nanoparticle or film), type of doped element, content of doped element, thickness of VO_2 layer, production method, number of glazing layers, type of filled gas, thickness of the gap, position of the thermochromic layer, etc. (Kamalisarvestani et al., 2013; S. Y. Li et al., 2012). System properties are the resultant properties of a product which are determined by the physical parameters. For example, the system properties of a thermochromic window include the transition temperature, U-factor, cold/hot state visible transmittance, cold/hot state solar transmittance, cold/hot state solar reflectance, cold/hot state infrared reflectance, solar heat gain coefficient (SHGC), etc.

Generally speaking, it is preferable to choose physical parameters as design variables, because they are what the developers truly manipulate. This is only going to work if the developer has a deep understanding of the underlying physics. However, if using system properties as design variables can provide certain benefits, such as reducing the computational complexity greatly, system properties should be chosen as design variables. Once the optimal system properties are obtained, a search should be conducted to find the corresponding physical parameters. Most previous product development studies used the backward approach and adopted system properties as design variables, which may not be the appropriate choice (Hoffmann et al., 2014; Kasinalis et al., 2014; Long & Ye, 2014; Loonen, 2018; Loonen et al., 2014; Saeli et al., 2010; Ye et al., 2013; Zeng et al., 2011). If physical parameters are chosen as design variables, the forward approach should be used. If system properties are chosen as design variables, the quasi-forward approach is recommended.

4.3.2 Constraint

The formulation of constraints also relies on a deep understanding of the underlying physics. According to their ranges, design variables can be categorized into technology-constrained ones and cost-constrained ones. The range of technology-constrained design variables is bounded on both ends. The bounds are determined by technological limits or physical laws. An example is the visible transmittance of a window, which is within the range of (0, 1). The range of cost-constrained design variables is bounded only on one end. The design variables can increase infinitely in theory on the other end because the value of these design variables is increased by means of addition or extension. An example is the R-value of a wall which can be increased infinitely by increasing the thickness of the insulation layer (Ozel, 2011). In practice, these design variables are usually constrained by the cost constraint imposed by the decision maker.

Physical parameters usually can be varied independently. The constraints on these parameters are formulated according to practical limitations. For example, increasing the doped content of Mg within a certain range can increase the visible transmittance monotonically. However, increasing the doped content of Mg beyond this range may incur undesirable consequences (S. Y. Li et al., 2012).

Since system properties depend on physical parameters, changing one physical parameter usually results in the variation of several system properties. For example, W doping in VO_2 will decrease the transition temperature of a thermochromic film and at the same time increase the visible transmittance (Granqvist, 2007). Also, applying low-e coatings to windows will simultaneously decrease the U-factor and visible transmittance (Hashemi & Gage, 2012). Therefore, most system properties cannot be varied independently. Proper constraints should be imposed to represent the correlation between them.

4.3.3 Objective Function

There can be one or more objective functions. If more than one objective function is adopted, the problem is usually called a multi-objective optimization problem. In a multi-objective optimization problem, conflicting objective functions are present, which means the value of one objective function can only be improved at the expense of the others. In this sense, the optimization problem transforms from a pure mathematical problem to a decision-making problem, as the trade-off between different objective functions hinges on the preferences of the decision-maker (Keeney & Raiffa, 1993). Based on how the preferences are articulated, the multi-objective optimization methods are divided into a priori articulation of preferences, a posteriori articulation of preferences, and no articulation of preferences (Marler & Arora, 2004).

A-priori-articulation methods allow the decision-makers to specify their preferences, which are usually expressed as some parameters to reflect the relative importance of different objectives. Using these parameters, the objective functions are combined into a utility function or transformed to one objective function with some constraints. Since the objective functions of a multi-objective optimization problem can be seen as a vector of objective functions and combining them into a utility functions is like the scalarization of a vector, this type of method is also called the scalarization method. Then, the optimization problem can be solved as one or a series of single-objective optimization problems. One of the most common a-priori-articulation methods is the weighted global criterion method. Its mathematical form is as follows:

$$Utility = \left\{ \sum_{i=1}^{n} {w_i}^p [F_i(\mathbf{x}) - F_i^o]^p \right\}^{\frac{1}{p}} \tag{11}$$

where *Utility* is the utility function; n is the number of objective functions; w_i is the weight of the ith objective function; $F_i(\mathbf{x})$ is the ith objective function, $\mathbf{x}$ is the vector of design variables; F_i^o is the utopia point; p is an exponent for a global criterion. The utopia point is defined as the point where all the objective functions are at their minima. If for $i = 1, 2, \ldots, n$, we choose $w_i = 1$ and $p = 2$, this method can be understood as finding the point that has the shortest distance to the utopia point. Another commonly used a-priori-articulation method is the weighted sum method. Its mathematical form is as follows:

$$Utility = \sum_{i=1}^{n} w_i F_i(\mathbf{x}) \tag{12}$$

It can be seen as a simplified version of the weighted global criterion method (Marler & Arora, 2004).

In contrast, in a-posteriori-articulation methods the preferences of a decision-maker are not articulated explicitly before running the optimization algorithm. Instead of generating only one optimal point that contains the preferences of the decision-maker, the a-posteriori-articulation methods provide the whole Pareto optimal set to the decision-maker. A point, $\mathbf{x}^* \in \mathbf{X}$, is Pareto optimal if there does not exist another point, $\mathbf{x} \in \mathbf{X}$, such that $\mathbf{F}(\mathbf{x}) \leqslant \mathbf{F}(\mathbf{x}^*)$, and $F_i(\mathbf{x}) < F_i(\mathbf{x}^*)$ for at least one function, where $\mathbf{X}$ is the feasible design space; $\mathbf{F}$ is the vector of objective functions. All Pareto optimal points constitute the Pareto optimal set (Keeney & Raiffa, 1993; Marler & Arora, 2004). After the whole Pareto optimal set has been obtained, the decision-maker can select a point from the set based on his/her preference. This method is more user-friendly as it circumvents the comparison of importance between different objective functions. The decision-maker can select the point with the most appealing objective function values or design variable values based on his preference, intuition, or experience directly. However, since all Pareto optimal points are generated, the a-posteriori-articulation methods are far more computation-intensive than the a-priori-articulation ones. The Pareto optimal set can be obtained using physical programming, normal boundary intersection method, normal constraint method, or genetic algorithm (Marler & Arora, 2004).

No-articulation methods can be seen as special cases of a-priori-articulation methods. In these methods, no parameters reflecting the decision-maker's preferences are required. The objective functions are combined into one objective function by performing some basic operations like summation and multiplication.

The scalarization of objective functions should be discouraged in the product development scenario unless reliable market research data are available. The weights in the scalarization methods are supposed to reflect the preferences of the decision maker. However, the weights assigned by product developers cannot faithfully reflect the preferences of the true decision maker, the consumer. A-posteriori-articulation methods or one objective function with multiple constraints are probably better options. The Pareto optimal set generated by a-posteriori-articulation methods can be used in the following market research. One objective function with multiple constraints guarantees that the product is superior to its counterparts on the market in some aspects and no worse than its counterparts in other aspects.

In terms of each single objective function, three types of values can serve as objective functions for product development optimization. The first one is system property. In this case, physical parameters are used as design variables and the objective is to achieve certain system properties by varying these physical parameters. For example, in the development of a thermochromic window, the objective function can be to maximize the cold state visible transmittance. The type of high-refractive-index dielectric coatings, the state of VO_2 (nanoparticle or film), doped elements and content, thickness of VO_2 layer, and production method can be chosen as design variables. Although choosing system properties as the objective function is simple and straightforward, it is not recommended by the author. There are several reasons. Firstly, using a single property as the objective function may lead to poor values of other properties. Secondly, even if multi-objective optimization is performed, the optimized properties may not perform as expected in the actual situation. Thirdly, this type of objective function can only be used in the optimization of a single ABE system. The interaction between different ABE systems is not taken into account. Therefore, investigating the optimization of ABE in practical situations is preferred.

The second type of objective function is building performance. In this case, the value of a building performance indicator in the actual situation, such as energy use intensity (EUI), thermal comfort criteria unmet hour, and daylight illuminance level at a certain point, is chosen as the objective function. Most optimization studies using backward approach adopt this type of objective function. This type of objective function reflects the performance of the product in practical applications, but cost is typically not considered. Therefore, the optimal solution may lead to an exorbitant cost.

The third type of objective function is monetary value, of which net present value (NPV) is an example. Using this type of objective function, the profit from improved performance is weighed against the additional investment. Thus, this is the most practical method for product development. To utilize a monetary value objective function, the researcher is required to not only have a deep understanding of the underlying physics but also have detailed information about the market conditions. This objective function can also be used to find out how the product should be priced in order to be competitive with similar products.

4.4 Building Design

The second and most common application scenario is building design. In this scenario, one needs to select a set of ABE technologies and then optimize the design parameters of the building and the design parameters of the ABE technologies selected. For the optimization of the design of buildings with optimized control, control optimization is contained in the design optimization. This case will be discussed in detail in the building operation scenario. All four approaches have been used by previous studies for building design. As explained in Section 4.1.2, the backward approach and quasi-backward approach have methodological flaws when used in practical situations. Thus, their usage is discouraged in the building design scenario. In contrast, the forward approach has methodological rigor and soundness but lacks generality and wholeness. For designers or engineers who are involved in an ongoing project, their task is to optimize the building and ABE systems that have already been specified by the architects or clients. The forward approach should be adopted. For designers or engineers who are involved in the planning or early design stage of a project, the quasi-forward approach should be adopted, as it is more general than the forward approach.

The first step of the optimization framework proposed here is to select a set of appropriate technologies. As shown in Table 2, there are various ABE technologies. Some of them take up the same position, some have similar functions, and others can work collaboratively. It is neither possible nor necessary to use all ABE technologies in one building. Selecting a set of appropriate ABE technologies is a critical step to a successful ABE application project. More than one technology combination may be selected as the candidates to be evaluated. The second step is to formulate the optimization problem. The third step is to solve the optimization problem. If more than one technology combination is selected, all combinations need to be optimized and their optimal objective function value should be compared to choose the best combination.

4.4.1 Selection of a Set of Technologies

This step is presented for designers or engineers who are involved in the planning or early design stage of a project. For designers or engineers who are involved in an ongoing project, this step may be skipped.

At present, the decision of selecting a set of appropriate technologies is made by experts. In the future, it is possible to leave this task to artificial intelligence. Before making the decision, preliminary analysis needs to be conducted to provide some essential information for the experts. Preliminary analysis includes location analysis, setting energy saving targets, and specifying the function of the building.

Location analysis includes climate analysis, potential analysis, and resource analysis. Climate analysis is conducted in every building design project. Important climatic factors, such as dry-bulb temperature, relative humidity, solar radiation, and wind speed and direction, should be extracted and visualized. Potential analysis is to analyze the energy saving potential of each weather variable in a location for a certain type of building using the method presented in CHAPTER 2. Resource analysis is to collect data on the local water quality and price, local energy (electricity, natural gas, etc.) price, and construction material price.

Energy saving targets should be set according to the requirements of the code or the clients. More radical energy saving targets usually need to be realized by more complicated and expensive ABE systems. The function of the building should be specified because different building functions have different requirements on daylight and comfort levels. For example, office buildings usually have higher requirements on the daylight control (sufficient daylight, no glare, continuous adjustment, etc.) than residential buildings.

Then, the information obtained in the preliminary analysis should be given to the experts who can synthesize all the information and combine this information with their expertise to make reasonable decisions. Such expertise includes incompatible ABE technologies, operation cost of each ABE technology, and risk of sub-design performance of each ABE technology. Incompatible technologies are those technologies that either cannot or should not be installed in the same position of a façade. They may be installed in different positions of building, but this is still discouraged considering the increased design, purchase, and installation cost. ABE technologies can be incompatible with each other for two reasons. The first is that they take up the same position. The second is that they have similar functions and adopting both of them will result in waste. The incompatible ABE technologies are summarized in Table 10.

Table 10 – Summary of incompatible ABE technologies

Technologies occupying the same position	
DSF	Adjustable louvers
DSF	Exterior movable insulation
DSF excluding box window	Radiative coating

DSF excluding box window	Dynamic façade
Adjustable louvers	Exterior movable insulation
Switchable window A	Switchable window B
Dynamic façade A	Dynamic façade B
Radiative coating A	Radiative coating B
Technologies with similar functions	
Switchable window	Adjustable louvers
Switchable window	Venetian blinds

Some operation cost is hard to be quantified in optimization, such as maintenance and cleaning cost. These costs should be estimated by the experts based on their experience and taken into account. The sub-design performance refers to the state of a system whose performance is worse than the expected performance due to malfunction or adverse influence of the environment. Generally speaking, systems with more movable or fine parts have higher risk of malfunction. And systems that have strict requirements on weather conditions are likely to be negatively influenced by the environment. It is recommended to replace these systems with more robust ones.

With all the information and their expertise, the experts are able to select one or several sets of appropriate ABE technologies to be optimized.

4.4.2 Design Variable

The optimization of the design of buildings with optimized control involves both design optimization and operation optimization. Correspondingly, the design variables can be divided into design parameters and operational parameters. The design parameters include the design parameters of the building and the design parameters of the ABE systems. The design parameters of the building include the geometry of the building, the window-to-wall ratio (WWR), etc. The design parameters of the ABE systems determine the variation range of the operational parameters and how they will be changed. For example, the configuration of the glazing system determines the upper limit of the U-factor of a window with movable insulation. The lower limit of the U-factor depends on the thickness and composition of the insulation layer and the airtightness of the insulation system. The U-factor of the window can only jump between the upper limit value and the lower limit value because the movable insulation only has two states, i.e., the open state and the closed state. The range of a design parameter can be either continuous or discrete, while that of an operational parameter can be continuous, multi-step, or binary.

4.4.3 Constraint

Similar to the product development scenario, the design parameters are also classified into technology-constrained and cost-constrained. For each ABE system, the operational parameters are constrained by the design parameters.

Other constraints include total cost, comfort level, daylight level, etc. It is worth noting that the constraints associated with building performance, such as comfort level and daylight level, are usually imposed on the building energy models and are not explicitly formulated in the optimization problem. For example, the comfort constraint is satisfied by maintaining the indoor air temperature within the comfortable range and the daylight constraint is satisfied by keeping the illuminance at a certain point below an upper limit. These constraints are called implicit constraints while those constraints formulated in the optimization problem are called explicit constraints.

The constraints expressed in the form of separate equations and inequations, as shown in Problem 10, are called hard constraints. For optimization algorithms, hard constraints cannot be violated in the slightest. Another type of constraints, called soft constraints, are adopted in some studies (Snyman, 2005). Soft constraints are most commonly used in control optimization problems where no feasible optimum can be obtained due to disturbances or inaccurate model parameters (Eric C. Kerrigan & Maciejowski, 2000; Mattingley, Wang, & Boyd, 2011). The way of applying soft constraints is to transform hard constraints into penalty terms and add them to the objective function to form a penalty function. In this sense, soft-constrained problems can be seen as a special type of multi-objective optimization problem. For Problem 10, the penalty function is as follows (Snyman, 2005):

$$F^*(\mathbf{x}) = F(\mathbf{x}) + \sum_{i=1}^{n} \alpha_i h_i^2(\mathbf{x}) + \sum_{j=1}^{m} \beta_j g_j^2(\mathbf{x}) \tag{13}$$

where $F(\mathbf{x})$ is the original objective function; α_i and β_j are penalty parameters. The values of the penalty parameters are assigned by the user. If the user wants to impose a hard constraint on the optimization problem—in which case little violation is allowed—a penalty parameter greater than certain lower bound should be selected (Eric C. Kerrigan & Maciejowski, 2000). In practice, an arbitrarily large penalty parameter can be used. If some degree of violation can be tolerated, a small penalty parameter can be selected (Corbin et al., 2013).

The application of soft constraints are demonstrated in some studies (Corbin et al., 2013; Loonen, 2018). There are three main reasons for using soft constraints. The first reason is that by adding soft constraints to the objective function, a constrained problem is transformed to an unconstrained problem, which can be solved by an unconstrained optimization algorithm (Snyman, 2005). The second reason is that in some cases the constraints associated with building performance do not need to be perfectly satisfied all the time. For instance, if the indoor air temperature is constrained between 22 and 24°C, extending this temperature range to 21.5–24.5°C will not even be noticeable to the occupants but may reduce the energy consumption greatly. Therefore, a trade-off needs to be made between the violation of a constraint and the improvement of the objective function in order to achieve better overall performance. The third reason is that soft-constrained problems are far less likely to become infeasible than hard-constrained ones.

4.4.4 Objective Function

As discussed in Section 4.3.3, there can be one or more objective functions. The methods for multi-objective optimization are the same as those introduced in Section 4.3.3. One thing to mention is that for operation optimization since it is impossible for the decision-maker to "manually" choose an optimal point from the Pareto optimal set at each step, only a-priori-articulation and no-articulation methods can be adopted (Favoino et al., 2017).

As for a single objective function, the objective function of a building design problem can be a subsystem objective function or an overall objective function. A subsystem objective function is a performance indicator of an ABE system and is used to optimize the performance of a single ABE system. For instance, for an evaporative cooling system the objective function can be the consumption of water, effectiveness, or cooling capacity (Rogdakis & Tertipis, 2015). In most cases overall objective functions are adopted. Similar to the product development scenario, the overall objective function can be divided into building performance and monetary value. Building performance objective functions include EUI, thermal comfort criteria unmet hour, daylight illuminance level at a certain point, etc. Monetary value objective functions include NPV, payback period, etc.

Objective functions and constraints are interchangeable. For instance, if daylight level is included in the objective function, it should not be used as a constraint anymore, and vice versa. Moreover, if one or more cost-constrained design variables are selected, a monetary value term should be used either as an objective function or as a constraint, or the optimization algorithm will not converge.

4.5 Building Operation

The third application scenario is building operation. In this scenario, two cases are considered. The first case, called “offline” optimization in the literature, is the optimization of the design of a building whose control also needs optimizing. The second case, called “real-time” or “online” optimization, is the control optimization of an existing building (Corbin et al., 2013). The second case can be seen as a sub-problem of the first case, as the in the first case both design optimization and control optimization are performed. In either case, the building itself and the ABE systems must be specified in sufficient detail before solving the control optimization problem. Thus, the forward approach is the only option. Nevertheless, there is a distinct difference between the two cases. Since the building in offline optimization is an imaginary building in the design stage, the computation time does not influence the optimization result. In contrast, the building in online optimization is a physical building in operation and the outputs of the optimization algorithm are directly sent to a building automation system or an actuator as control signals. Therefore, the computation time is restricted by the length of an execution horizon. The user needs to choose the appropriate building model and optimization algorithm in order to strike a balance between the simulation and optimization accuracy and acceptable computation time (Corbin et al., 2013; Loonen, 2018).

4.5.1 The Nested Optimization Framework

In the optimization of buildings with optimized control, both the design parameters and operational/control parameters need to be optimized. However, they are not optimized at the same level. As shown in Figure 32, nested optimization should be used to optimize the design parameters and control parameters. The optimization of design parameters is at a higher level than that of control parameters. In each iteration of the design optimization, a set of design parameter values are selected. These design parameters either influence the evaluation of the objective function of or set constraints on the optimization of control parameters. The control parameters are optimized for each time step over a period of time. For buildings with light-weight construction (e.g. glazing wall), the optimization only needs to consider the current time step and rule-based control (RBC) also works. For buildings with heavy-weight construction (e.g. concrete wall), the optimization needs to take the current time step as well as the following time steps (within a selected time horizon) into account due to the thermal storage effect of the construction. In this case, model predictive control (MPC) is required (Borrelli, Bemporad, & Morari, 2017). After the control parameters of all the time steps are optimized, the aggregate objective function values of all the time steps are used as the objective function value of the design optimization. The aggregation operation can be summation, integration, averaging, or finding the maximum/minimum value. Then, the design optimization proceeds to the next iteration. This process is repeated until the optimal design parameters are obtained. It can be seen that although control parameters are optimized in the process, the purpose of this nested optimization problem is to obtain the optimal design parameters. Control optimization is only a necessary step to achieve this goal. As will be shown in Section 5.3, poor designs with optimal control may outperform good designs with suboptimal control.

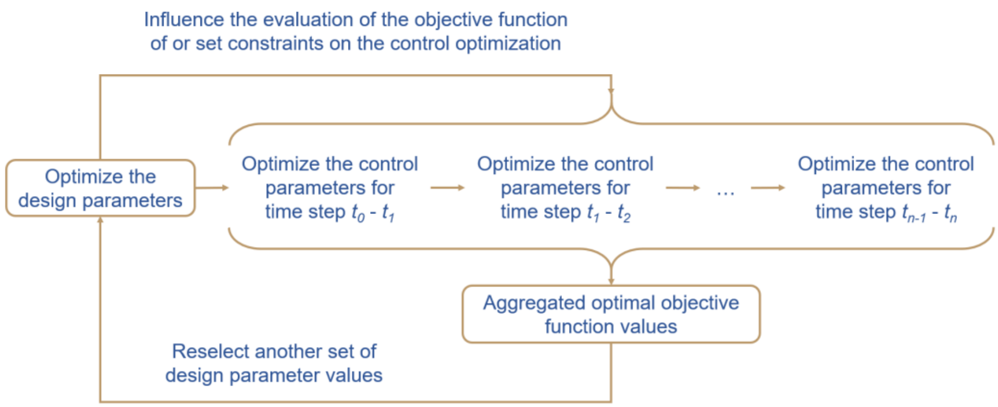

Figure 32 – The nested optimization framework for building design optimization

4.5.2 Model Predictive Control

4.5.2.1 Introduction

Model predictive control (MPC), also known as receding horizon control (RHC), is a feedback control strategy that solves an optimization problem at the current time step to determine a plan of action over a fixed time horizon. The first *N* inputs from this plan are executed. At the *N*th time step counting from the current one we repeat the planning process, solving a new optimization problem with the time horizon shifted *N* steps forward. The optimization problem takes into account estimates of future quantities based on available information at the current time step (Mattingley et al., 2011).

The most distinct difference between RBC and MPC is that the decision of the former is made only based on the measurements of the current and/or past states of the controlled system, while the decision of the latter relies not only on the measurements of current and past states of the controlled system, but on the prediction of the effect of the control action on future building states as well (Favoino et al., 2016). This feature of MPC makes it an ideal control strategy for building systems involving temporal energy shift, i.e., building energy storage systems. In a broad sense, buildings with heavy thermal mass and distributed energy generation systems (either stand-alone or connected to the grid) all belong to this category. MPC is also suitable for buildings located in the regions with variable electricity price. By properly arranging the power of the HVAC system in different time periods, a saving in total utility cost can be achieved (Killian & Kozek, 2016; Y. Ma, Kelman, Daly, & Borrelli, 2012).

The essential components of a model predictive controller used in buildings are (1) a dynamic building model, (2) predictions of the disturbances (e.g. weather variables, occupancy, etc.), (3) an objective function combining conflicting goals and constraints, and (4) a real-time optimization algorithm (Killian & Kozek, 2016). The greatest obstacle to the commercial application of MPC is the difficulty in constructing building models. The building models can be categorized into while-box models (physics-based), black-box models (data-driven), and grey-box models (a combination of white-box and black-box models) (Henze, 2019; Killian & Kozek, 2016). Among the three types of models, white-box models have a good prediction accuracy over a wide range of operating conditions but have to be constructed by experts in building simulation and take a great amount of engineering effort to construct and calibrate. Black-box models can be constructed automatically by programs using measured data as inputs but require long training and validation periods and are limited to building operation conditions covered during the training period (Killian & Kozek, 2016). Thus, currently there are no simple ways of obtaining widely applicable building models.

Another thing worth mentioning is that in MPC problems with hard constraints, often a disturbance drives the system into a region where the MPC problem is infeasible and hence no control action can be computed. The solution is to "soften" the constraints by adding slack variables to the objective function, as shown in Equation 13 (Eric C. Kerrigan & Maciejowski, 2000; Mattingley et al., 2011; Morari & H. Lee, 1999). An example of how hard constraints can make the problem infeasible will be presented in Section 5.3.

4.5.2.2 Optimization horizons

In MPC, there are several "horizons" that are of paramount importance in the formulation of the optimization problem. Their definitions are given below (Corbin et al., 2013):

- Planning horizon – The time horizon over which the control sequence is determined in each optimization step.
- Cost horizon – The time horizon over which the objective function is evaluated.
- Execution horizon – The time horizon over which the control sequence determined in the optimization problem is implemented. The rest of the control sequence is discarded. It is also the interval between two adjacent optimization steps.
- Termination horizon – When the cost horizon is longer than the planning horizon, the part of the cost horizon that does not overlap with the planning horizon is called

the termination horizon. Existence of termination horizon indicates that the effect of the control decisions extends beyond the end of the planning horizon.

- Pre-conditioning horizon – If the building model used in MPC is a commercial tool that does not allow the user access to the state variables, at the beginning of each optimization iteration a period of re-simulation using previous weather data and previously implemented control sequence is required to resume the thermal states of the model to the end of last optimization step.

The execution horizon should be no longer than the planning horizon, and the planning horizon should be no longer than the cost horizon. The relationship between different optimization horizons is shown in Figure 33.

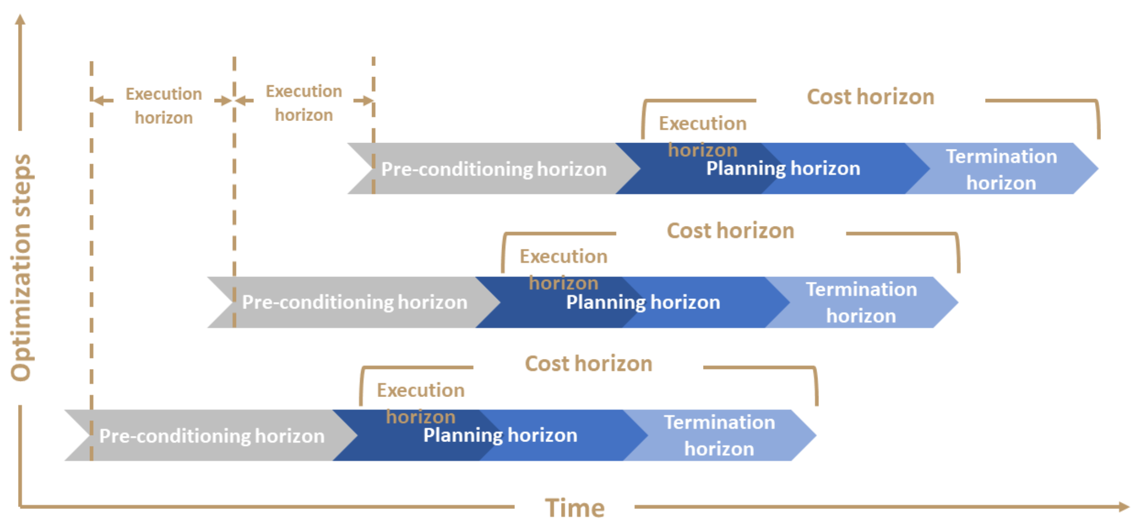

Figure 33 – Relationship between different optimization horizons (Corbin et al., 2013)

CHAPTER 5. APPLICATION STUDIES

So far, a generic framework for the formulation of ABE optimization problems has been presented. In order to enrich this framework and give the readers paradigms for using this framework, three application studies are presented, each corresponding to one application scenario. An overview is presented at the beginning of each application study to explain the purpose of the application study and how it is related to previous sections. The three application studies are summarized in Table 11.

Table 11 – Summary of the three application studies

	Application scenario	Design variable	Objective function
1.	**Building design**	· WWR · Type of glazing system · Thickness of the movable insulation layer	· EUI · LCC
2.	**Product development**	· Solar reflectance · Visible reflectance	· EUI · Useful daylight illuminance (UDI)
3.	**Building operation**	· SHGC of the insulation layer · U-factor of the insulation layer · Thickness of the concrete layer	· Total HVAC energy cost

5.1 Application Study 1: Optimization of a Façade with Movable Insulation

5.1.1 Overview

This application study is intended to enrich and serve as a paradigm for using the optimization framework in the building design scenario. To be specific,

- This application study adopts the forward approach as recommended by Section 4.4.

- Two types of objective functions (building performance and monetary value) as introduced in Section 4.4.4 are used in the two scenarios of this application study. For different objective functions, proper design variables as introduced in Section 4.3.1 are selected accordingly.
- This application study demonstrates how to revise the objective function if the optimization result is undesirable from a practical perspective. The revised objective function employs the scalarization technique of multi-objective optimization as introduced in Section 4.3.3.
- This application study demonstrates how to properly construct the cost model for a monetary value objective function based on real cost data.
- The result reveals two key features of ABE. Firstly, the prescriptive criteria in building codes do not apply to ABE. Secondly, ABE can reduce the sensitivity of building performance to design parameters of the building.

5.1.2 Problem Description

In this study, the south façade of a residential building with movable insulation will be optimized, while the rest of the façades remain unchanged. The reason for selecting movable insulation is that it is an ideal example of ABE's ability to block the adverse factors in the outdoor environment while admit the favorable ones. Optimization will be performed for two scenarios, either with a different objective function, as shown in Figure 34. The objective function of the first scenario is a building performance one, the energy use intensity, while that of the second scenario is a monetary value one, the life-cycle cost (LCC). For different objective functions, different design variables and constraints are selected accordingly. In the first scenario, after solving the original optimization problem it is found that the result is invalid from a practical perspective. Therefore, the objective function of the problem is revised, and a second round of optimization is performed. In practice, the optimization of ABE should often be conducted in an iterative manner, because it is very difficult to directly formulate the problem perfectly at the beginning. Improper formulation of the problem will lead to results that are valid from a mathematical perspective but invalid from a practical perspective. In these cases, the formulation has to be revised and then another round of optimization needs to be performed.

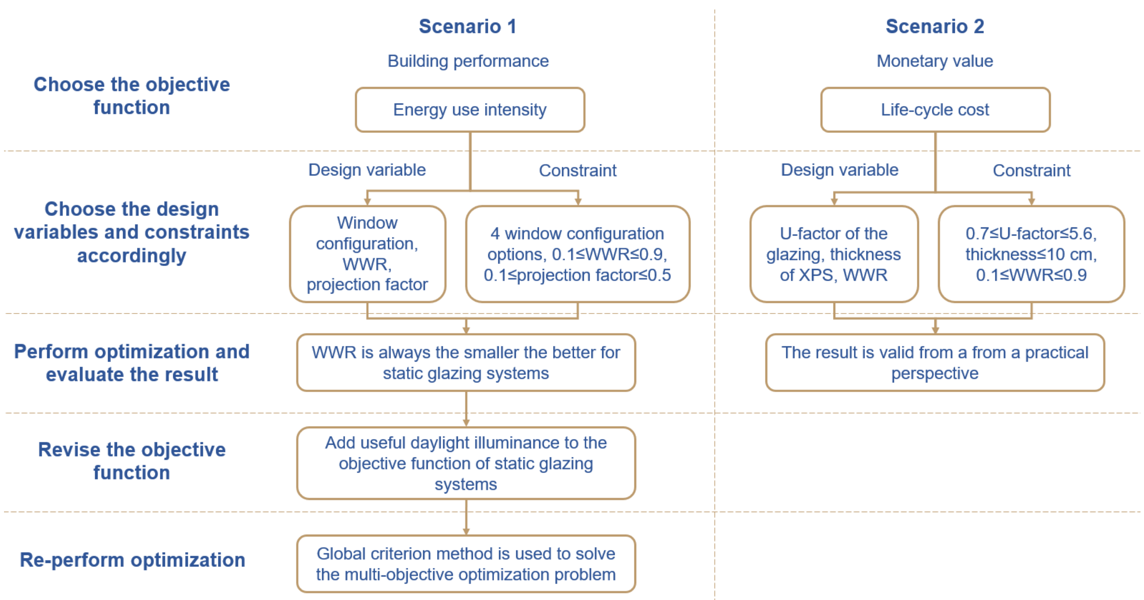

Figure 34 – Structure of application study 1

5.1.3 The Building Model of This Study

The residential prototype building model developed by PNNL is adopted for this application study (Pacific Northwest National Laboratory, 2013). The location of the building is Atlanta, Georgia. The only change made to the prototype building model is the geometry conversion from a two-story building to a one-story building, so that there is only one window on each façade. This change is done in OpenStudio (National Renewable Energy Laboratory, 2019), and will greatly reduce the difficulty of altering the model in the optimization process. The building model after conversion is shown in Figure 35. The north, east, and west façades have a fixed WWR of 30%, while the south window has a fixed height and a variable width, as shown in Figure 36. An overhang is placed over the window on the south façade. Other windows only have interior blinds. The construction of the building is compliant with 2012 International Energy Conservation Code (IECC) (International Code Council, 2011). The cooling setpoint is constantly 23.88°C and the heating setpoint is constantly 22.22°C. There are three occupants living in this building. The details of lighting schedule, electric equipment schedule, and gas equipment schedule can be found in (Pacific Northwest National Laboratory, 2013). The heating source of the HVAC system is a gas furnace.

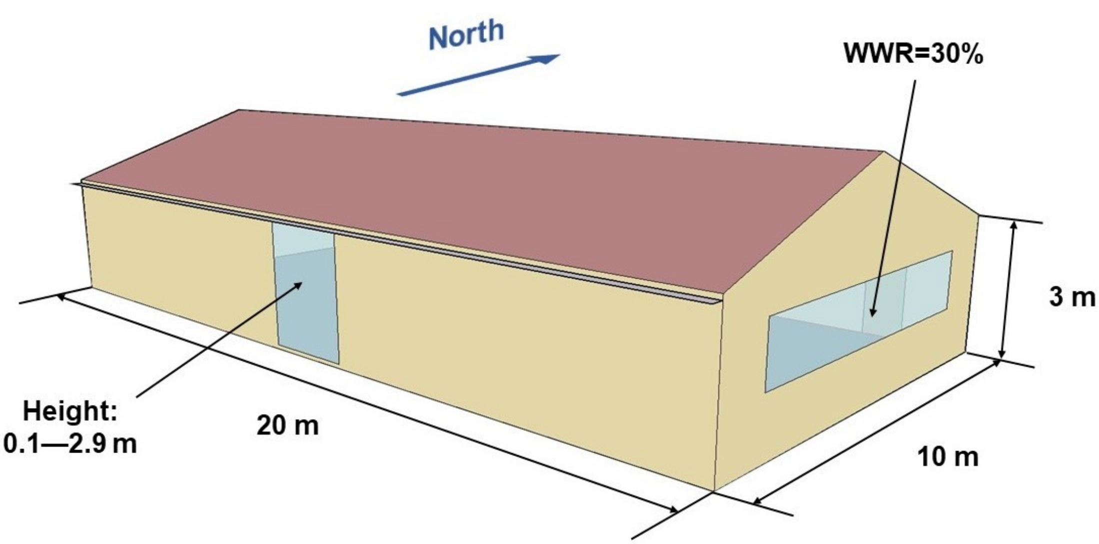

Figure 35 – The residential building model used in application study 1

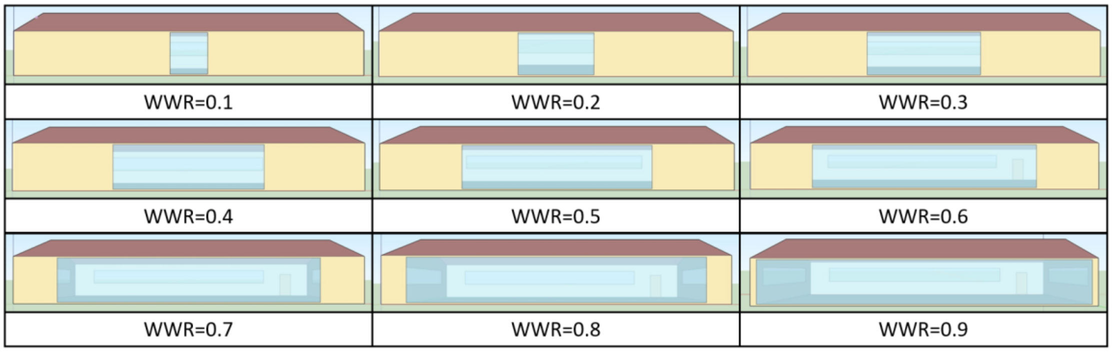

Figure 36 – Different layouts of the south façade

5.1.4 Formulation of the Optimization Problem

Table 12 – Formulation of the optimization problem of application study 1

Scenario 1		**Scenario 2**	
Objective function	Energy use intensity	**Objective function**	Life-cycle cost
Design variable	Window configuration	**Design variable**	U-factor of the glazing
	WWR		Thickness of XPS
	Projection factor		WWR
Constraint	Options of window configuration: double glazed window, triple glazed window, single glazed window + movable insulation, double glazed window + movable insulation	**Constraint**	0.7 W/(m^2·K) $\leq$ U-factor of the glazing $\leq$ 5.6 W/(m^2·K)
	$0.1 \leq$ WWR ≤ 0.9		Thickness of XPS $\leq$ 10 cm
	$0.1 \leq$ Projection factor ≤ 0.5		$0.1 \leq$ WWR ≤ 0.9

The formulation of the optimization problem of application study 1 is shown in Table 12. The assumption is that movable insulation has been selected by an expert as the

ABE technology for consideration due to its low cost and great potential to reduce cooling/heating need. Conventional static windows will also be included in the comparison.

In scenario 1, the objective function is the source energy use intensity in kWh/(m^2·year), which is calculated as follows:

$$\mathrm{EUI} = \frac{R_{grid}\left(E_c + E_f\right) + R_{ng} \cdot E_h}{A_f} \tag{14}$$

where R_{grid} and R_{ng} are the source-site ratios for grid electricity and natural gas, respectively (R_{grid} = 2.80 and R_{ng} = 1.05 from (Energy Star, 2018) is used); E_c is the annual electricity consumption for cooling, kWh; E_f is the annual electricity consumed by fans in the HVAC system, kWh; E_h is the annual natural gas consumption for heating, kWh; A_f is the total floor area of the buildings, m^2.

The design variables selected in this scenario are window configuration, WWR, and projection factor. Window configuration is a design parameter of the ABE system, while WWR and projection factor are design parameters of the buildings. For window configuration, there are four discrete values to choose from, which are double-glazed window, triple-glazed window, single-glazed window + movable insulation, and double-glazed window + movable insulation. Although the single-glazed window is not a viable option for buildings compliant with the prescriptive envelope criteria of ASHRAE 90.2 anymore (American Society of Heating Refrigerating and Air-Conditioning Engineers, 2007), combining single-glazed windows with movable insulation may yield a solution that has better performance than the windows compliant with ASHRAE 90.2 do. The design of the insulation layer should take durability, fire-resistance, mold-resistance, light weight, strength, health issue, and economy into account. The insulation layer is placed on the outside of the glazing because the thermal resistance of the insulation is far higher than the glazing. If it is placed on the inside of the glazing, moisture would enter the space between the insulation and the glazing and condense, thus causing mold problem. The insulation layer used in this study comprises from outside to inside a layer of aluminum foil, a 4-cm-thick extruded polystyrene layer, a 1-cm-thick gypsum board, and a layer of latex paint. The aluminum foil not only protects the insulation layer from weathering but also reduces the radiation heat transfer with its low emissivity. The data of the material properties are from ASHRAE Handbook Fundamentals (American Society of Heating Refrigerating and Air-Conditioning Engineers, 2013). The calculated total R-value of this insulation layer is 1.40 $m^2 \cdot K/W$. Based on ISO 10077-1 (International Organization for Standardization, 2006), the total U-factor of the window with an additional insulation layer is calculated by:

$$U_t = \frac{1}{\frac{1}{U_g} + 0.95 \times R_I + 0.17} \tag{15}$$

where U_g is the U-factor of the glazing layer, $W/(m^2 \cdot K)$; R_I is the thermal resistance of insulation layer, $m^2 \cdot K/W$. The properties of different window configurations are shown in Table 13. Since EUI is a building performance objective function and there is no constraint on the total cost, cost-constrained design variables (e.g. the thickness of insulation layer) should not be adopted. Therefore, an insulation layer with a typical thickness is used in this scenario. WWR is the ratio of the total area of the windows on a façade to the total area of the façade. In this application study, the WWR takes the values from 0.1 to 0.9 with a step of 0.1. Projection factor is the ratio of the length of the overhang to the vertical distance from the overhang to the sill. In this application study, the projection factor takes the values from 0.1 to 0.5 with a step of 0.1.

Table 13 – The properties of different window configurations in scenario 1

Window configuration	Single-glazed	Double-glazed	Triple-glazed	Single-glazed with insulation	Double-glazed with insulation
U-factor [W/(m²·K)]	4.5	1.99	0.7	0.58	0.5
SHGC	0.25	0.25	0.25	0.03	0.03
T_{vis}	0.57	0.45	0.4	0	0

In scenario 2, the objective function is the life-cycle cost (LCC) of the façade, which is calculated as the sum of the initial investment in the façade and the operation cost of the HVAC system for the next 25 years. The selection of 25 years is due to the fact that customers are expecting warranties of 20 years for window products (Sbar et al., 1999), which means the lifespan of a window should be longer than 20 years. The initial investment in the façade includes the investment in the glazing, insulation layer, control system of movable insulation, and wall. It is very difficult for researchers in academia like the author to get the accurate cost of the materials, equipment, and labor. Therefore, the estimation of the investment in the façade is based on the data mainly from (Plotner, Babbitt, Charest, Elsmore, & Gomes, 2015) and partly from journal papers and Alibaba.com.

Although LCC contains the trade-off between the initial investment and the operation cost, the real situation is far more complicated than just adding the initial investment and the operation cost up. Firstly, all investments involve an element of risk. In the calculation of operation cost, we use a discount rate to represent the decreasing value of money spent in the future to the decision maker. Many other factors may also depreciate future savings or earnings, such as inflation and the decrease of energy prices. Even if the investment in an advanced façade is bound to be profitable, it is still a failed investment if investing elsewhere has a higher rate of return. Secondly, the decision maker may not be the one who pays the energy bills. In this application study, the decision maker is the developer or the owner of the house. The developer is mainly concerned about the initial cost of the house in order to boost sales and increase profits. The owner will not care about the energy bills if he rent the house to others and the tenants will pay the energy bills. It is also possible that the decision maker does own and live in the house, but he moves away and sells the house a few years later, which makes the operation cost less relevant to him. Therefore, LCC is not a universally applicable monetary value objective function. It is only used as an illustrative example here. In real situations, the decision maker should make a comprehensive assessment of all the risks and possibilities before making the decision.

If a renovation project instead of construction project is considered, another monetary value called payback period could be chosen as the objective function. The payback period refers to the amount of time required to recover the cost of an investment. Since investing in ABE systems does not generate profits, we need to compare the (additional) investment with the saved energy cost relative to a baseline case in order to obtain the payback period.

The design variables in this scenario are U-factor of the glazing, thickness of extruded polystyrene (XPS), and WWR. The first two are design parameters of the ABE system, while the last one is a design parameter of the building. The U-factor of the glazing takes the values 0.7, 1.24, 1.99, 3.2, 4.5, and 5.6 W/($m^2 \cdot K$), which represent the U-factor of a high-end triple-glazed window, a low-end triple-glazed window, an average double-glazed window, a low-end double-glazed window, a high-end single-glazed window, and a low-end single-glazed window, respectively. The thickness of XPS takes the values 1, 2, 4, 6, 8, 10 cm, and the resultant R-value of the insulation layer is 0.40, 0.73, 1.40, 2.06, 2.73, and 3.40 $m^2 \cdot K/W$, respectively. The values of WWR are the same as those in scenario 1.

Since we want to see the value of the objective function over the whole design space and computation time is not a main concern, brute-force search is adopted to solve the optimization problem.

5.1.5 Control of Movable Insulation

Since the building considered is a residential building with light-weight construction, RBC instead of MPC is adopted for movable insulation which can shorten the time required for solving the optimization problem significantly. A control system as shown in Figure 37 is used for the control of movable insulation. The outdoor and indoor thermometers measure the outdoor and indoor dry-bulb temperatures, respectively. The pyranometer measures the incident solar radiation (both direct and diffuse) on each window. The black bulb temperature sensor measures the mean radiant temperature of the environment surrounding each window. When the sun is shining, the black bulb temperature sensor should be shaded from the sun or just simply disabled. The reason for adding the long-wave radiation term to the heat balance equation is that during clear nights, the sky has a strong cooling effects on the window. However, during clear days, sunshine is the dominant factor and direct exposure to sunlight will cause the black bulb temperature sensor to malfunction. The infrared detector detects the presence of occupants. The access to daylight is given priority over building load reduction. Thus, the movable insulation will remain open as long as the house is occupied and the incident solar radiation on the window exceeds 20 W/m^2. The user input information, including the cooling and heating set points, window U-factor, window average transmittance, window average absorptance, and window outside face emissivity, is used to calculate the energy balance of the window. If the window average transmittance and window average absorptance are not available, the user can simply input the SHGC and the system will estimate these values using the method explained in (Arasteh, Kohler, & Griffith, 2009). The control step is set as 15 minutes.

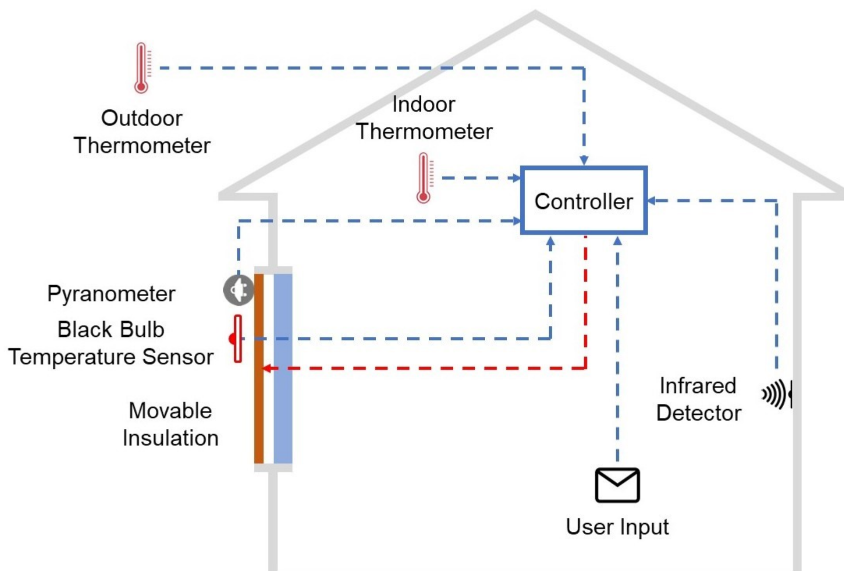

Figure 37 – The control system for movable insulation

The control algorithm is based on the energy balance calculation of the window. The method employed in this study is similar to that used by EnergyPlus (U.S. Department of Energy, 2016b). The diagram of the heat balance calculation when the movable insulation is open is shown in Figure 13. In this model, we consider the glazing system as an equivalent single layer. The equivalent thermal conductance U_{eq} is calculated according to (Arasteh et al., 2009). The portion of incident solar radiation absorbed by the glazing system is split equally and added to surface 8 and surface 9. The heat balance equations for surface 8 and surface 9 are as follows:

$$h_{or}\left(T_{o,r} - T_8\right) + h_{oc}\left(T_{o,db} - T_8\right) + U_{eq}(T_9 - T_8) + \frac{1}{2}Ab_{sol}I_{sol} = 0 \qquad (16)$$

$$h_i(T_i - T_9) + U_{eq}(T_8 - T_9) + \frac{1}{2}Ab_{sol}I_{sol} = 0 \qquad (17)$$

where h_{or} is the equivalent outside radiation heat transfer coefficient and is calculated by $h_{or} = \sigma\varepsilon_8\left(T_{o,r}^2 + T_8^2\right)\left(T_{o,r} + T_8\right)$, W/(m^2·K); $T_{o,r}$ is the mean radiant temperature of the exterior environment, K; $T_{o,db}$, T_8, T_9, and T_7 are the outdoor dry-bulb temperature, temperature of surface 8, surface 9, and indoor environment, respectively, K; Ab_{sol} is the solar absorptance of the glazing; I_{sol} is the incident solar radiation, W/m^2; h_{oc} is the outside surface convection heat transfer coefficient, W/(m^2·K); h_i is the inside surface heat transfer coefficient, which takes both convection and radiation into account, W/(m^2·K). From Equations 16 and 17 we can solve for the temperatures of surface 8 and surface 9 and then the conduction heat flux through the window is calculated by:

$$Q_{c0} = U_{eq}(T_8 - T_9) \qquad (18)$$

The solar radiation transmitted through the window is calculated by:

$$Q_{s0} = Tr_{sol} I_{sol} \tag{19}$$

where Tr_{sol} is the solar transmittance of the glazing, which depends on the incident angle and temperature. Here a constant average value is used. The total heat transfer rate through the window when the movable insulation is open is as follows:

$$Q_0 = Q_{c0} + Q_{s0} \tag{20}$$

When the movable insulation is closed, the transmittance of window is reduced to 0. All the absorbed solar radiation should be added to surface 8. The conduction heat flux through the window in this case, Q_1, can be calculated using similar heat balance equations.

When $T_{in} > 23.4$°C, the control system will compare Q_0 and Q_1 and choose the smaller one as the movable insulation status to reduce heat gain through the window. When $T_{in} < 22.7$°C, the control system will choose the greater one of Q_0 and Q_1 as the movable insulation status to increase heat gain through the window. The reason why the control of movable insulation uses 22.7°C and 23.4°C instead of 22.22°C and 23.88°C as thresholds is that with the HVAC system working properly, the indoor temperature will fluctuate slightly around 22.22°C when heating is on and 23.88°C when cooling is on. The adoption of 22.7°C and 23.4°C as thresholds will ensure that load reduction is always effective when the HVAC system is on. It should be noted that the movable insulation only has two statuses, on and off. This is because partially opening the movable insulation will make it lose its airtightness, in which case the movable insulation becomes an ordinary shutter.

The Energy Management System actuator: Construction State in EnergyPlus is used to simulate the control of movable insulation (U.S. Department of Energy, 2016a). This actuator is able to reselect the construction state of a building surface according to a control program during the simulation. The control program is written in the EnergyPlus Runtime Language (U.S. Department of Energy, 2016a). At the beginning of each time step, the construction state of the window on the south façade is reset. Then, the simulation is performed.

5.1.6 Results of Scenario 1

The EUI colour map for static windows is shown in Figure 38. The x-axis is WWR and the y-axis is projection factor. Both windows have the same optimal point, (WWR = 0.1, projection factor = 0.4). For both windows when WWR is between 0.1 and 0.8, EUI decreases almost linearly with the decrease of WWR and EUI is insensitive to projection factor. When WWR is greater than 0.8, greater projection factor leads to lower EUI. Overall, the triple-glazed window has better energy performance than the double-glazed window and the difference increases with the increase of WWR.

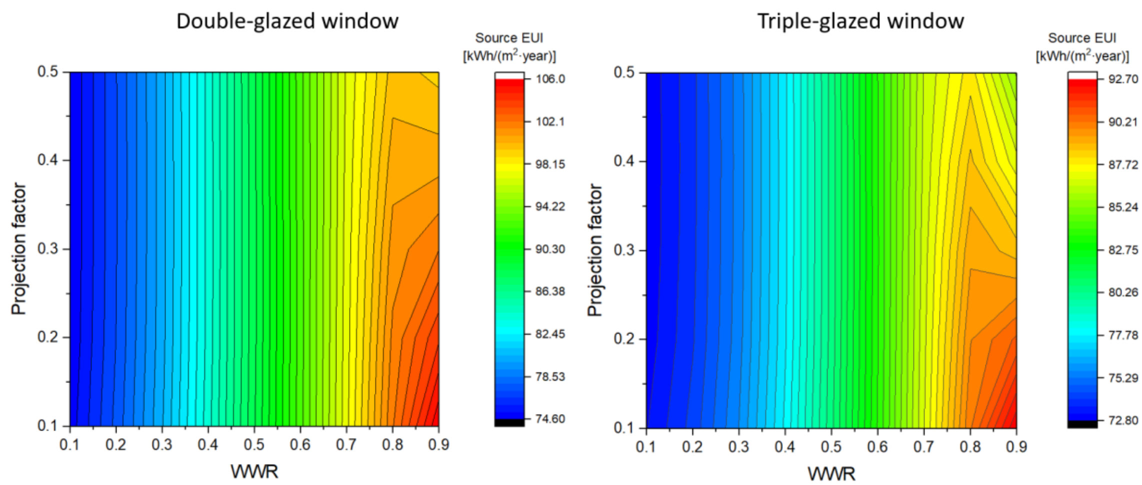

Figure 38 – The EUI colour map for static windows

From a practical perspective this optimization result is invalid, because although an extremely small window area or even no window at all is good for energy conservation, it is unable to meet the occupants' need for daylight and view to the outside. Therefore, this design strategy cannot be implemented in real situations. The reason for this invalid result is the flawed formulation of the optimization problem. To solve this problem, a term reflecting the occupants' need for daylight or view to the outside should be added to either the constraint or the objective function. After the formulation is revised, optimization should be re-performed.

The EUI colour map for windows with movable insulation is shown in Figure 39. For the single-glazed window with movable insulation the optimal point is the same as that for static windows, (WWR = 0.1, projection factor = 0.4), and the changing trend of EUI is also similar to that for static windows. The main difference between this window and the static windows is that the range of EUI for this window is much narrower than the static windows. The lowest EUI for this window is 73.15 kWh/(m^2·year), which is close to that for the triple-glazed window, 72.80 kWh/(m^2·year). However, the highest EUI for this window is only 82.30 kWh/(m^2·year), while that for the triple-glazed window is as high as 92.70 kWh/(m^2·year). This result gives us two important pieces of information. The first is that although a single-glazed window alone is not allowed by the prescriptive envelope criteria of ASHRAE 90.2 (American Society of Heating Refrigerating and Air-Conditioning Engineers, 2007), the energy performance of a single-glazed window with movable insulation is as good as or even better than that of a triple-glazed window. This means that the prescriptive criteria in building codes do not apply to ABE, and performance-based criteria should be adopted instead (Foliente, 2000). The second is that ABE systems (movable insulation) can reduce the sensitivity of building performance (EUI) to design parameters (WWR) significantly, which gives building designers more freedom to change the design parameters of the building without worrying too much about its performance. This conclusion is also supported by the result in Section 5.3.7.

For the double-glazed window with movable insulation, the situation is quite different. The optimal point is (WWR = 0.3, projection factor = 0.3), which shows that the superior thermoregulation ability of this window can compensate for its lower R-value compared to the wall. This design, (WWR = 0.3, projection factor = 0.3), not only achieves the optimal energy performance, but also meets the occupants' need for daylight and view to the outside. The difference in the changing trends of EUI with WWR between the two windows with movable insulation is probably because the thermal insulation of the single-glazed window is so bad that in the heating season movable insulation has to be closed for most of the time and the window cannot exploit free solar energy. In this sense, the window works like an opaque wall but with a lower R-value than the actual wall. Thus, the smaller

WWR, the better the overall thermal insulation of the façade. This explanation is supported by two pieces of evidence. The first is that the difference in heating energy consumption between the single-glazed window and double-glazed window dominates the difference in EUI between the two windows. For example, for the case (WWR = 0.5, projection factor = 0.3), the difference in electricity consumption (cooling + fan) is 108.5 kWh, while the difference in natural gas consumption is 880.7 kWh. The second is that on average movable insulation is open for 36.2% of the time in a whole year for the single-glazed window, while it is open for 39.2% of the time in a whole year for the double-glazed window. This means that the double-glazed window with movable insulation can better utilize solar energy to heat the building in the heating season.

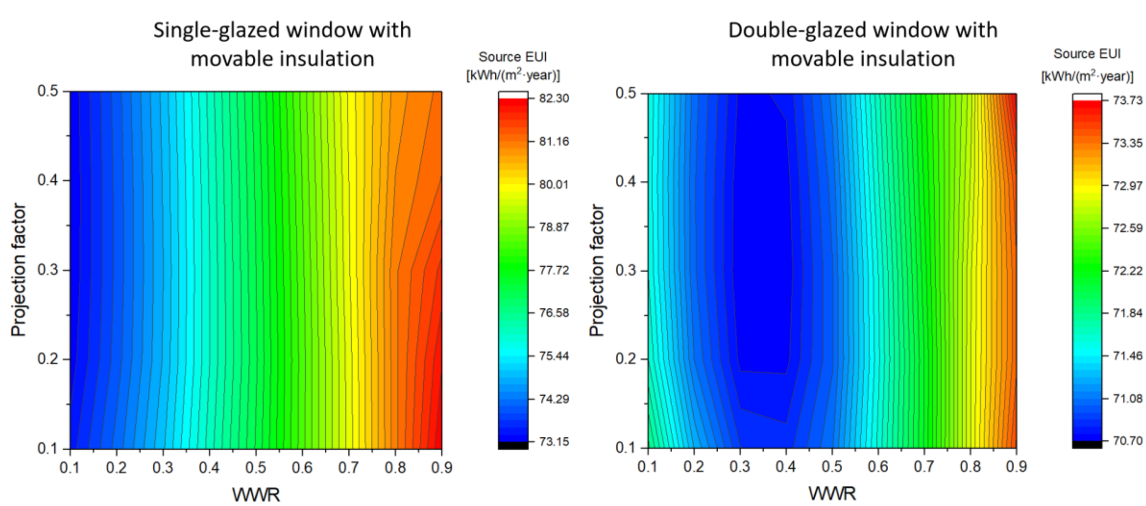

Figure 39 – The EUI colour map for windows with movable insulation

5.1.7 Revision of the Formulation of the Optimization Problem

As shown in the last section, for static windows the smaller the WWR, the lower the EUI, which is undesirable from a practical perspective. In this section, we will revise the formulation of the optimization problem by adding a term reflecting the occupants' need for daylight to the objective function. Useful daylight illuminance (UDI) is adopted as the indicator of daylight quality, which is defined as the percentage of time in the day in a whole year when the daylight illuminance of a point falls within the useful range (Nabil & Mardaljevic, 2006). The useful range is defined by the user, which in this case is 300–2000 lux. The illuminance at 30 points in the working plane are measured, as shown in Figure 40, and the average UDI of these points is used as the indicator of daylight in the objective function. The average UDI colour map for the double-glazed window is shown in Figure 41, and that for the triple-glazed window is similar to this. We can see that the average UDI increases with the increase of WWR.

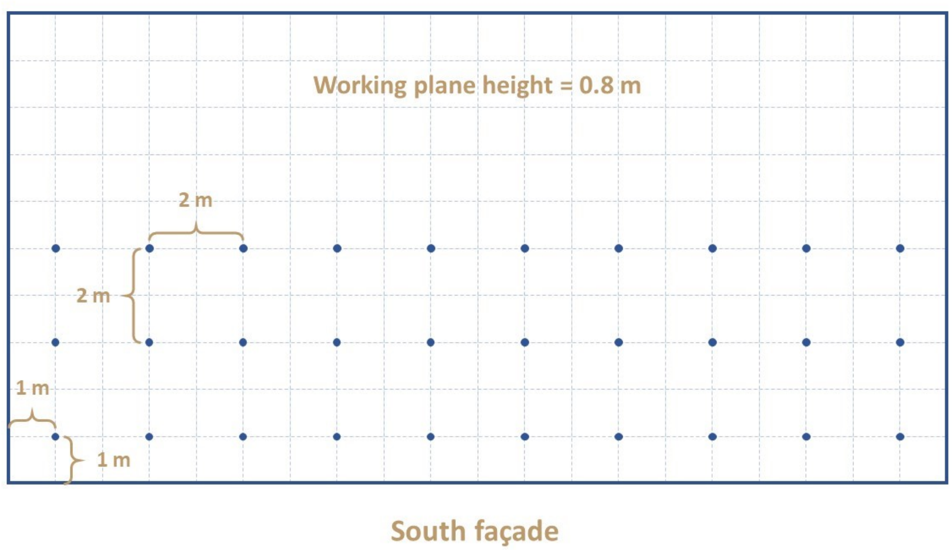

Figure 40 – The position of the points at which the illuminance is measured for application study 1

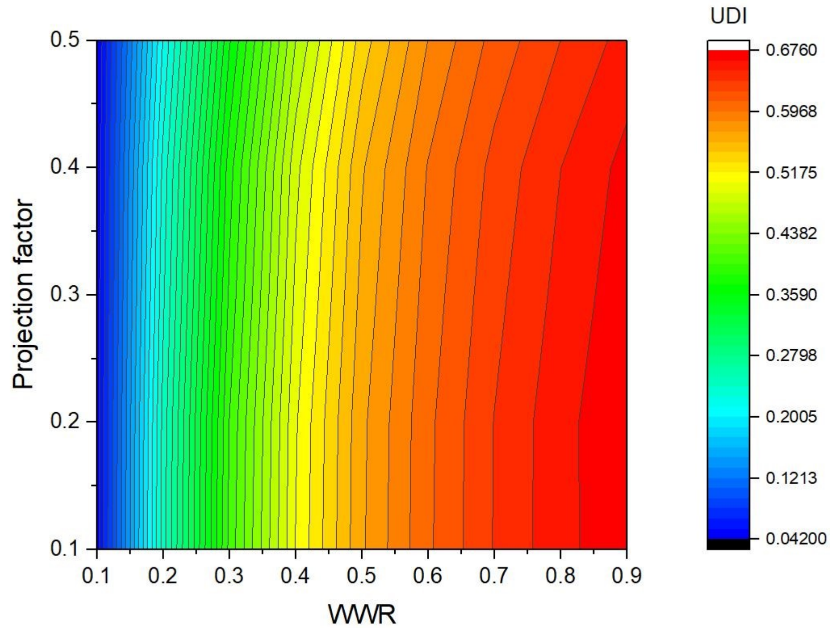

Figure 41 – The average UDI colour map for the double-glazed window

Since UDI and EUI are two objective functions in different dimensions, multi-objective optimization should be used. The weighted global criterion method as shown in Equation 11 is adopted to unify UDI and EUI into a utility function. UDI itself is a normalized value (between 0 and 1), so we need to normalize EUI as well. EUI is normalized as follows:

$$\mathrm{nEUI} = \frac{\mathrm{EUI} - 70\ \mathrm{kWh/(m^2 \cdot year)}}{(106 - 70)\ \mathrm{kWh/(m^2 \cdot year)}} \tag{21}$$

where 106 kWh/(m^2·year) and 70 kWh/(m^2·year) are the highest and lowest EUI seen in the optimization process. From Equation 11, the utility function is calculated as follows:

$$Utility = \sqrt{(1 - \mathrm{UDI})^2 + 4 \cdot \mathrm{nEUI}^2} \tag{22}$$

Since the target is to minimize the utility function, which is opposite to the target for UDI (higher UDI is preferred), we replace UDI with (1 – UDI) in Equation 22. The weights for UDI and nEUI are 1 and 4, respectively. The values of these weights should be carefully selected to represent the relative importance of different objectives in the decision maker's view. This process is not easy even for the decision maker himself. The ways of quantifying a person's preferences, such as soliciting indifference curves, can be found in (Keeney & Raiffa, 1993). The reason for giving nEUI a higher weight is that the residential building is only occupied for a small portion of the time during the day, so energy saving is more important than sufficient daylight. The utility function colour map for static windows is shown in Figure 42. The optimal points for the double-glazed window and triple-glazed window are (WWR = 0.3, projection factor = 0.2) and (WWR = 0.4, projection factor = 0.2), respectively.

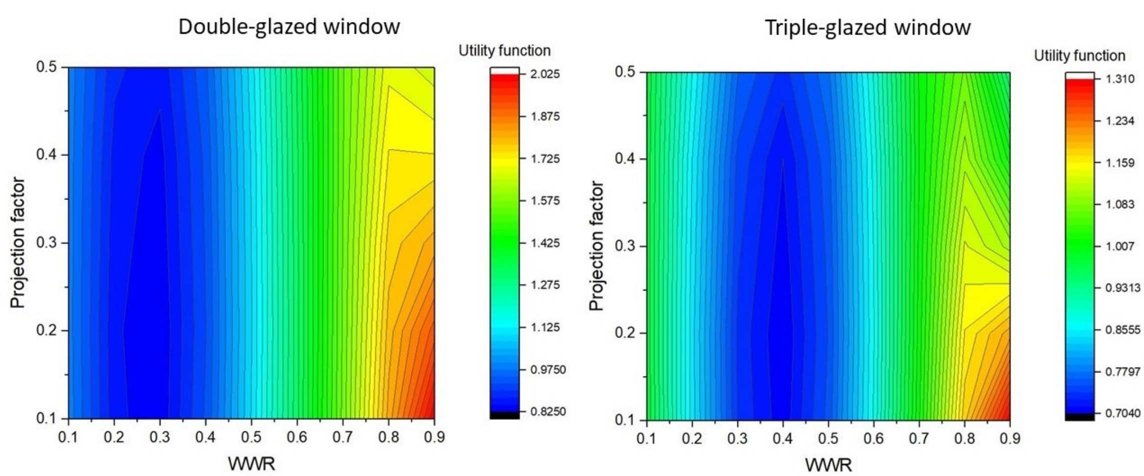

Figure 42 – The utility function colour map for static windows

5.1.8 Cost Model of Scenario 2

The objective function of scenario 2 is life-cycle cost, which includes the initial investment in the façade. Therefore, we need to estimate the initial cost of each part of the façade. First, a model describing the relationship between the area of a window and its cost is developed. From (Plotner et al., 2015), we find the cost of double-glazed windows of different sizes, as shown in Table 14. From these data, a linear regression model is constructed as follows:

$$Cost = 232.32A_w + 203.61\ [\mathrm{U.S.\$}] \quad (23)$$

where A_w is the area of the window, m^2. However, this cost model only applies to double-glazed windows. The second model describes the relationship between the cost of windows and their U-factor. Based on the data from multiple resources (Menzies & Wherrett, 2005; Pikas, Thalfeldt, & Kurnitski, 2014), it is reasonable to assume that the cost of a high-end triple-glazed window (U-factor = 0.7 $W/(m^2 \cdot K)$) is 30% percent higher than that of an average double-glazed window (U-factor = 1.99 $W/(m^2 \cdot K)$). Since single-glazed windows are not allowed by most building codes, it is difficult to find the cost data for them. From Alibaba.com, we found that the cost of a low-end single-glazed window (U-factor = 5.6 $W/(m^2 \cdot K)$) is roughly half that of an average double-glazed window (U-factor = 1.99 $W/(m^2 \cdot K)$). Based on these data, a quadratic regression model is constructed as follows:

$$Relative\ cost = 0.0192U_w^2 - 0.2842U_w + 1.4895 \quad (24)$$

where U_w is the U-factor of the window, $W/(m^2 \cdot K)$. This relative cost is the ratio of the cost of a window to that of an average double-glazed window of the same size.

Table 14 – Cost of double-glazed windows of different sizes

Window area [m²]	0.836	1.30	1.86	2.79
Cost [U.S. $]	420	505	590	875

The third model describes the relationship between the cost of XPS and its thickness. Based on the data from (Plotner et al., 2015) as shown in Table 15, a linear regression model is constructed as follows:

$$Cost = 2.522 l_{XPS} + 8.576 \text{ [\$/m}^2\text{]} \tag{25}$$

where l_{XPS} is the thickness of XPS, cm. The rest of the insulation layer cost \$25.19/m² in total. Also based on the data from (Plotner et al., 2015), the cost of the R-15 wall used in the prototype building is estimated to be \$262.85/m². The cost of items used in the control system is shown in Table 16, the total being \$253.5. For windows without movable insulation, the cost of the insulation layer and control system will not be included.

Table 15 – Cost of materials used in the insulation layer

Material	XPS 2.54 cm	XPS 5.08 cm	XPS 7.62 cm	Gypsum board 1 cm	Latex	Aluminium foil
Cost [\$/m²]	14.64	22.07	27.45	10.55	4.31	10.33

Table 16 – Cost of items used in the control system

Item	Thermometer	Infrared detector	Pyranometer	Actuator	Controller	Black bulb temperature sensor	Wire
Unit price [U.S. \$]	5	3.5	100	40	30	20	50
Number	2	1	1	2	1	1	1

The operation cost of the HVAC system consists of the electricity bills and the natural gas bills. Electricity is used for cooling and powering the fans, and natural gas is used for heating. According to (U.S. Energy Information Administration, 2019a), the average price of electricity provided to residential consumers in the U.S. is \$0.13/kWh. According to (U.S. Energy Information Administration, 2019b, 2019c), the average heat content and price of natural gas delivered to residential consumers in the U.S. are 1037 Btu/ft^3 and \$12.6 kft^3, respectively.

The total operation cost of the HVAC system is calculated as follows:

$$C_{HVAC} = \sum_{i=1}^{n} \frac{C_{HVAC,1}}{(1+d)^{i-1}} \tag{26}$$

where n is the number of years considered; $C_{HVAC,1}$ is the operation cost of the HVAC system in the first year, \$; d is the discount rate (3% is selected in this study, which is the DOE discount rate for projects related to energy conservation, renewable energy resources, and water conservation (Lavappa & Kneifel, 2018)).

5.1.9 Results of Scenario 2

In scenario 2, the life-cycle cost of the south façade, which is the sum of the initial investment and HVAC operation cost, is optimized. Intuitively, glazing with higher U-factor and thicker insulation layer require higher initial investment but will lead to lower operation cost. In addition, the cost of the wall is lower than double-glazed windows but higher than single-glazed windows. Therefore, there are a lot of trade-offs to be made.

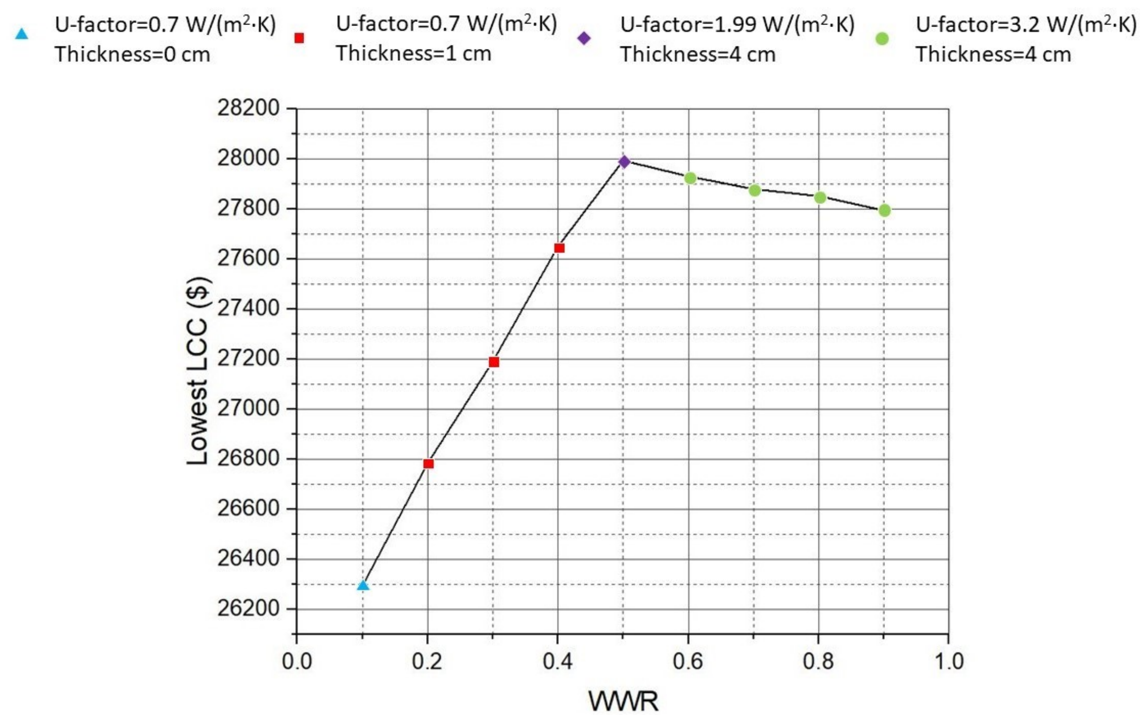

Figure 43 – Lowest LCC and the corresponding window configuration for different WWRs

Figure 43 shows the lowest LCC for different WWRs. The minimum lowest LCC occurs when WWR = 0.1, and the maximum lowest LCC occurs when WWR is 0.5. When WWR is lower than 0.5, the lowest LCC increases rapidly and almost linearly with the increase of WWR. When WWR is higher than 0.5, the lowest LCC decreases slowly and almost linearly with the increase of WWR. For different WWRs, the optimal window configuration is also different. For WWR = 0.1 the optimal window configuration is a high-end triple-glazed window (U-factor = 0.7 W/(m^2·K)) without movable insulation. For WWR from 0.2 to 0.4, the optimal window configuration is a high-end triple-glazed window (U-factor = 0.7 W/(m^2·K)) with XPS thickness = 1 cm. For WWR = 0.5, the optimal window configuration is an average double-glazed window (U-factor = 1.99

W/(m^2·K)) with XPS thickness = 4 cm. For WWR greater than 0.5, the optimal window configuration is a low-end double-glazed window (U-factor = 3.2 W/(m^2·K)) with XPS thickness = 4 cm.

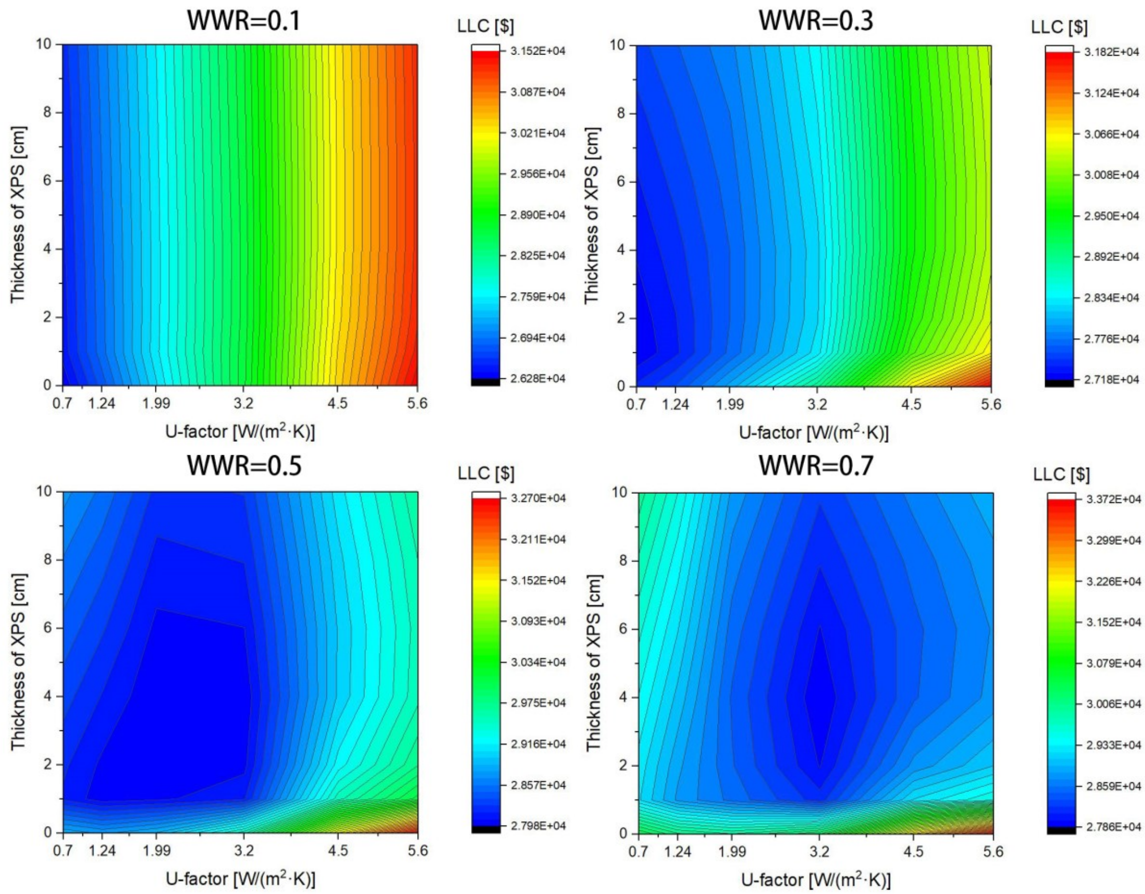

Figure 44 – LCC colour map for four typical WWRs

Figure 44 shows the LCC colour map for four typical WWRs. The x-axis is the U-factor of the glazing and the y-axis is the thickness of XPS. In each colour map, there is a basin where the LCC is lower than the surrounding areas. As the WWR increases, this basin moves gradually from the bottom left corner to the middle right. This trend can be explained as follows:

- The cost of the movable insulation system is comprised of fixed cost and variable cost. Fixed cost is the cost of the control system. Once movable insulation is adopted, this part of cost has to be included. It does not change with the thickness of XPS or the area of the window. Variable cost is the cost of the insulation layer. It depends on the thickness of XPS and the area of the window.
- The benefit of adopting movable insulation increases with the increase of WWR. Windows with lower U-factor and thicker XPS can save more operation cost, but their initial investment is also higher.
- When WWR is 0.1, the energy savings by using movable insulation cannot compensate for the additional cost (mainly fixed cost) of movable insulation. Instead, a high-end triple-glazed window has fairly good thermal resistance. Although the unit cost of the high-end triple-glazed window is high, the total cost is still acceptable due to the small window area.
- When WWR is 0.2–0.4, there is larger window area to share the fixed cost of movable insulation, causing the unit cost of movable insulation to drop. Larger window area also increases the benefit of adopting movable insulation. Therefore, adopting movable insulation becomes profitable. Since the window area is not too large, the total cost of a high-end triple-glazed window is still acceptable. Since the high-end triple-glazed window already has fairly good thermal resistance, the thinnest XPS layer is selected.
- When WWR is larger than 0.4, a triple-glazed window will be too costly. Thus, a standard double-glazed window is selected for WWR of 0.5 and a low-end double-glazed window is selected for WWR larger than 0.5. These windows have so-so

thermal resistance and significantly lower cost. Thicker XPS is selected to make up for the reduction in window thermal resistance.

Taking both energy and daylight into consideration, WWRs of 0.2 or 0.3 are most common. In these cases, a high-end triple-glazed window with movable insulation with 1-cm-thick XPS should be selected from an economic perspective.

5.2 Application Study 2: Optimization of a Selective Reflective Coating

5.2.1 Overview

This application study is intended to enrich and serve as a paradigm for using the optimization framework in the product development scenario. To be specific,

- This application study presents a modified forward approach whose implementation is based on the deep understanding of the underlying physics, which is emphasized in Section 4.3. In this approach, system properties, as introduced in Section 4.3.1, are selected as design variables and the calculation of system properties from physical parameters is replaced by constraints on the system properties. This arrangement can reduce the computational complexity greatly.
- This application study demonstrates how to use a-posterior-articulation methods to obtain the Pareto optimal set of a multi-objective optimization problem, as introduced in Section 4.3.3, and how to interpret the Pareto optimal set in comparison with a baseline product.
- The optimization result strongly depends on the constraints imposed, which once again reflects the importance of a deep understanding of the underlying physics.

5.2.2 *Problem Description*

A building's energy performance highly depends on the properties of its windows. For buildings with large internal heat gains or located in cooling dominated climate zones, people usually want their windows to have low SHGC or solar transmittance but also be able to provide sufficient daylight. At present, low SHGC or solar transmittance is usually realized by using tinted glass or applying a reflective coating to the glazing system. Both methods will impair the visible transmittance of the glazing system and decrease the amount of daylight available. To solve this problem, a research group at Georgia Institute of Technology developed a type of selective reflective coating that has a high reflectance in the near infrared part of the spectrum and a high transmittance in other parts of the spectrum. This type of coating, called the distributed Bragg reflector (DBR) in material science, is formed by multiple bilayers (Bachevillier et al., 2019). Each bilayer is comprised of a layer of low-refractive-index material and a layer of high-refractive-index material, as shown in Figure 45. By changing the physical parameters of the coating, i.e., refractive index difference of the alternating layers, the thickness of the alternating layers, and the number of bilayers (called the period in material science), the width, height, and position of the high-reflectance band can be modulated at will within a certain range, as shown in Figure 46.

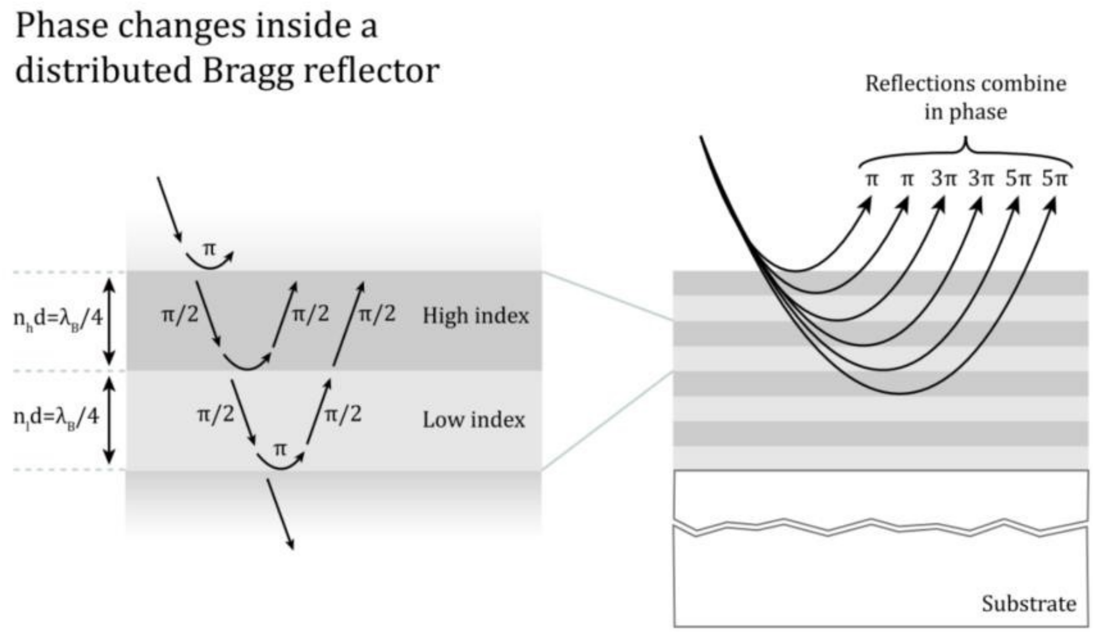

Figure 45 – The structure of DBRs

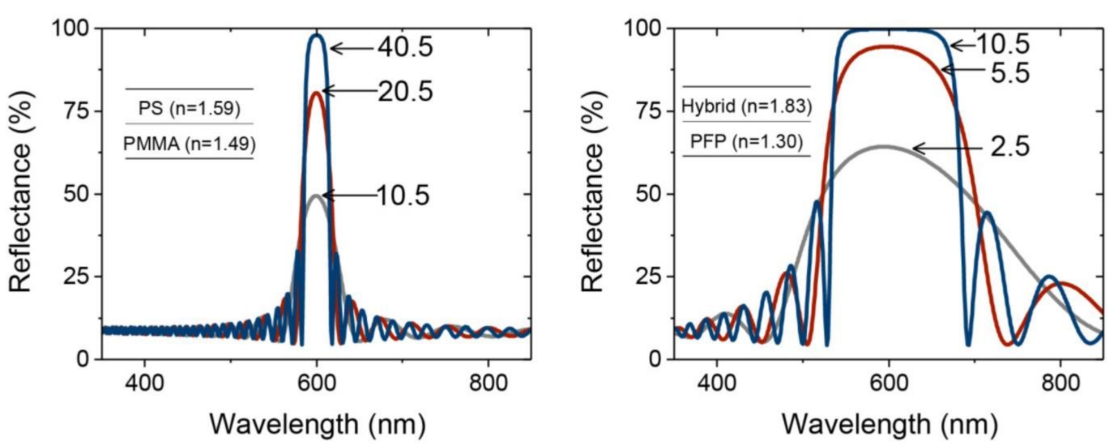

Figure 46 – The modulation of the width, height, and position of the high-reflectance band (Bachevillier et al., 2019)

The purpose of this application study is to find the physical parameters of the coating that lead to the optimal window performance. As discussed in Section 4.3, the forward approach is suitable for product development optimization. However, directly using the physical parameters (the refractive index difference of the alternating layers, the thickness of the alternating layers, and the number of bilayers) as the design variables is too computationally intensive. In BEM programs, weighted average properties, such as visible reflectance and solar reflectance, instead of spectral properties are mostly used as inputs. If the physical parameters are used as design variables, for each iteration we need to first calculate the spectral properties from the physical parameters using transfer-matrix method (TMM) (Bachevillier et al., 2019) and then calculate the weighted average properties from the spectral properties, both of which require massive computation. In addition, there may be more than one physical parameter combination that corresponds to the same weighted average property value and thus leads to the same window performance, which makes the optimization process very inefficient. Therefore, the forward approach should be modified to make the optimization process more efficient.

As shown in Figure 47, a modified forward approach is proposed to reduce the computational complexity. In the original forward approach workflow, there are three steps involving massive computation, which are the TMM modelling, weighted average calculation, and BEM. These steps have to be repeated every optimization iteration, which is highly inefficient. In the modified forward approach, the TMM modelling and weighted average calculation do not need to be performed every optimization iteration. Instead, the developer will need to vary the physical parameters to find the feasible region of the weighted average properties prior to the optimization step. This shouldn't be an arduous task for an experienced material scientist because only the extreme cases need to be tested. For instance, for the selective reflective coating in question, the developer only needs to test extremes cases like minimum number of periods, maximum number of periods, maximum refractive index difference, maximum difference between visible reflectance and infrared reflectance, etc. After the feasible region is obtained, it will be used as constraints in the optimization step. The optimization step will yield the optimal weighted average properties. Next, a search for the corresponding physical parameters needs to be performed. This modified forward approach is different from the quasi-forward, quasi-backward and backward approaches in that the technological characteristics of the selective reflective coating are fully specified in the pre-optimization steps and reflected in the constraints.

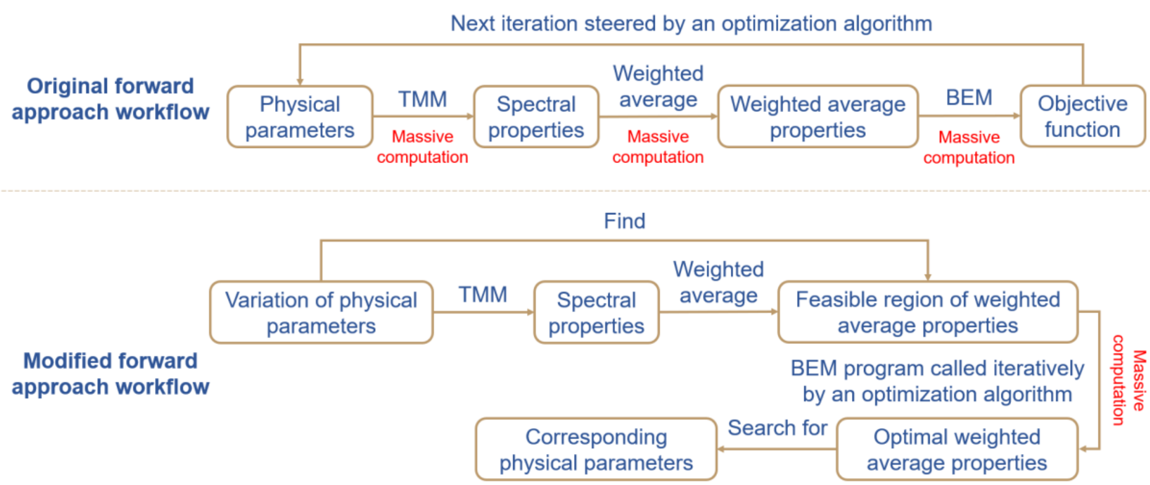

Figure 47 – Comparison of the original forward approach workflow and the modified forward approach workflow

5.2.3 The Building Model of This Study

The Medium Office Commercial Reference Building EnergyPlus model developed by National Renewable Energy Laboratory (NREL) is adopted for this study (Deru et al., 2011). The building is located in Atlanta whose climate zone is 3A. Since the author only has limited computational power, the original model, a three-story building with 18 zones, is simplified to reduce the computation time. A perimeter zone, as shown in Figure 48, is extracted from the original building. The schedules, materials, constructions and WWR are all inherited from the original model. The changes made to the original model are as follows:

- The original HVAC system is replaced by an Ideal Loads Air System. The cooling source is a chiller with a seasonal COP of 3 and the heating source is a gas furnace with an efficiency of 0.9;
- The outside boundary conditions of all surfaces except the exterior surface are set as adiabatic, since it is assumed that this room is adjacent to similar conditioned rooms;
- The window construction is changed from a Window Material: Simple Glazing System object to a Construction object, as the investigation of a window coating requires more detailed modelling of the window than just using U-factor, SHGC, and visible transmittance.

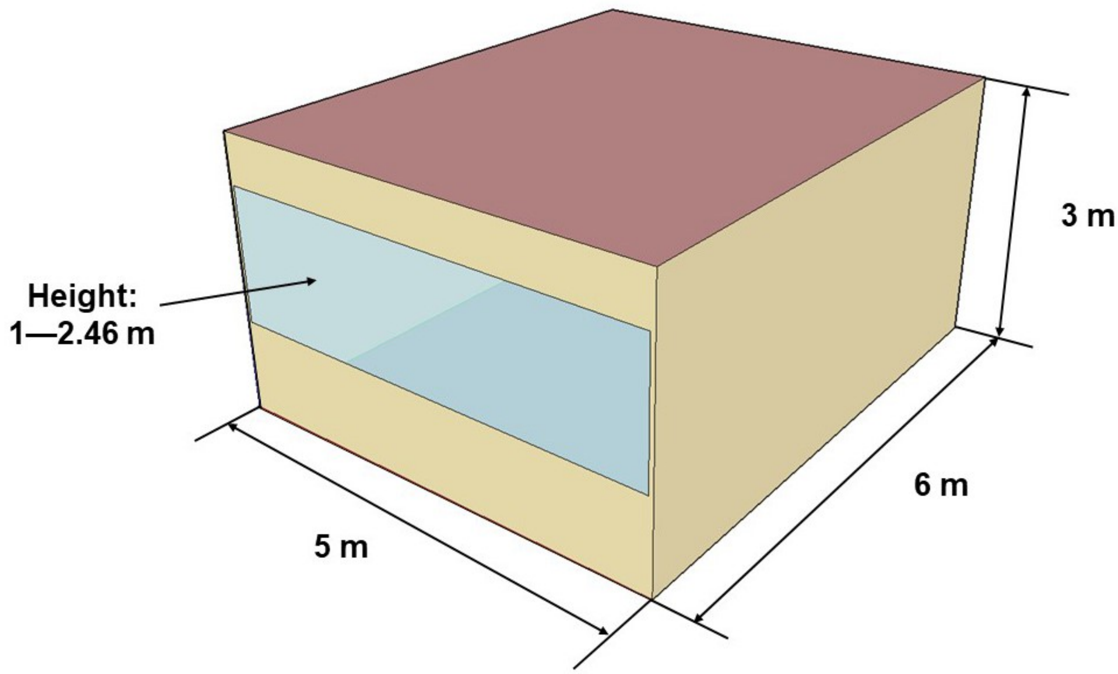

Figure 48 – The adapted single-zone building model for application study 2

5.2.4 Formulation of the Optimization Problem

Since people want to make the energy consumption related to windows as low as possible and at the same time maintain a high level of useful daylight, the objective function of this optimization problem should take both energy consumption and daylight into account. Thus, multi-objective optimization is adopted for the development of the selective reflective coating. As introduced in Section 4.3.3, a-priori-articulation methods are discouraged in product development unless the weights can faithfully reflect the preference of the potential consumers (which is theoretically impossible). In this application study, an a-posteriori-articulation method is adopted to generate a Pareto optimal set that will be used in the following market research. Since minimizing Equation 11 is both necessary and sufficient for Pareto optimality (Marler & Arora, 2004), we can obtain a Pareto optimal set by continuously changing the value of w_i. Besides, there is a study showing that using higher values for p increases the effectiveness of the method in providing the complete Pareto optimal set. Therefore, we set $p = 4$.

UDI and source HVAC energy consumption, as introduced in Section 5.1, are selected as the indicators of energy consumption and daylight respectively in this application study. The position of the photometers in this application study is shown in Figure 49. Since the optimization algorithms try to minimize the objective function, we replace UDI with (1 – UDI) in the objective function so that smaller objective function value represents better daylighting performance. We also need to normalize the source HVAC energy consumption to make it comparable to (1 – UDI). The normalized source HVAC energy consumption is calculated as follows:

$$nE_{HVAC} = \frac{R_{grid} \cdot E_{c,id}/\mathrm{COP} + R_{ng} \cdot E_{h,id}/\eta_h}{8000\ \mathrm{kWh}} \tag{27}$$

where R_{grid} and R_{ng} are the source-site ratios for grid electricity and natural gas, respectively (R_{grid} = 2.80 and R_{ng} = 1.05 from (Energy Star, 2018) is used); $E_{c,id}$ is the annual ideal cooling energy need, kWh; COP is the seasonal cooling COP of the HVAC system, 3; $E_{h,id}$ is the annual ideal heating energy need, kWh; η_h is the efficiency of the heating system, 0.9; 8000 kWh is an arbitrary number used to normalize the source HVAC energy consumption. The utility function of this optimization problem is as follows:

$$Utility = (w_1^4 \cdot (1 - UDI)^4 + w_2^4 \cdot nE_{HVAC}^4)^{\frac{1}{4}} \tag{28}$$

where w_1 and w_2 are the weights of the daylight term and the energy consumption term, respectively.

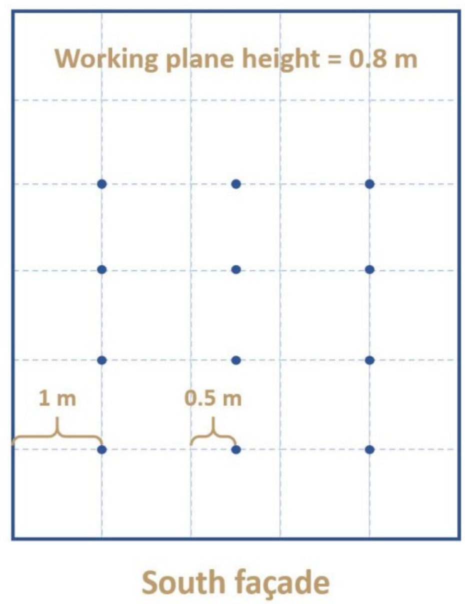

Figure 49 – The position of the points at which the illuminance is measured for application study 2

EnergyPlus is used as the BEM program. In EnergyPlus, the inputs of glazing radiation properties are visible reflectance, visible transmittance, solar reflectance, solar transmittance, and emissivity. We can see from Figure 46 that by modulating the width, height, and position of the high-reflectance band, solar reflectance and visible reflectance can be varied independently within a certain range. Out of this range, changing one property will influence the other. Therefore, we choose solar reflectance and visible reflectance as design variables and impose proper constraints to represent their correlations. The solar transmittance and visible transmittance can be calculated by:

$$Tr_{sol} = 1 - Re_{sol} - Ab_{sol}$$

$$Tr_{vis} = 1 - Re_{vis} - Ab_{vis} \tag{29}$$

where Re_{sol} and Re_{vis} are the solar reflectance and visible reflectance, respectively; Ab_{sol} and Ab_{vis} are the solar absorptance and visible absorptance, respectively.

Originally, we planned to use the data provided by the group that developed this selective reflective coating to find the feasible region of the design variables. However, due to some unknown issues, the data are still unavailable by the time this section is written. Therefore, we have to use some pseudo data chosen by the author. Although the data are chosen based on the author's experience, this method applies to the real data as well.

The selective reflective coating has to be applied to a substrate, i.e., a layer of glass. A Vinyl-framed double-glazed window with a U-factor and an SHGC that are the same as the requirements of ASHRAE 90.1 is chosen as the baseline window (American Society of Heating Refrigerating and Air-Conditioning Engineers, 2016). The properties of this window, as shown in Table 17, are modelled by Window 7.6, a window-modelling tool developed by LBNL (Curcija, Vidanovic, Hart, Jonsson, & Mitchell, 2018). Since this window uses a tinted glass with high absorptance to reduce solar heat gain, applying the selective reflective coating to this window will restrict the variation of the window's solar transmittance and visible transmittance to a very small region. Therefore, another window whose solar absorptance and visible absorptance are 0.2 and 0.15 respectively is created as the substrate window. The selective reflective coating is applied to the exterior surface of this window. The reason for choosing the exterior surface is that the target buildings of this coating are the commercial buildings with high internal heat gain located in cooling dominated climates so that reducing solar heat gain is a high priority all year round. The emissivity of the exterior surface is a constant value of 0.5. All other parameters of the substrate window are the same as those of the baseline window. The constraints on the solar reflectance and visible reflectance of the outer side of the substrate window are as follows:

$$\begin{gathered} 0.086 \leq Re_{sol} \leq 0.7 \\ 0.158 \leq Re_{vis} \leq 0.6 \\ Re_{sol} \leq 1.5Re_{vis} \\ Re_{sol} \leq Re_{vis} + 0.2 \end{gathered} \tag{30}$$

To generate the Pareto optimal set, this optimization problem is solved 99 times using pattern search algorithm provided by Matlab (MathWorks, 2019). Pattern search algorithm is selected because it can solve a constrained optimization problem in Matlab whose objective function is calculated by an external program (EnergyPlus) and the objective function of this problem has at most one local optimum. In these 99 cases, w_1 in Equation 28 is varied from 0.01 to 0.99 with a step of 0.01 and w_2 is calculated as $(1 - w_1)$.

Table 17 – The properties of the bare window that the selective reflective coating is applied to

	ID	Thick	T_{sol}	$R_{sol}1$	$R_{sol}2$	T_{vis}	$R_{vis}1$	$R_{vis}2$	T_{ir}	E1	E2	Cond
Glass1	9769	5.9	0.240	0.086	0.213	0.491	0.158	0.267	0.000	0.840	0.215	1
Gap	2 (Argon)	12.7										

Glass2	103	5.7	0.771	0.070	0.070	0.884	0.080	0.080	0.000	0.840	0.840	1

	U-factor (W/m^2·K)	SHGC	T_{vis}
Glazing system	1.730	0.289	0.444
Window	1.870	0.252	0.370

5.2.5 Results

The Pareto optimal set of the selective reflective coating is shown in Figure 50. Due to the defect of the pattern search algorithm provided by Matlab, only discrete points on the Pareto optimal set are obtained and the distribution of the Pareto optimal points is not very uniform. Nevertheless, we can clearly see the shape of the Pareto optimal set in this figure. The UDI and source EUI of the baseline window (the light blue point) that can be seen as an existing product on the market are also shown in Figure 50. If we set this point as the origin, the two-dimensional objective space can be divided into four quadrants. Points in quadrant 1 represent the design decisions whose daylight performance is better than that of the baseline window but energy performance is worse. The daylight performance and energy performance of design decisions in quadrant 2 are both superior to the baseline window. Design decisions in quadrant 3 have worse daylight performance and better energy performance compared to the baseline window. Design decisions in quadrant 4 have worse daylight performance and energy performance compared to the baseline window and thus should be discarded unless they have a prominent cost advantage.

As we can see in Figure 50, none of the points in the Pareto optimal set lies in quadrant 4, which means all the design decisions are at least superior to the baseline window in one aspect. Of paramount interest are the points in quadrant 2, as these design decisions surpass the baseline window in both aspects. The solar reflectance and visible reflectance of the three points in quadrant 2 shown in Figure 50 are (0.479, 0.319), (0.494, 0.329), and (0.509, 0.339), respectively. Other design decisions that may also be of interest are those in quadrant 3. When the UDI decreases from 0.519 to 0.473, the source EUI drops significantly from 87.8 kWh/(m^2·year) to 66.3 kWh/(m^2·year), which means at the expense of 8.86% UDI degradation, the source EUI is improved by 24.5%. This trade-off may be attractive enough for certain customers.

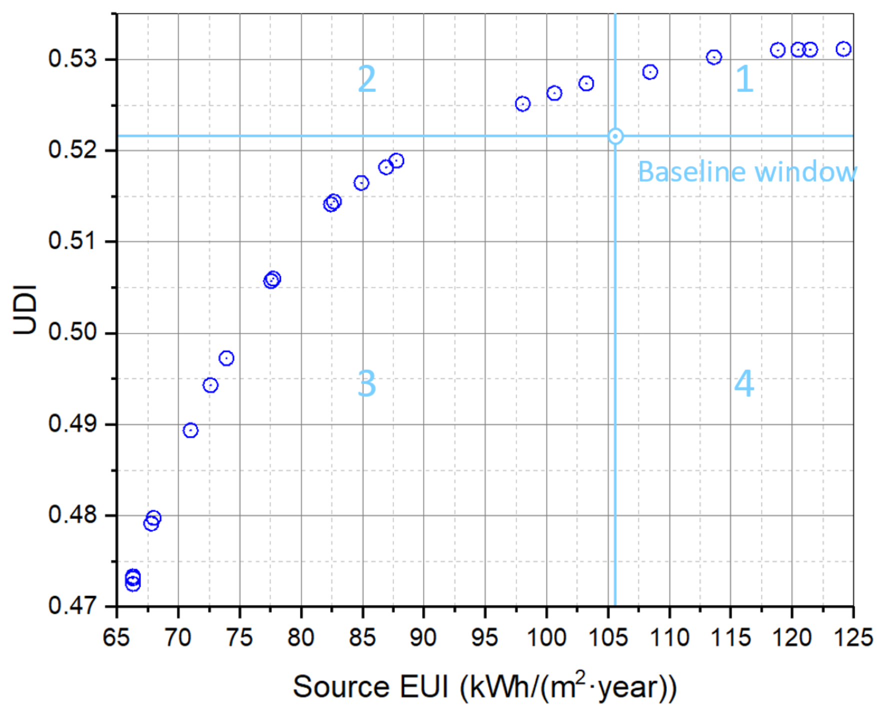

Figure 50 – The Pareto optimal set of the selective reflective coating

Figure 51 shows the feasible region of the selective reflective coating. All the Pareto optimal points lie on the lower boundary of the feasible region, i.e., the last two inequality constraints in Equation 30 are active constraints. This reminds us again of the importance of imposing proper constraints on the optimization problem based on the characteristics of the technology in question.

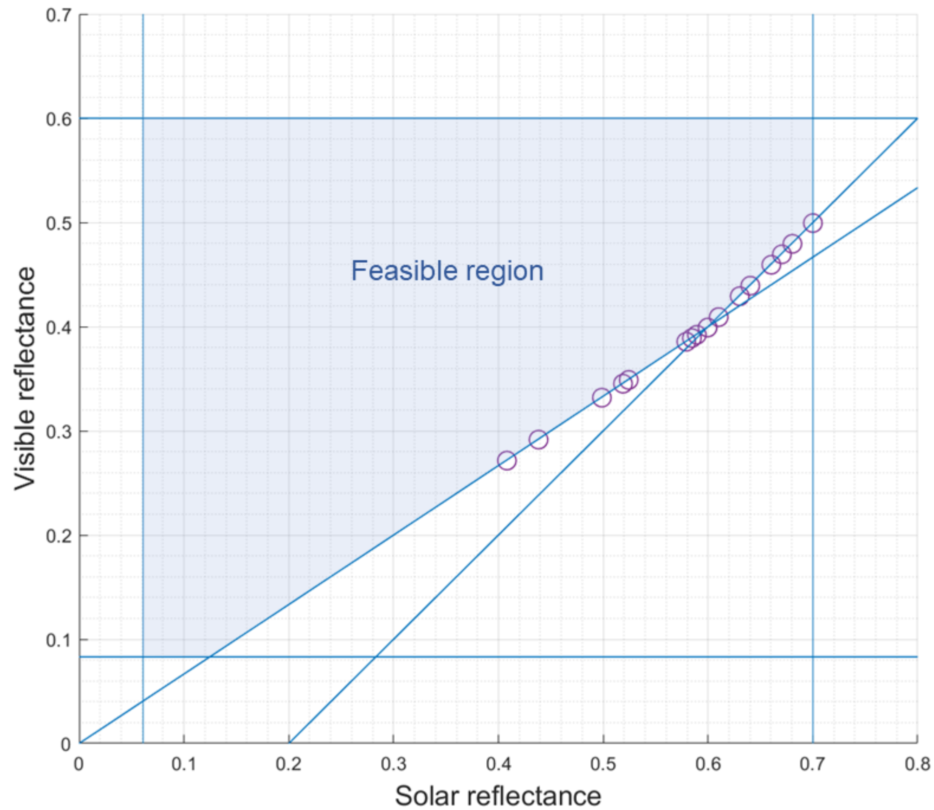

Figure 51 – The feasible region of the selective reflective coating

5.3 Application Study 3: Optimization of a Ventilated Façade with MPC

5.3.1 Overview

This application study is intended to enrich and serve as a paradigm for using the optimization framework in the building operation scenario. To be specific,

- This application study adopts the forward approach as discussed in Section 4.5.
- In this application study, the finite-difference model introduced in Section 1.3.5 is adopted for MPC studies and the model is coded in Matlab. The reason for choosing this model is that its state variables can be read, stored, and assigned, thus

eliminating the need for a pre-conditioning horizon, and its functionality is less limited than that of commercial programs in terms of modelling ABE systems.

- This application study demonstrates how to use the nested optimization framework as introduced in Section 4.5.1 to formulate the design optimization problem of a building with optimized control.
- This application study demonstrates how to properly formulate an MPC problem using the concepts introduced in Section 4.5.2.
- The result proves the statements in Section 4.5.1 that the design parameters have a significant impact on the control optimization result, and that the performance of each design case hinges on the optimality of its control decisions.

5.3.2 Problem Description

As mentioned in Section 4.5.1, for building design scenarios where optimized control is adopted, the nested optimization framework should be used. In this study, the application of this framework is demonstrated through the optimization of a ventilated façade with MPC. The reason for selecting this ventilated façade is that it has multiple design parameters as well as a control parameter, which can be used to demonstrate the interaction between design optimization and control optimization. Besides, the thermal storage function of this ventilated façade entails the adoption of MPC.

The ventilated façade considered in this study consists of three functional layers, as shown in Figure 52. The outermost layer is a translucent insulation layer with a low U-factor and a low thermal mass. In the middle is an air channel with a fan that can either serve as an insulation layer when the fan is off or an airflow channel when the fan is on.

The innermost layer is a thermal mass layer made of concrete. Placing the thermal mass close to the inside leads to better energy performance than placing the thermal mass elsewhere (El Mankibi et al., 2015; Koenders et al., 2018).

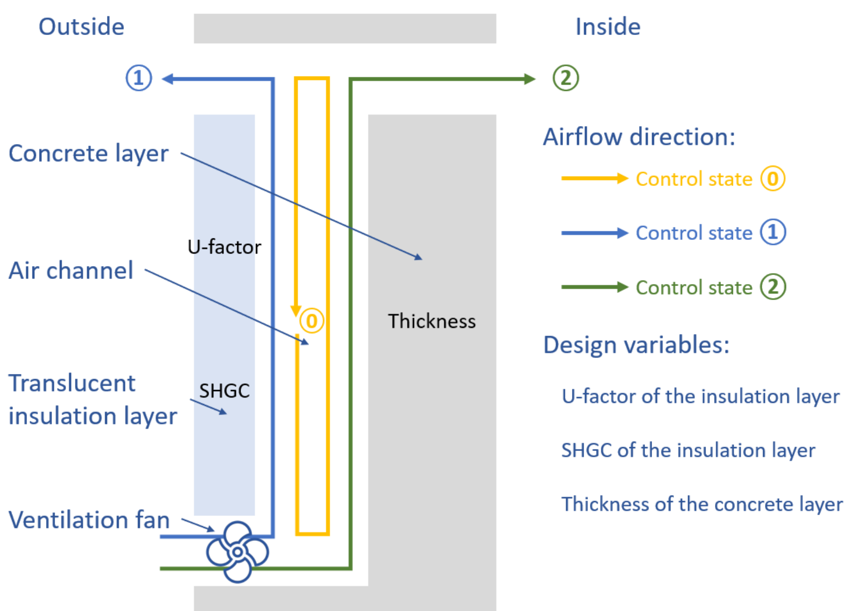

Figure 52 – The configuration and control states of the ventilated façade

This ventilated façade has three control states, denoted as state 0, 1, and 2. In state 0, the fan is off and the stagnant air in the air channel serves as an insulation layer with no mass. In state 1, the fan is on and blows the outdoor air into the channel. After going through the channel, the air is exhausted to the outside. In state 2, the only difference from state 1 is that after going through the channel, the air is delivered to the inside. The MPC problem in this study is to find the optimal control state of the ventilated façade for each control step.

The control optimization of the ventilated façade is only the lower level optimization. At the higher level is the design optimization, which is performed based on the results of the control optimization. In each design case, optimization is performed to ensure that the control decisions are optimal for this case, because the quality of the control decisions has a great impact on the evaluation of the design parameters. For instance, a poor design with optimal control may outperform a good design with suboptimal control, thus misleading the designer into the wrong decision. On the other hand, the design parameter values selected in each design case also influence the evaluation of the objective function of the control optimization problem or set constraints on the control optimization problem. For different design parameter values, the optimal control sequence is likely to be different. In this study, the design parameters to be optimized are the U-factor of the insulation layer, the SHGC of the insulation layer, and the thickness of the thermal mass layer.

5.3.3 Model Predictive Control Parameters

In this study, the execution horizon is set as 1 day. A cost horizon of 3 days is selected to take the lasting effects of the control decisions into account. The planning horizon is the same as the cost horizon. The control step is 2 hours in the execution horizon and 6 hours in the rest of the planning horizon. A longer control step in the last two days can reduce the computation time greatly. There are 12 control decisions in the first day of the planning horizon and 4 control decisions in either of the last two days. This results in a 20-dimensional optimization problem. In each dimension, there are three candidate options, which are control state 0, 1, and 2. Genetic algorithm is adopted, as it can solve constrained integer nonlinear optimization problem relatively efficiently.

The objective function of this study is the total HVAC energy cost in the cost horizon, which is calculated by:

$$C_{HVAC} = C_{elec}\left(\frac{E_{c,id}}{\text{COP}} + E_{fan}\right) + C_{ng} \cdot E_{h,id}/\eta_h \tag{31}$$

where C_{elec} is the unit price of grid electricity, \$/kWh; $E_{c,id}$ is the total ideal cooling energy need, kWh; COP is the seasonal cooling COP of the HVAC system, 3; E_{fan} is the total electricity consumption of the ventilated façade fan, kWh; C_{ng} is the unit price of natural gas, \$/kWh; $E_{h,id}$ is the total ideal heating energy need, kWh; η_h is the efficiency of the heating system, 0.9. According to (U.S. Energy Information Administration, 2019a), the average price of electricity provided to residential consumers in the U.S. is \$0.13/kWh. According to (U.S. Energy Information Administration, 2019b, 2019c), the average heat content and price of natural gas delivered to residential consumers in the U.S. are 1037 Btu/ft^3 and \$12.6 kft^3, respectively.

5.3.4 The Finite-Difference Model of This Study

The single-zone building model used in application study 2 is also adopted in this study. However, the finite-difference model from Section 1.3.5 that is coded in Matlab instead of EnergyPlus is used to perform the simulation. This decision is made based on two considerations.

- Computation time. Since EnergyPlus does not allow the user access to the state variables, at the beginning of each optimization iteration a period of re-simulation using previous weather data and previously implemented control sequence in addition to EnergyPlus's default warm-up period is required to resume the thermal states of the model to the end of last optimization step. In (Corbin et al., 2013), a pre-conditioning horizon of 21 days and a cost horizon of 3 days are adopted, which means more than 87.5% of the computation time is spent on warming up. By using the finite-difference model, all the state variables can be read, stored, and assigned, thus eliminating the need for an additional warm-up period.

- Controllability. As stated in Section 3.1.2, in EnergyPlus we can only control the ABE systems through the actuators provided by EnergyPlus. Unfortunately, we cannot create a ventilated façade in EnergyPlus that has the desired functions and design parameters. In contrast, the finite-difference model does not impose any limitation on the design and operation of the ventilated façade.

If MPC is not adopted like in the first two application studies, EnergyPlus is still preferred over the finite-difference model, because (1) EnergyPlus has a mature user interface, so the construction of the model takes less effort; (2) EnergyPlus has been extensively validated; and (3) EnergyPlus can simulate more complex physical phenomena, such as daylight illumination.

Figure 53 shows the diagram of the finite-difference model used in this application study. The stability criterion of Explicit Euler method requires for node k

$$\frac{\Delta t \mathbf{B}_{k,k}}{\mathbf{A}_{k,k}} \leq 2 \tag{32}$$

where $\mathbf{A}$ and $\mathbf{B}$ are defined in Figure 13. If the thermal mass ($\mathbf{A}_{k,k}$) of a node is very small, we have to reduce the time step to maintain stability. Therefore, the size of the time step is restricted by the thermal mass of the node with smallest thermal mass, i.e., the room node

(node 9 in Figure 53). Usually we want to make the time step larger so that the computation time can be reduced. In order to use a reasonably large time step (6 to 10 minutes), we have to increase the thermal mass of the room node. The original EnergyPlus reference building model uses a room node to represent the air inside the room and a separate Internal Mass node to represent the furniture. This arrangement results in a very small room node thermal mass, around 108 kJ/K. In order to add more thermal mass to the room node, we merge the room air and the furniture into one node. In EnergyPlus this is realized by using the Zone Capacitance Multiplier: Research Special object. The original thermal mass of the room air will be multiplied by this multiplier to get the new thermal mass that includes the thermal mass of the furniture. In this model, a multiplier of 4.5 (This value is recommended by Prof. Godfried Augenbroe in his Computational Building Simulation course.) and a simulation time step of 6 minutes are selected.

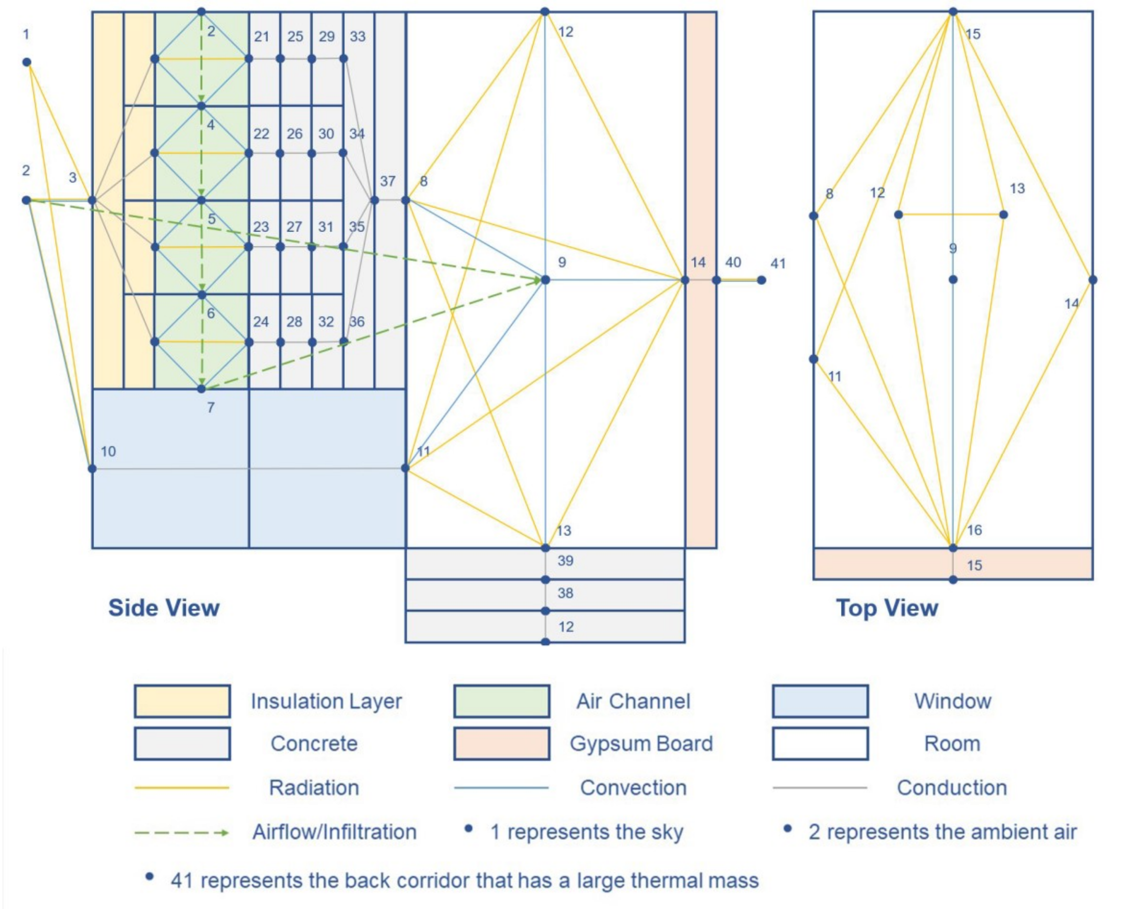

Figure 53 – Diagram of the finite-difference model used in application study 3

The equation set of this model is adapted from that shown in Figure 13. Since this ventilated façade has three control states, three different equation sets are constructed to model these three control states. When the ventilated façade is in control state 0, the air channel serves as an insulation layer. The convective heat transfer coefficient of a vertical cavity is calculated based on the formula provided by ISO 15099 (International Organization for Standardization, 2003):

$$Nu = (Nu_1, Nu_2)_{\max} \tag{33}$$

$$Nu_1 = 0.0673838Ra^{1/3} \quad 5 \times 10^4 < Ra$$

$$Nu_1 = 0.028154Ra^{0.4134} \quad 10^4 < Ra \leq 5 \times 10^4$$

$$Nu_1 = 1 + 1.7596678 \times 10^{-10} Ra^{2.2984755} \quad Ra \leq 10^4$$

$$Nu_2 = 0.242 \left(\frac{Ra}{AR}\right)^{0.272}$$

where *Nu* is the Nusselt number; *Ra* is the Rayleigh number; AR is the aspect ratio of the cavity. The width of the air gap in this study is 0.05 m. We assume the temperature difference between the two walls of this air gap is 2°C. The calculated convective heat transfer coefficient is 1.02 W/(m^2·K). Besides convective heat transfer, there is also radiative heat transfer between the two walls. Since the width of the air gap (0.05 m) is far smaller than the dimensions of the wall (5 m × 3 m), this problem can be seen as the radiative heat transfer between two infinite parallel plates. The radiative heat transfer coefficient is calculated by:

$$h_{rad} = \frac{\sigma(T_1 + T_2)(T_1^2 + T_2^2)}{\frac{1}{\varepsilon_1} + \frac{1}{\varepsilon_2} - 1} \tag{34}$$

where σ is the Stefan-Boltzmann constant, 5.67×10^{-8} W/(m^2·K^4); ε_1 and ε_2 are the emissivity of the two walls, respectively; T_1 and T_2 are the temperatures of the two walls, respectively, K. Assuming $\varepsilon_1 = \varepsilon_2 = 0.9$ and $T_1 = T_2 = 298$ K, we get $h_{rad} = 4.91$ W/(m^2·K). Taking both convective heat transfer and radiative heat transfer into account, the total heat transfer coefficient of the air channel is 5.93 W/(m^2·K).

When the ventilated façade is in control state 1 or 2, a fan is turned on to drive the air to flow through the channel. While the air is flowing through the channel, it exchanges heat with the two channel walls. The calculation of the convective heat transfer coefficient is based on the forced-convection correlations provided by ASHRAE Handbook: Fundamentals (American Society of Heating Refrigerating and Air-Conditioning Engineers, 2013):

$$Nu = 0.037Re^{4/5}Pr^{1/3} \tag{35}$$

where *Re* is the Reynolds number; *Pr* is the Prandtl number. Since the façade is separated into two parts by a horizontal window, we make the air flow horizontally inside the air channel and assume that the air velocity is uniform everywhere. In this study, a fan with a flow rate of 277 m^3/h is adopted which results in an air velocity of 1 m/s. Substituting this value into Equation 35 we can get a convective heat transfer coefficient of 4.39 $W/(m^2 \cdot K)$. It should be noted that this convective heat transfer coefficient measures the heat transfer rate between the wall and the air stream, while that in the last paragraph measures the heat transfer rate between the two walls of the air channel.

It is assumed that within the same time step, the air stream is in steady state, i.e., its temperature distribution does not change with time. The temperature of the air stream is calculated by:

$$v_{air}A_{sec}\rho_{air}c_{air}(T_{m+1}^{n+1} - T_m^{n+1}) = \left(T_{w1} - \frac{T_{m+1}^n + T_m^n}{2}\right)h_{conv}A_w \tag{36}$$

$$+\left(T_{w2}-\frac{T_{m+1}^{n}+T_{m}^{n}}{2}\right)h_{conv}A_{w}$$

where v_{air} is the air velocity, m/s; A_{sec} is the sectional area of the air channel, m^2; ρ_{air} is the density of air, kg/m^3; c_{air} is the specific heat of air, J/(kg·K); T_m is the temperature of the mth air stream node, °C; T_{w1} and T_{w2} are the temperatures of the two walls, °C; h_{conv} is the convective heat transfer coefficient, W/(m^2·K); A_w is the area of the air channel wall, m^2. As shown in Figure 53, the airflow channel is discretized into five nodes, which is a trade-off between computation time and simulation accuracy. In the channel, the air flows from node 2 to node 4, 5, 6, and 7 successively. The calculation of the temperatures of the air stream nodes starts from node 2, whose temperature is the same as the outdoor dry-bulb temperature. Then, the temperature of node 4, 5, 6, and 7 can be calculated from Equation 36 one by one. After the temperatures of all the nodes are obtained, the first iteration is completed. This process needs to be repeated in order for the temperature of the air stream to converge. In Equation 36, the superscript n of T_m denotes that the temperature's value is calculated in the nth iteration. It takes 4 or 5 iterations for the temperature to converge.

When the SHGC of the translucent insulation layer is greater than 0, part of the solar radiation incident on the façade is transmitted through the insulation layer. In the calculation of the finite-difference model, 0.7 of the transmitted solar radiation is added to the outer surface of the concrete layer directly, as the solar absorptance of concrete is 0.7. The rest is split evenly between the inner surface of the insulation layer and the outer surface of the concrete layer.

In order to determine the power of the fan, we find the product specifications of 17 ventilation fans at Alibaba.com, and fit a linear regression model using their power and flow rate, as shown in Figure 54. Since the fan used in this study has a flow rate of 277 m^3/h, its power, according to the regression equation, is 29.17 W.

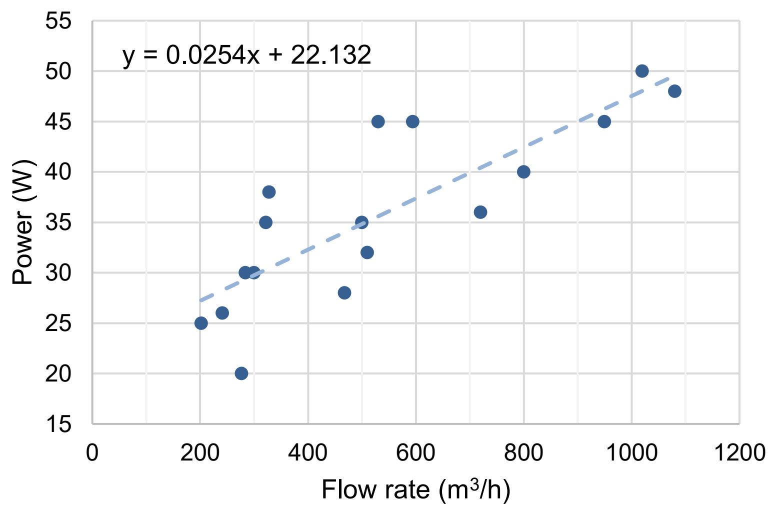

Figure 54 – Linear regression of fan power versus flow rate

5.3.5 Verification of the Finite-Difference Model

Before we use the finite-difference model to perform any simulation, we first need to verify this model by comparing its result with that of an EnergyPlus model with identical settings. EnergyPlus, as a BEM program, has been widely validated (U.S. Department of Energy, 2015). The weather data (including outdoor dry-bulb temperature, sky temperature, direct normal irradiance, and global horizontal irradiance), geometry, construction, and schedules of the finite-difference model are directly copied from the EnergyPlus model. Then, we let EnergyPlus output all the convective and radiative heat transfer coefficients and use their monthly averages in the finite-difference model.

A comparison between the hourly ideal cooling energy in May of the EnergyPlus model and the finite-difference model is shown in Figure 55. In this comparison, the control state of the ventilated façade is 0 at all times. We can see that the hourly ideal cooling energy of the finite-difference models is almost identical to that of the EnergyPlus model. A comparison between the indoor air temperature in May of the EnergyPlus model and the finite-difference model is shown Figure 56. We can see that the indoor air temperature profile of the finite-difference model follows that of the EnergyPlus model quite well. Only in a few short periods are there discernible discrepancies and the difference is at most 0.8°C. Based on these two comparisons, we can conclude that the results of the finite-difference model are reliable.

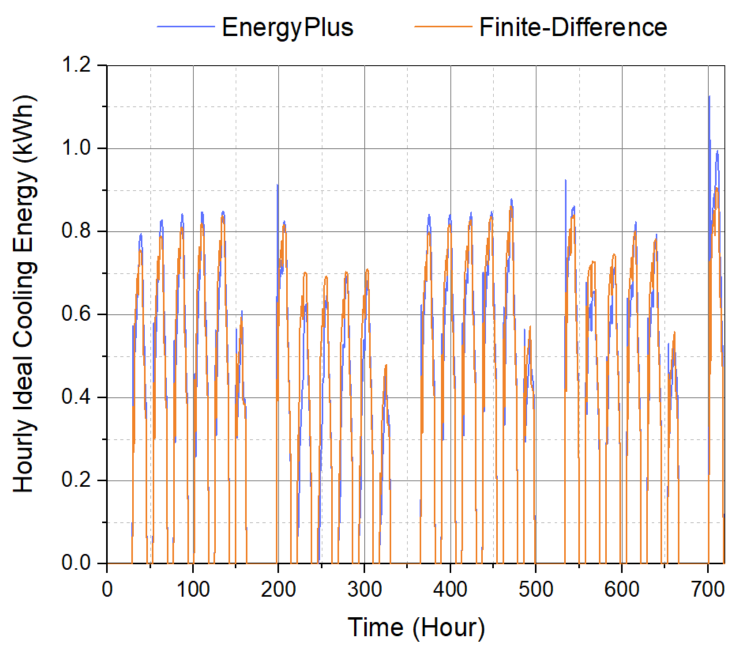

Figure 55 – A comparison between the hourly ideal cooling energy in May of the EnergyPlus model and the finite-difference model

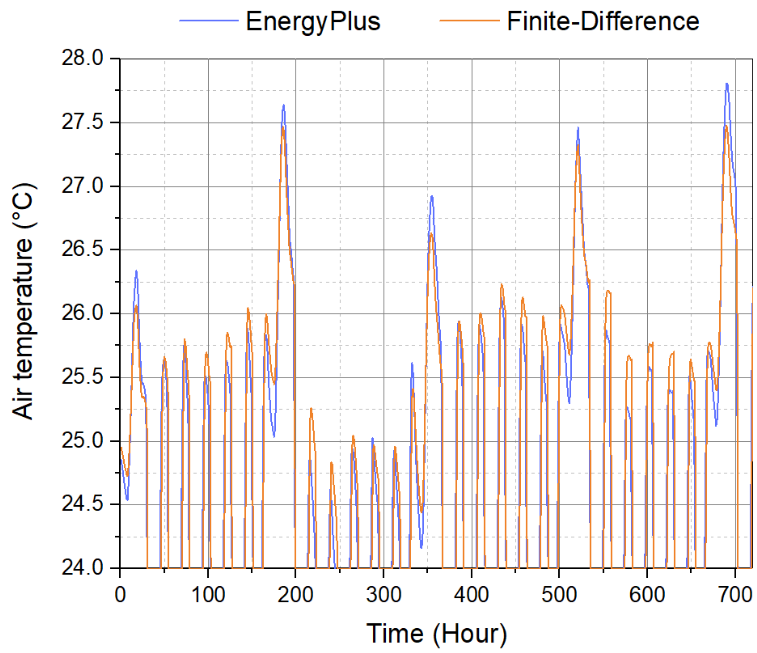

Figure 56 – A comparison between the indoor air temperature in May of the EnergyPlus model and the finite-difference model

5.3.6 Explicit Constraint and Implicit Constraint

In the MPC problems discussed here, thermal comfort does not appear in the objective function, but rather it serves as a constraint. The ideal air system of this building maintains the room air temperature between 21 and 24°C during the occupied hours, which is assumed to be a sufficient condition for thermal comfort. However, this constraint may fail in some cases. In May, the ventilated façade tends to exploit the cold outside air during the night to cool the thermal mass. Chances are that the cooling of the ventilated façade is so effective that at the beginning of the occupied hours the operative temperature of the room is below the comfort threshold, 21°C. There are two ways of handling it. The first way is to change the controlled variable of the HVAC system from air temperature to operative temperature. Thermostats that measure mean radiant temperature are already available on the market, as shown in Figure 57. Where the relative air speed is smaller than 0.2 m/s, or where the difference between mean radiant and air temperature is smaller than 4°C, the operative temperature can be calculated by (American Society of Heating Refrigerating and Air-Conditioning Engineers, 2010):

$$T_{op} = \frac{T_{mr} + T_{i,a}}{2} \tag{37}$$

where T_{mr} is the mean radiant temperature, °C; $T_{i,a}$ is the indoor air temperature, °C. HVAC systems configured in this way can ensure that the thermal comfort constraint is satisfied. Since this kind of constraint does not appear explicitly in the optimization formulation, it is called the implicit constraint. The implicit constraint impacts the optimization result through the evaluation of the objective function. In this case, changing the controlled variable from air temperature to operative temperature will inevitably increase the heating energy need which is reflected in the objective function. The optimizer will try to strike a balance between reducing the cooling energy need with night cooling and reducing the heating energy need induced by overcooling.

Figure 57 – A thermostat that measures mean radiant temperature

The second way is to explicitly add a thermal comfort constraint to the objective function in the form of a slack variable (Y. Ma et al., 2012). Since this kind of constraint can be explicitly seen in the optimization formulation, it is called the explicit constraint. The penalty function used in this study is as follows:

$$F^*(\mathbf{x}) = C_{elec}\left(\frac{E_{c,id}}{\mathrm{COP}} + E_{fan}\right) + \frac{C_{ng} \cdot E_{h,id}}{\eta_h} + \alpha\left|T_{ht} - T_{op}\right| \quad (38)$$

where α is the penalty parameter; T_{ht} is the heating setpoint, °C; T_{op} is the operative temperature, °C. The penalty parameter should be properly chosen so that the penalty term is at least one order of magnitude larger than the rest of the penalty function but not too large to impair the optimization algorithm's efficiency and accuracy. By trial and error, we found that 0.02 is a proper value. Violating the thermal comfort constraint will cause the objective function's numerical value to rise dramatically. Thus, the optimizer will reduce the time when the thermal mass is cooled by the cold outside air during the night to avoid violation of this constraint.

In order to compare the performance of implicit constraint and explicit constraint, we run a simulation from May 10th to 14th using four different control methods, as shown in Table 18. The period from May 1st to 9th is used for warming up. In this case, the insulation layer is opaque and has a U-factor of 0.7 W/(m^2·K). The thickness of the concrete layer is 20 cm. In all four control methods, the cooling system is triggered once the air temperature rises above 24°C during the occupied hours (6:00 to 24:00 on weekdays and 6:00 to 17:00 on Saturday). The trigger mechanism for the heating system differs for different control methods. The first control method, labelled as "No constraint", has no heating setpoint and thus no heating energy cost, so the optimizer will try to make the best of night cooling to minimize the cooling energy cost. The second control method, labelled as "Implicit constraint", uses the operative temperature as the controlled variable for heating. When the operative temperature falls below 21°C, the heating system is turned on. The third control method, labelled as "Explicit constraint", also has no heating setpoint. However, a soft constraint is imposed on the optimization problem to penalize any operative temperature below 21°C, as shown in Equation 38. The fourth control method, labelled as "No MPC", uses the air temperature as the controlled variable for heating and in this method the ventilated façade is always in state 0.

Table 18 – Comparison of the four control methods

Control method	Cooling criterion	Heating criterion	Objective function	Control

No constraint	$T_{air} > 24°C$	No heating setpoint	C_{HVAC}	MPC
Implicit constraint	$T_{air} > 24°C$	$T_{op} < 21°C$	C_{HVAC}	MPC
Explicit constraint	$T_{air} > 24°C$	No heating setpoint	$C_{HVAC} + \alpha\lvert T_{ht} - T_{op}\rvert$	MPC
No MPC	$T_{air} > 24°C$	$T_{air} < 21°C$	C_{HVAC}	Always 0

The comparison of operative temperature between the four control methods is shown in Figure 58 and the comparison of control decisions of the first three control methods is shown in Figure 59. The operative temperature of “No MPC” is prominently higher than that of the rest, because it does not take advantage of free cooling at all. The operative temperature of “No constraint” falls below 21°C at the begging of the occupied hours on all five days. On the second day, which is the coldest day, the operative temperature does not rise above 21°C until 10:00 a.m. The operative temperature of both “Implicit constraint” and “Explicit constraint” satisfies the thermal comfort constraint, but different strategies are used. We call the action of intentionally turning off the ventilation fan to avoid overcooling as “brake”. On day 3 and day 4, “Explicit constraint” control brakes from 22:00 to 24:00. At 6:00 in the next morning, the operative temperature is a little lower than 21°C, so heating system is turned on to bring the operative temperature up to 21°C rapidly. In contrast, “Implicit constraint” control brakes from 4:00 to 6:00, right before the occupied hours, to avoid violation of the thermal comfort constraint.

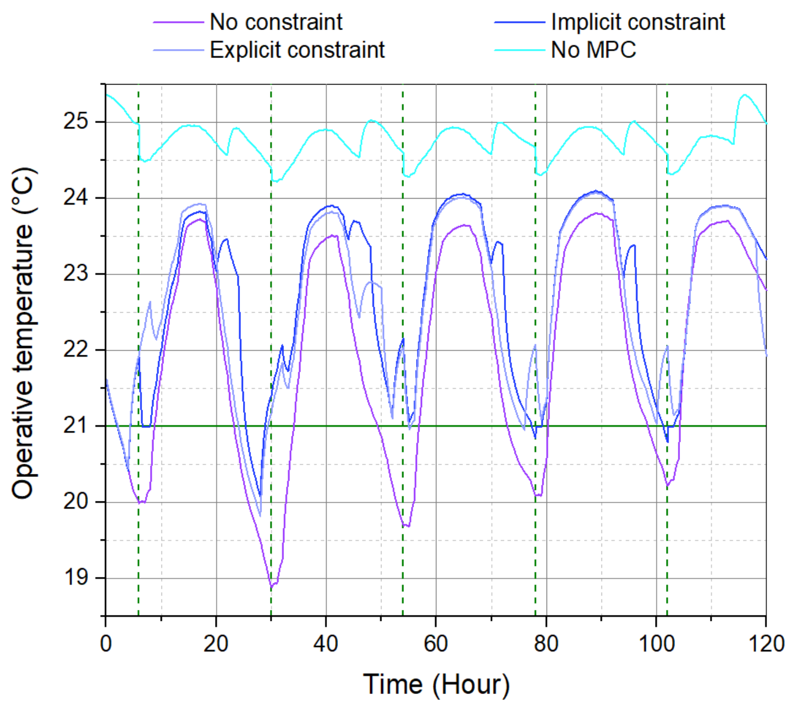

Figure 58 – The comparison of operative temperature between the four control methods (The solid olive line marks the thermal comfort threshold (21°C) and the dashed olive lines mark the beginning of the occupied hours each day (6:00).)

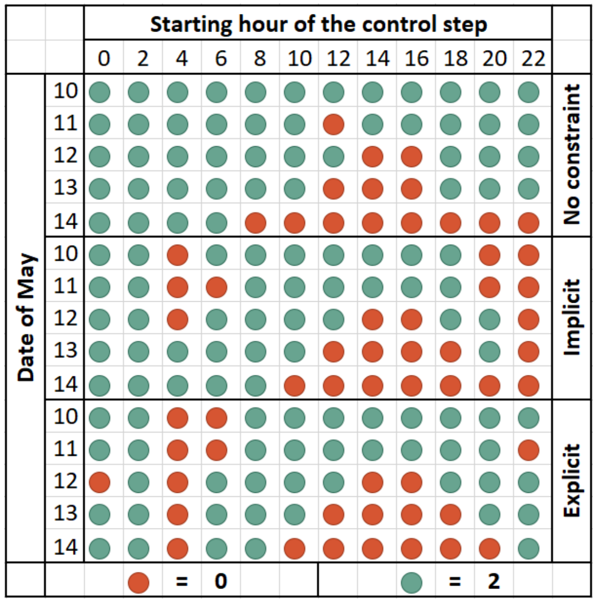

Figure 59 – The comparison of control decisions of the three control methods

It is worth mentioning that it is only possible to use the lower bound of the comfort zone ($\alpha|T_{ht} - T_{op}|$) as an explicit constraint on the control optimization problem. If the upper bound of the comfort zone ($\alpha|T_{op} - T_{cl}|$, where T_{cl} is the cooling setpoint, °C) is used as an explicit constraint and the cooling system is removed, the optimization problem will be infeasible. The reason is that during the day the outdoor air temperature is close to or even higher than the cooling setpoint, 24°C, which means that the ventilated façade is unable to reduce the operative temperature during the day regardless of which control state is used. If the user insists on using $\alpha|T_{op} - T_{cl}|$ as a penalty term, the optimizer will output some very inefficient control decisions, e.g. choosing control state 2 all the time. This is still not the worst case. If the user imposes $T_{op} \leq T_{cl}$ on the problem as a hard constraint, the optimizer may just crash without yielding any control decisions. This explains why soft constraints are always recommended over hard constraints in MPC.

The comparison of energy cost between the four control methods is shown in Figure 60. It is obvious that the total energy cost of "No MPC" is the highest, \$1.63, and the total energy cost of "No constraint" is the lowest, \$0.56, at the expense of violation of thermal comfort constraint. The total energy costs of "Implicit constraint" and "Explicit constraint" are both \$0.66. Although their energy performance is almost identical, the two types of constraint have their respective pros and cons. The implicit constraint is robust and versatile, but it has some requirements on the physical building systems. In this case, the implicit constraint can handle both heating constraint and cooling constraint and work effectively all year round. However, it requires the building to be equipped with a sufficiently large heating system and a sufficiently large cooling system, which may be exorbitant in some cases. As can be seen in Figure 60, the energy cost profile of "Implicit constraint" has some spikes after 6:00 a.m. These spikes reflect the large capacity of the heating system. The explicit constraint, on the other hand, affects the optimizer instead of the physical building systems. However, its application is limited to certain scenarios and it has the possibility of making the optimization problem infeasible. Therefore, the selection of constraint should be based on a comprehensive assessment.

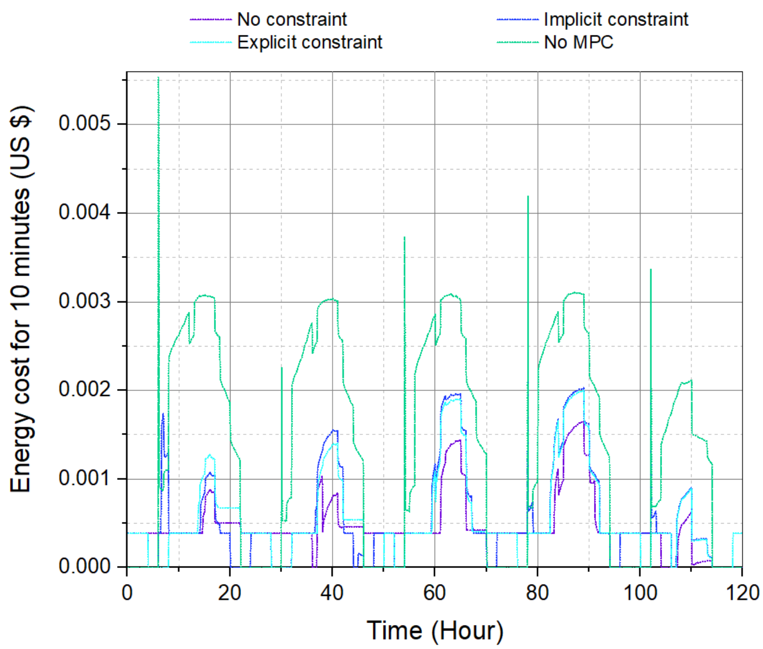

Figure 60 – The comparison of energy cost between the four control methods

5.3.7 Design Optimization with Nested MPC

As discussed in Section 4.5.1, for design problems with MPC the nested optimization framework should be used. In this section, we assume that the insulation layer of the ventilated façade is built of translucent materials and its SHGC and U-factor can be changed by using different materials. Numerous translucent wall manufacturers can be found on the internet, such as Duo-Gard, Kalwall, and Extech. The third design variable is the thickness of the concrete layer. Brute-force search is adopted for the design optimization. The design variables and their levels are shown in Table 19. A total of 5 × 5 × 3 = 75 design cases are simulated. Ideally, we should evaluate the objective function of a design case over the whole year in order to obtain an unbiased evaluation of the design. However, due to the massive computation required by MPC, we can only afford to run 14 days in the winter and 14 days in the summer for each design case. We will use the objective function value over these 28 days as an approximation of that over the whole year. In the winter, the warm-up period is from January 1st to 7th and the simulation period is from January 8th to 21st. In the summer, the warm-up period is from July 1st to 7th and the simulation period is from July 8th to 21st. The implicit constraint is adopted, and the operative temperature is used as the controlled variable for both heating and cooling. Genetic algorithm is adopted to solve the control optimization problem. It takes around 1.3 hours to complete the simulation of one design case over 14 days with MPC. Since genetic algorithm is a population-based algorithm and cannot guarantee the true optimality of its output, we have to run the optimization multiple times and manually combine the best control decisions of different design cases to obtain a set of control decisions that is close to true optimality.

Table 19 – Design variables and their levels for the nested optimization

Design variable 1	Levels	Design variable 2	Levels	Design variable 3	Levels
SHGC of the translucent insulation layer	0	Thickness of the concrete layer (cm)	10	U-factor of the translucent layer (W/(m^2·K))	0.7
	0.2		15		1
	0.4		20		1.3
	0.6		25		
	0.8		30		

The optimized control decisions of three different design cases are shown in Figure 61. It can be seen that the design parameter, SHGC, has a great impact on the optimized control decisions. When the SHGC is 0, i.e. the insulation layer is opaque, most of the control states are 0. When the SHGC rises to 0.4, significantly more control states 2 are used to neutralize the additional solar heat gain. When the SHGC reaches 0.8, the number of control state 2 increases again and at 12:00 noon control state 1 is used to expel the hot air in the channel to the outside.

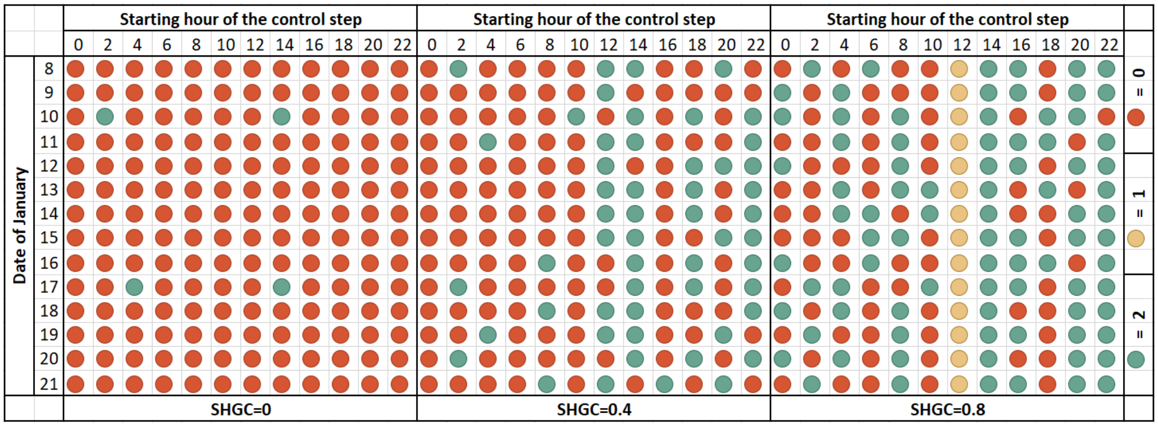

Figure 61 – The optimized control decisions of different design cases

Figure 62 shows the total HVAC energy cost (U.S. $) of different design cases. It consists of four parts. The top left part shows the energy cost in January without MPC. By comparing it with the top right part (the energy cost in January with MPC), we can see that MPC has the ability of reducing the difference of performance between good and poor designs, which supports the conclusion made in Section 5.1.6 that ABE systems can reduce the sensitivity of building performance to design parameters. Without MPC, the energy cost of the worst design is 7.41 times that of the best design. With MPC, this value is reduced to 3.63. This is great news for architects, because now they can focus on the aesthetic aspect of the building and do not need to worry about the performance too much as long as MPC is adopted.

In January, there are two almost equally optimal designs. One is SHGC = 0, thickness = 30 cm, and U-factor = 0.7 W/(m^2·K). The other is SHGC = 0, thickness = 15 cm, and U-factor = 1.3 W/(m^2·K). Since the building is cooling dominated during the day in January, the first design uses high insulation to block the solar heat, while the second design uses low insulation to release the heat in the room to the cold outside. In July, the optimal design is SHGC = 0 and U-factor = 0.7 W/(m2·K). The impact of thickness on the energy cost is negligible. In terms of whole year performance, the optimal design is SHGC = 0, thickness = 30 cm, and U-factor = 0.7 W/(m^2·K), but the impact of both thickness and U-factor are very small compared to SHGC. In this case, other factors like initial investment, structural stability, and noise-cancelling ability should be considered to make the final decision.

January no MPC

U-factor of the translucent layer [W/(m^2·K)]	SHGC of the translucent layer	Thickness of the concrete layer [cm]: 10	15	20	25	30
0.7	0	1.810	1.672	1.556	1.516	1.457
0.7	0.2	3.387	3.222	3.165	3.124	2.981
0.7	0.4	5.261	5.377	5.299	5.208	5.163
0.7	0.6	8.021	7.851	7.534	7.619	7.529
0.7	0.8	10.801	10.641	10.522	10.395	10.106
1	0	1.734	1.740	1.681	1.554	1.458
1	0.2	3.018	2.855	2.750	2.695	2.590
1	0.4	4.757	4.834	4.757	4.622	4.566
1	0.6	7.314	7.114	6.778	6.869	6.773
1	0.8	9.964	9.767	9.609	9.445	9.132
1.3	0	1.443	1.401	1.619	1.625	1.582
1.3	0.2	2.745	2.580	2.456	2.394	2.305
1.3	0.4	4.357	4.431	4.328	4.163	4.100
1.3	0.6	6.739	6.517	6.191	6.295	6.183
1.3	0.8	9.283	9.067	8.884	8.695	8.369

January

U-factor of the translucent layer [W/(m^2·K)]	SHGC of the translucent layer	Thickness of the concrete layer [cm]: 10	15	20	25	30
0.7	0	1.623	1.514	1.439	1.273	1.207
0.7	0.2	1.985	1.848	1.718	1.649	1.605
0.7	0.4	2.470	2.056	1.826	1.794	1.649
0.7	0.6	3.718	3.393	3.027	2.776	2.619
0.7	0.8	4.379	3.809	3.676	3.383	3.394
1	0	1.527	1.521	1.516	1.416	1.358
1	0.2	1.908	2.022	1.664	1.569	1.564
1	0.4	2.432	1.996	1.724	1.769	1.546
1	0.6	3.674	3.262	3.016	2.735	2.019
1	0.8	4.304	3.668	3.555	3.271	3.244
1.3	0	1.280	1.216	1.420	1.440	1.437
1.3	0.2	1.892	2.004	1.655	1.527	1.559
1.3	0.4	2.415	1.985	1.684	1.730	1.509
1.3	0.6	3.477	3.085	2.995	2.741	2.357
1.3	0.8	4.260	3.581	3.445	3.161	3.109

July

U-factor of the translucent layer [W/(m^2·K)]	SHGC of the translucent layer	Thickness of the concrete layer [cm]: 10	15	20	25	30
0.7	0	7.002	7.032	7.078	7.085	7.080
0.7	0.2	7.717	7.739	7.767	7.773	7.761
0.7	0.4	8.683	8.623	8.648	8.674	8.697
0.7	0.6	10.010	9.923	9.765	9.736	9.754
0.7	0.8	11.083	11.133	11.096	11.065	10.853
1	0	7.085	7.108	7.123	7.165	7.191
1	0.2	7.683	7.703	7.729	7.732	7.716
1	0.4	8.612	8.549	8.569	8.590	8.608
1	0.6	9.891	9.795	9.657	9.597	9.614
1	0.8	11.069	11.035	11.004	10.965	10.798
1.3	0	7.265	7.289	7.224	7.188	7.220
1.3	0.2	7.654	7.673	7.697	7.697	7.678
1.3	0.4	8.552	8.487	8.503	8.520	8.535
1.3	0.6	9.792	9.688	9.558	9.481	9.492
1.3	0.8	10.980	10.947	10.915	10.926	10.621

January + July

U-factor of the translucent layer [W/(m^2·K)]	SHGC of the translucent layer	Thickness of the concrete layer [cm]: 10	15	20	25	30
0.7	0	8.625	8.546	8.516	8.359	8.286
0.7	0.2	9.702	9.587	9.485	9.423	9.366
0.7	0.4	11.153	10.679	10.474	10.468	10.346
0.7	0.6	13.728	13.316	12.792	12.512	12.373
0.7	0.8	15.463	14.942	14.772	14.449	14.247
1	0	8.611	8.629	8.639	8.581	8.550
1	0.2	9.591	9.726	9.393	9.300	9.279
1	0.4	11.044	10.546	10.293	10.359	10.154
1	0.6	13.566	13.057	12.673	12.331	11.632
1	0.8	15.373	14.703	14.559	14.236	14.042
1.3	0	8.545	8.506	8.644	8.628	8.656
1.3	0.2	9.546	9.677	9.353	9.224	9.237
1.3	0.4	10.967	10.472	10.187	10.250	10.044
1.3	0.6	13.269	12.773	12.553	12.222	11.849
1.3	0.8	15.239	14.528	14.360	14.087	13.730

Figure 62 – The total HVAC energy cost (U.S. \$) of different design cases

In order to quantify the sensitivity of HVAC energy cost to changes in the design parameters and control parameter, an analysis of variance (ANOVA) test is run for HVAC energy cost in January using Minitab (Minitab LLC., 2019). SHGC, U-factor, and thickness are chosen as continuous predictors, and whether MPC control is adopted is chosen as a categorical predictor. The second-order interactions between different predictors are also included in the model. The report is shown below. The F-value can be seen as an indicator of the relative importance of the predictors. We can see that the predictors that have the greatest impact on HVAC energy cost are SHGC*Control and SHGC, which means SHGC is the most important design parameter and the optimal control sequence heavily depends on SHGC. The impact of all other predictors on the response is far less significant. The impact of Thickness and U-factor*Thickness is so trivial that these two predictors should probably be removed from the model. Therefore, for this ventilated façade in January, it is better to choose SHGC based on the nested optimization result, choose U-factor and thickness according to other criteria, such as structural stability, and then optimize the control sequence for the chosen design parameters.

```
Analysis of Variance

Source               DF   Adj SS   Adj MS  F-Value  P-Value
Regression           10   988.80   98.880   763.09    0.000
  SHGC                1    75.07   75.066   579.31    0.000
  U-factor            1     0.66    0.664     5.13    0.025
  Thickness           1     0.01    0.010     0.08    0.784
  Control             1     1.26    1.258     9.71    0.002
  SHGC*U-factor       1     2.26    2.256    17.41    0.000
  SHGC*Thickness      1     1.46    1.465    11.30    0.001
  U-factor*Thickness  1     0.01    0.008     0.06    0.802
  SHGC*Control        1   161.18  161.179  1243.87    0.000
  U-factor*Control    1     4.24    4.241    32.73    0.000
  Thickness*Control   1     0.44    0.444     3.43    0.066
Error               139    18.01    0.130
Total               149  1006.82
```

CHAPTER 6. CLOSURE

6.1 Contributions of This Thesis

This thesis is a comprehensive review of previous studies on ABE and lays the foundation for future ones by developing some critical concepts and methods. Different from most previous studies on ABE that only focus on a specific aspect of the subject, this thesis looks at the overall picture and the methods proposed by this thesis are intended to benefit all the research in this field. For previous studies, this thesis unifies the inconsistent or even contradictory definitions of some concepts in the literature into one concept system, summarizes the existing modelling methods for ABE technologies, and critically reviews the optimization approaches adopted by previous studies. For future studies, this thesis identifies four weather variables that determine the energy saving potential of ABE systems and proposes methods to calculate the energy saving potential associated with each of them, develops modelling methods for ABE technologies that cannot be modelled by existing methods, makes recommendations for choosing the suitable optimization approaches in different application scenarios, and proposes a generic optimization framework for ABE that can guide the formulation of optimization problems in future application studies.

6.1.1 The Energy Saving Potential of ABE Technologies

This thesis identifies four weather variables (outdoor dry-bulb temperature, outdoor wet-bulb temperature, sky temperature, and solar radiation) that dictate the energy saving potential of ABE technologies. All ABE technologies can be associated with one or several of these weather variables. Methods to calculate the energy saving potential of utilizing these weather variables are presented, which can be used in the preliminary analysis and selection of appropriate ABE technologies for a building.

6.1.2 Modelling Methods for ABE Technologies

This thesis summarizes and develops modelling methods for ABE technologies using EnergyPlus. In general, the modelling method of an ABE system consists of a control module, a physical module, and an interface. Some ABE systems, such as electrochromic windows, dynamic louvers/blinds, and PCM systems, can be modelled by existing modules in EnergyPlus. Others have to be modelled with some workarounds proposed by this thesis. These modelling methods will benefit future ABE researchers and designers who want to integrate ABE technologies into their designs.

6.1.3 A Generic Optimization Framework for ABE

A generic optimization framework for ABE is proposed. In this framework, four application scenarios are discussed, which are product development, building design, building operation, and theoretical research. This framework makes recommendations for selecting the appropriate optimization approach and offers detailed guidance on how to formulate optimization problems in different application scenarios. Following this framework, the researchers, developers, and designers can select the appropriate optimization approach to their problems, formulate the optimization problems efficiently, and avoid making mistakes that are common in previous studies.

This thesis also presents three application studies that demonstrate how to use this framework in three application scenarios, i.e. product development, building design, and building operation. These application studies not only enrich the framework but also can be used as paradigms for formulating and solving ABE optimization problems.

6.2 Limitations of This Thesis

6.2.1 Solving ABE Optimization Problems

In an ABE optimization project, the next step of formulating the optimization problem is to solve the optimization problem. Solving an optimization problem involves the construction of the building model, the use of a toolchain that integrates different building performance simulation programs and the optimization program, and the selection of proper optimization algorithms. In this thesis, the construction of the building model is discussed in CHAPTER 3. Modelling Methods of ABE Systems and application study 3, but the use of toolchains and the selection of proper optimization algorithms are not discussed at length. The reason is that these topics have been thoroughly discussed in a number of studies while the discussion on the formulation of the optimization problem in the literature is scarce. Nevertheless, the formulation of optimization problems and the selection of optimization algorithms are sometimes interrelated. A proper optimization algorithm is able to reach the global optimum efficiently while an inappropriate optimization algorithm may either have trouble finding the global optimum or spend an excessive amount of time doing so. Although the formulation of optimization problems is an intriguing and unexplored field itself, inclusion of optimization algorithms in the discussion will make the thesis more complete.

6.2.2 Cost Model

In scenario 2 of application study 1 (Section 5.1.8), some cost models are developed to estimate the initial investment of the façade. The data that these cost models are based on are from multiple sources, including journal papers (Menzies & Wherrett, 2005; Pikas et al., 2014), RSMeans Building Construction Cost Data 2016(Plotner et al., 2015), and Alibaba.com. The cost data from the first source may not be representative enough of the products on the market and may be outdated. The cost data from the second source are reliable, but they may be outdated and are U.S. national average values and cannot reflect the difference between different regions. The cost data from the third source are the prices provided by the manufacturers, which may be unreliable and inaccurate.

In the calculation of operation cost in application study 1 and application study 3, the cost of electricity and natural gas is estimated based on national average prices, which cannot reflect the difference between different regions. All the maintenance cost is not considered, because its value is highly uncertain, and it is beyond the author's ability to even make a rough estimation of its value.

6.2.3 Characteristics of the Selective Reflective Coating

In application study 2, the original plan is to use the authentic characteristics of this coating to determine the feasible region of the optimization problem. Unfortunately, the authentic characteristics of this coating are still unavailable by the time application study 2 was conducted. As a result, some pseudo characteristics of the coating are chosen by the author based on his experience to generate the feasible region. Since the purpose of application study 2 is to demonstrate the implementation of the optimization framework in product development, using authentic or pseudo characteristics does not influence the demonstration of the method.

6.3 Future Work

6.3.1 The Energy Saving Potential of ABE Technologies

The energy saving potential of ABE systems comes from two sources, i.e. blocking the adverse factors in the outdoor environment and admitting the favorable ones. In this thesis, the modelling methods associated with the four weather variables can only account for the energy saving potential that stems from the second source. Thus, the usage of energy saving potential is limited to the preliminary analysis and selection of appropriate ABE technologies for a building, and DOP can only be used to measure the performance of a few ABE systems, such as ventilated façade and evaporative cooling systems. In the next step, we will try to find a way to quantify the energy saving potential that stems from the first source and make DOP a universal measure of the performance of ABE systems.

6.3.2 The Selection of ABE Technologies

In this thesis, the task of selecting the appropriate ABE technology combination is performed by experts. This is by far the most practical and efficient method. However, experienced experts are not always available, and their service can be costly. Besides, even the judgement of an experienced experts may be biased and unreliable sometimes. The ideal solution is to leave this task to an intelligent tool. There are three possible ways of doing it. The first is to create a database that includes all the ABE studies and applications. Then, this database can directly make selection decisions using artificial intelligence or provide recommendations for an expert. This method takes a tremendous amount of effort but can benefit the largest number of people. The second way is to create a generic tool that can yield quick results based on simplified normative models. This method is relatively easy to implement and helpful for early-stage designs, but its rough results may be of little use to detailed designs. The third way is to train an artificial neural network model which can make the selection based on the location and type of the building. However, this method requires large volumes of data and its predictive power is limited to scenarios covered by the training data.

6.3.3 MPC

There are a number of interesting topics about MPC to be investigated. The first and also the most critical one is how to improve the computational efficiency model predictive controllers. There are several ways to realize this. The first is to employ reduced-order building models, such as resistance-capacitance models (Y. Ma et al., 2012). The computational effort can be greatly reduced when the model is linearized in some manner and linearization is the only method that has found any wider use in industry beyond demonstration projects (Morari & H. Lee, 1999). The second way is to extract control rules from the control decisions made by model predictive controllers and express these rules in some simple models (May-Ostendorp, Henze, Corbin, Rajagopalan, & Felsmann, 2011). Other ways include dividing the planning horizons into blocks (Corbin et al., 2013), combining MPC and RBC, etc. All of these methods require further investigation and development.

Another interesting topic is the comparison between MPC and RBC. When using the same control step, MPC always performs better than RBC. However, it is possible to adopt a control step as short as a few minutes for RBC, but for MPC the order of magnitude of control step is usually hours due to the limitation of computation time. Besides, the investment on a model predictive controller is usually much higher than a proportional-integral-derivative (PID) controller. Therefore, two questions need to be answered before deciding on which control method to use. First, as the control step of MPC gets longer, is its performance still better than RBC? Second, provided that the performance of MPC is indeed superior to RBC, is the better performance worth the extra investment?

REFERENCES

Al-Nimr, M. A., Asfar, K. R., & Abbadi, T. T. (2009). Design of a Smart Thermal Insulation System. *Heat Transfer Engineering, 30*(9), 762-769. doi:10.1080/01457630802678664

Al-Saadi, S. N., & Zhai, Z. (2013). Modeling phase change materials embedded in building enclosure: A review. *Renewable and Sustainable Energy Reviews, 21*, 659-673. doi:https://doi.org/10.1016/j.rser.2013.01.024

American Society of Heating Refrigerating and Air-Conditioning Engineers. (2007). ANSI/ASHRAE Standard 90.2-2007: Energy-Efficient Design of Low-Rise Residential Buildings. In: ASHRAE, Inc.

American Society of Heating Refrigerating and Air-Conditioning Engineers. (2010). ANSI/ASHRAE standard 55-2010: thermal environmental conditions for human occupancy. In. Atlanta, Ga.: ASHRAE, Inc.

American Society of Heating Refrigerating and Air-Conditioning Engineers. (2013). *ASHRAE Handbook: Fundamentals* [1 online resource (1 volume (various pagings)) : illustrations](SI edition. ed.). Retrieved from http://app.knovel.com/hotlink/toc/id:kpASHRAEC1/2013-ashrae-handbook

http://proxy.library.carleton.ca/login?url=http://app.knovel.com/hotlink/toc/id:kpASHRAEC1/2013-ashrae-handbook

American Society of Heating Refrigerating and Air-Conditioning Engineers. (2014). *2014 ASHRAE Handbook: Refrigeration*(Vol. 1).

American Society of Heating Refrigerating and Air-Conditioning Engineers. (2016). ANSI/ASHRAE Standard 90.1-2016: Energy Standard for Buildings Except Low-Rise Residential Buildings. In: ASHRAE, Inc.

Arasteh, D., Kohler, C., & Griffith, B. (2009). *Modeling windows in Energy Plus with simple performance indices*. Retrieved from http://gaia.lbl.gov/btech/papers/2804.pdf

Arens, E., & Zhang, H. (2006). 16 - The skin's role in human thermoregulation and comfort. In N. Pan & P. Gibson (Eds.), *Thermal and Moisture Transport in Fibrous Materials* (pp. 560-602): Woodhead Publishing.

Babulanam, S. M., Eriksson, T. S., Niklasson, G. A., & Granqvist, C. G. (1987). Thermochromic VO2 films for energy-efficient windows. *Solar Energy Materials, 16*(5), 347-363. doi:https://doi.org/10.1016/0165-1633(87)90029-3

Bachevillier, S., Yuan, H.-K., Strang, A., Levitsky, A., Frey, G. L., Hafner, A., . . . Stingelin, N. (2019). Fully Solution-Processed Photonic Structures from Inorganic/Organic Molecular Hybrid Materials and Commodity Polymers. *Advanced Functional Materials, 29*(21), 1808152. doi:10.1002/adfm.201808152

Baetens, R., Jelle, B. P., & Gustavsen, A. (2010). Properties, requirements and possibilities of smart windows for dynamic daylight and solar energy control in buildings: A state-of-the-art review. *Solar Energy Materials and Solar Cells, 94*(2), 87-105. doi:https://doi.org/10.1016/j.solmat.2009.08.021

Balcomb, J. D., Hedstrom, J. C., & Mcfarland, R. D. (1977). Simulation Analysis of Passive Solar Heated Buildings - Preliminary-Results. *Solar Energy, 19*(3), 277-282. doi:Doi 10.1016/0038-092x(77)90071-8

Balocco, C. (2002). A simple model to study ventilated facades energy performance. *Energy and Buildings, 34*(5), 469-475. doi:https://doi.org/10.1016/S0378-7788(01)00130-X

Bechinger, C., Ferrere, S., Zaban, A., Sprague, J., & Gregg, B. A. (1996). Photoelectrochromic windows and displays. *Nature, 383*(6601), 608-610. doi:10.1038/383608a0

Benson, D. K., Potter, T. F., & Tracy, C. E. (1994). Design of a Variable-Conductance Vacuum Insulation. *SAE Transactions, 103*, 176-181. Retrieved from http://www.jstor.org/stable/44581241

Berge, A., Hagentoft, C.-E., Wahlgren, P., & Adl-Zarrabi, B. (2015). Effect from a Variable U-Value in Adaptive Building Components with Controlled Internal Air Pressure. *Energy Procedia, 78*, 376-381. doi:https://doi.org/10.1016/j.egypro.2015.11.677

Bergeron, B. V., White, K. C., Boehme, J. L., Gelb, A. H., & Joshi, P. B. (2008). Variable Absorptance and Emittance Devices for Thermal Control. *The Journal of Physical Chemistry C, 112*(3), 832-838. doi:10.1021/jp076336d

Berry, R., Livesley, S. J., & Aye, L. (2013). Tree canopy shade impacts on solar irradiance received by building walls and their surface temperature. *Building and Environment, 69*, 91-100. doi:https://doi.org/10.1016/j.buildenv.2013.07.009

Blanchard, B. S., & Fabrycky, W. J. (2005). *Systems Engineering and Analysis* (4th ed.). Englewood Cliffs, NJ: Prentice Hall.

Borrelli, F., Bemporad, A., & Morari, M. (2017). *Predictive Control for Linear and Hybrid Systems*. Cambridge: Cambridge University Press.

Brahme, R., O'Neill, Z., Sisson, W., & Otto, K. (2009). *Using existing whole building energy tools for designing net-zero energy buildings–challenges and workarounds*.

Paper presented at the Eleventh International IBPSA Conference, Glasgow, Scotland.

Chae, Y. T., & Strand, R. K. (2013). Modeling ventilated slab systems using a hollow core slab: Implementation in a whole building energy simulation program. *Energy and Buildings, 57*, 165-175. doi:https://doi.org/10.1016/j.enbuild.2012.10.036

Chan, A. L. S., Chow, T. T., Fong, K. F., & Lin, Z. (2009). Investigation on energy performance of double skin façade in Hong Kong. *Energy and Buildings, 41*(11), 1135-1142. doi:https://doi.org/10.1016/j.enbuild.2009.05.012

Chan, H. Y., Riffat, S. B., & Zhu, J. (2010). Review of passive solar heating and cooling technologies. *Renewable & Sustainable Energy Reviews, 14*(2), 781-789. doi:10.1016/j.rser.2009.10.030

Chun, W., & Chen, K. (2002). Test results of a bi-directional thermodiode system for solar energy utilization. *Solar Energy, 73*(4), 269-280. doi:https://doi.org/10.1016/S0038-092X(02)00064-6

Chun, W., Chen, K., & Kim, H. T. (2002). Performance Study of a Bi-Directional Thermodiode Designed for Energy-Efficient Buildings. *Journal of Solar Energy Engineering, 124*(3), 291-299. doi:10.1115/1.1498849

Ciampi, M., Leccese, F., & Tuoni, G. (2003). Ventilated facades energy performance in summer cooling of buildings. *Solar Energy, 75*(6), 491-502. doi:https://doi.org/10.1016/j.solener.2003.09.010

Corbin, C. D., Henze, G. P., & May-Ostendorp, P. (2013). A model predictive control optimization environment for real-time commercial building application. *Journal of Building Performance Simulation, 6*(3), 159-174. doi:10.1080/19401493.2011.648343

Cuce, P. M., & Riffat, S. (2016). A state of the art review of evaporative cooling systems for building applications. *Renewable and Sustainable Energy Reviews, 54*, 1240-1249. doi:https://doi.org/10.1016/j.rser.2015.10.066

Cupelli, D., Pasquale Nicoletta, F., Manfredi, S., Vivacqua, M., Formoso, P., De Filpo, G., & Chidichimo, G. (2009). Self-adjusting smart windows based on polymer-dispersed liquid crystals. *Solar Energy Materials and Solar Cells, 93*(11), 2008-2012. doi:https://doi.org/10.1016/j.solmat.2009.08.002

Curcija, C., Vidanovic, S., Hart, R., Jonsson, J., & Mitchell, R. (2018). *WINDOW Technical Documentation*. Retrieved from

de Gracia, A., Navarro, L., Castell, A., Ruiz-Pardo, Á., Alvárez, S., & Cabeza, L. F. (2013). Experimental study of a ventilated facade with PCM during winter period. *Energy and Buildings, 58*, 324-332. doi:https://doi.org/10.1016/j.enbuild.2012.10.026

de Gracia, A., Navarro, L., Castell, A., Ruiz-Pardo, Á., Álvarez, S., & Cabeza, L. F. (2013). Thermal analysis of a ventilated facade with PCM for cooling applications. *Energy and Buildings, 65*, 508-515. doi:https://doi.org/10.1016/j.enbuild.2013.06.032

Deru, M., Field, K., Studer, D., Benne, K., Griffith, B., Torcellini, P., . . . Crawley, D. (2011). *U.S. Department of Energy Commercial Reference Building Models of the National Building Stock* (TP-5500-46861). Retrieved from

Downey, J. A., & Lemons, D. E. (1994). Chapter 13 - Human Thermoregulation. In J. A. Downey, S. J. Myers, E. G. Gonzalez, & J. S. Lieberman (Eds.), *The Physiological Basis of Rehabilitation Medicine (Second Edition)* (pp. 351-363): Butterworth-Heinemann.

El Mankibi, M., Zhai, Z., Al-Saadi, S. N., & Zoubir, A. (2015). Numerical modeling of thermal behaviors of active multi-layer living wall. *Energy and Buildings, 106*, 96-110. doi:https://doi.org/10.1016/j.enbuild.2015.06.084

Energy Star. (2018). *Portfolio Manager Technical Reference*. Retrieved from

Evins, R. (2015). Multi-level optimization of building design, energy system sizing and operation. *Energy, 90*, 1775-1789. doi:https://doi.org/10.1016/j.energy.2015.07.007

Favoino, F., Fiorito, F., Cannavale, A., Ranzi, G., & Overend, M. (2016). Optimal control and performance of photovoltachromic switchable glazing for building integration in temperate climates. *Applied Energy, 178*, 943-961. doi:https://doi.org/10.1016/j.apenergy.2016.06.107

Favoino, F., Jin, Q., & Overend, M. (2017). Design and control optimisation of adaptive insulation systems for office buildings. Part 1: Adaptive technologies and simulation framework. *Energy, 127*, 301-309. doi:https://doi.org/10.1016/j.energy.2017.03.083

Favoino, F., Overend, M., & Jin, Q. (2015). The optimal thermo-optical properties and energy saving potential of adaptive glazing technologies. *Applied Energy, 156*, 1-15. doi:https://doi.org/10.1016/j.apenergy.2015.05.065

Feng, W., Zou, L., Gao, G., Wu, G., Shen, J., & Li, W. (2016). Gasochromic smart window: optical and thermal properties, energy simulation and feasibility analysis. *Solar Energy Materials and Solar Cells, 144*, 316-323. doi:https://doi.org/10.1016/j.solmat.2015.09.029

Ferguson, S., Siddiqi, A., Lewis, K., & Weck, O. L. d. (2007, September 4-7). *Flexible and reconfigurable systems: Nomenclature and review.* Paper presented at the ASME 2007 International Design Engineering Technical Conferences & Computers and Information in Engineering Conference, Las Vegas, Nevada, US.

Foliente, G. C. (2000). Developments in performance-based building codes and standards. *Forest Products Journal, 50*(7/8), 12-21.

Georg, A., Georg, A., Graf, W., & Wittwer, V. (2008). Switchable windows with tungsten oxide. *Vacuum, 82*(7), 730-735. doi:https://doi.org/10.1016/j.vacuum.2007.10.020

Ghaffarianhoseini, A., Ghaffarianhoseini, A., Berardi, U., Tookey, J., Li, D. H. W., & Kariminia, S. (2016). Exploring the advantages and challenges of double-skin façades (DSFs). *Renewable and Sustainable Energy Reviews, 60*, 1052-1065. doi:https://doi.org/10.1016/j.rser.2016.01.130

Ghosh, A., Norton, B., & Duffy, A. (2015). Measured overall heat transfer coefficient of a suspended particle device switchable glazing. *Applied Energy, 159*, 362-369. doi:https://doi.org/10.1016/j.apenergy.2015.09.019

Granqvist, C. G. (2007). Transparent conductors as solar energy materials: A panoramic review. *Solar Energy Materials and Solar Cells, 91*(17), 1529-1598. doi:https://doi.org/10.1016/j.solmat.2007.04.031

Gratia, E., & De Herde, A. (2004). Optimal operation of a south double-skin facade. *Energy and Buildings, 36*(1), 41-60. doi:https://doi.org/10.1016/j.enbuild.2003.06.001

Grynning, S., Gustavsen, A., Time, B., & Jelle, B. P. (2013). Windows in the buildings of tomorrow: Energy losers or energy gainers? *Energy and Buildings, 61*, 185-192. doi:https://doi.org/10.1016/j.enbuild.2013.02.029

Hammad, F., & Abu-Hijleh, B. (2010). The energy savings potential of using dynamic external louvers in an office building. *Energy and Buildings, 42*(10), 1888-1895. doi:https://doi.org/10.1016/j.enbuild.2010.05.024

Hashemi, A., & Gage, S. (2012). Technical issues that affect the use of retrofit panel thermal shutters in commercial buildings. *Building Services Engineering Research and Technology, 35*(1), 6-22. doi:10.1177/0143624412462906

Heiselberg, P. (2012). *ECBCS Annex 44 Integrating Environmentally Responsive Elements in Buildings Project Summary Report*. Retrieved from St Albans, UK:

Henze, G. P. (2019). Modeling and simulation in building automation systems. In *Building Performance Simulation for Design and Operation* (2nd Edition ed.). London, UK: Taylor & Francis Group.

Henze, G. P., Felsmann, C., & Knabe, G. (2004). Evaluation of optimal control for active and passive building thermal storage. *International Journal of Thermal Sciences, 43*(2), 173-183. doi:https://doi.org/10.1016/j.ijthermalsci.2003.06.001

Hoes, P., Trcka, M., Hensen, J. L. M., & Hoekstra Bonnema, B. (2011). Investigating the potential of a novel low-energy house concept with hybrid adaptable thermal storage. *Energy Conversion and Management, 52*(6), 2442-2447. doi:https://doi.org/10.1016/j.enconman.2010.12.050

Hoffmann, S., Lee, E. S., & Clavero, C. (2014). Examination of the technical potential of near-infrared switching thermochromic windows for commercial building applications. *Solar Energy Materials and Solar Cells, 123*, 65-80. doi:https://doi.org/10.1016/j.solmat.2013.12.017

Home Ideas. (2016). How Much Do Smart Windows Cost? Retrieved from https://modernize.com/home-ideas/32437/smart-windows-cost

Hosseinzadeh Khaligh, H., Liew, K., Han, Y., Abukhdeir, N. M., & Goldthorpe, I. A. (2015). Silver nanowire transparent electrodes for liquid crystal-based smart windows. *Solar Energy Materials and Solar Cells, 132*, 337-341. doi:https://doi.org/10.1016/j.solmat.2014.09.006

Huang, Y. J., Akbari, H., Taha, H., & Rosenfeld, A. H. (1987). The Potential of Vegetation in Reducing Summer Cooling Loads in Residential Buildings. *Journal of Climate and Applied Meteorology, 26*(9), 1103-1116. doi:10.1175/1520-0450(1987)026<1103:TPOVIR>2.0.CO;2

Imbabi, M. S.-E. (2012). A passive–active dynamic insulation system for all climates. *International Journal of Sustainable Built Environment, 1*(2), 247-258. doi:https://doi.org/10.1016/j.ijsbe.2013.03.002

International Code Council. (2011). *2012 International Energy Conservation Code*.

International Organization for Standardization. (2003). ISO 15099: Thermal performance of windows, doors and shading devices — Detailed calculations. In: ISO.

International Organization for Standardization. (2006). ISO 10077-1: Thermal performance of windows, doors and shutters — Calculation of thermal transmittance — Part 1: General. In: ISO.

International Organization for Standardization. (2008). ISO 13790: Energy performance of buildings- — Calculation of energy use for space heating and cooling. In: ISO.

iPHA. (2018). Active for more comfort: Passive House. In: International Passive House Association.

Jin, Q., Favoino, F., & Overend, M. (2017). Design and control optimisation of adaptive insulation systems for office buildings. Part 2: A parametric study for a temperate climate. *Energy, 127*, 634-649. doi:https://doi.org/10.1016/j.energy.2017.03.096

Joe, J., Choi, W., Kwak, Y., & Huh, J.-H. (2014). Optimal design of a multi-story double skin facade. *Energy and Buildings, 76*, 143-150. doi:https://doi.org/10.1016/j.enbuild.2014.03.002

Kamalisarvestani, M., Saidur, R., Mekhilef, S., & Javadi, F. S. (2013). Performance, materials and coating technologies of thermochromic thin films on smart windows. *Renewable and Sustainable Energy Reviews, 26*, 353-364. doi:https://doi.org/10.1016/j.rser.2013.05.038

Kasinalis, C., Loonen, R. C. G. M., Cóstola, D., & Hensen, J. L. M. (2014). Framework for assessing the performance potential of seasonally adaptable facades using multi-objective optimization. *Energy and Buildings, 79*, 106-113. doi:https://doi.org/10.1016/j.enbuild.2014.04.045

Keeney, R. L., & Raiffa, H. (1993). *Decisions with Multiple Objectives: Preferences and Value Trade-Offs*. Cambridge: Cambridge University Press.

Kerrigan, E. C., Bemporad, A., Mignone, D., Morari, M., & Maciejowski, J. M. (2000, 28-30 June 2000). *Multi-objective prioritisation and reconfiguration for the control of constrained hybrid systems.* Paper presented at the Proceedings of the 2000 American Control Conference. ACC (IEEE Cat. No.00CH36334).

Kerrigan, E. C., & Maciejowski, J. M. (2000). *Soft constraints and exact penalty functions in model predictive control*. Paper presented at the UKACC International Conference (Control 2000), Cambridge, UK.

Khudhair, A. M., & Farid, M. M. (2004). A review on energy conservation in building applications with thermal storage by latent heat using phase change materials. *Energy Conversion and Management, 45*(2), 263-275. doi:https://doi.org/10.1016/S0196-8904(03)00131-6

Killian, M., & Kozek, M. (2016). Ten questions concerning model predictive control for energy efficient buildings. *Building and Environment, 105*, 403-412. doi:https://doi.org/10.1016/j.buildenv.2016.05.034

Kim, D., Cox, S. J., Cho, H., & Yoon, J. (2018). Comparative investigation on building energy performance of double skin façade (DSF) with interior or exterior slat blinds. *Journal of Building Engineering, 20*, 411-423. doi:https://doi.org/10.1016/j.jobe.2018.08.012

Kim, Y.-J., & Park, C.-S. (2017). Multi-criterion stochastic optimal selection of a double glazing system. *Building Simulation, 10*(1), 1-9. doi:10.1007/s12273-016-0311-6

Kimber, M., Clark, W. W., & Schaefer, L. (2014). Conceptual analysis and design of a partitioned multifunctional smart insulation. *Applied Energy, 114*, 310-319. doi:https://doi.org/10.1016/j.apenergy.2013.09.067

Kirimtat, A., Koyunbaba, B. K., Chatzikonstantinou, I., & Sariyildiz, S. (2016). Review of simulation modeling for shading devices in buildings. *Renewable and Sustainable Energy Reviews, 53*, 23-49. doi:https://doi.org/10.1016/j.rser.2015.08.020

Koenders, S. J. M., Loonen, R. C. G. M., & Hensen, J. L. M. (2018). Investigating the potential of a closed-loop dynamic insulation system for opaque building elements. *Energy and Buildings, 173*, 409-427. doi:https://doi.org/10.1016/j.enbuild.2018.05.051

Konstantoglou, M., & Tsangrassoulis, A. (2016). Dynamic operation of daylighting and shading systems: A literature review. *Renewable and Sustainable Energy Reviews, 60*, 268-283. doi:https://doi.org/10.1016/j.rser.2015.12.246

Langdon, W. K. (1980). *Movable Insulation: A Guide to Reducing Heating and Cooling Losses Through the Windows in Your Home*. Emmaus, US: Rodale Press.

Lavappa, P. D., & Kneifel, J. D. (2018). *Energy Price Indices and Discount Factors for Life-Cycle Cost Analysis - 2018* Retrieved from

Lee, E., Selkowitz, S., Bazjanac, V., Inkarojrit, V., & Kohler, C. (2002). *High-performance commercial building façades*. Retrieved from

Lee, E. S., & DiBartolomeo, D. L. (2002). Application issues for large-area electrochromic windows in commercial buildings. *Solar Energy Materials and Solar Cells, 71*(4), 465-491. doi:https://doi.org/10.1016/S0927-0248(01)00101-5

Lee, E. S., DiBartolomeo, D. L., & Selkowitz, S. E. (1998). Thermal and daylighting performance of an automated venetian blind and lighting system in a full-scale private office. *Energy and Buildings, 29*(1), 47-63. doi:https://doi.org/10.1016/S0378-7788(98)00035-8

Lee, E. S., Selkowitz, S. E., Clear, R. D., DiBartolomeo, D. L., Klems, J. H., Fernandes, L. L., . . . Yazdanian, M. (2006). *A design guide for early-market electrochromic windows*. Retrieved from Berkeley, California, USA:

Lee, E. S., & Tavil, A. (2007). Energy and visual comfort performance of electrochromic windows with overhangs. *Building and Environment, 42*(6), 2439-2449. doi:https://doi.org/10.1016/j.buildenv.2006.04.016

Li, D. H. W., Yang, L., & Lam, J. C. (2013). Zero energy buildings and sustainable development implications – A review. *Energy, 54*, 1-10. doi:https://doi.org/10.1016/j.energy.2013.01.070

Li, S. Y., Niklasson, G. A., & Granqvist, C. G. (2012). Thermochromic fenestration with VO2-based materials: Three challenges and how they can be met. *Thin Solid Films, 520*(10), 3823-3828. doi:https://doi.org/10.1016/j.tsf.2011.10.053

Long, L., & Ye, H. (2014). How to be smart and energy efficient: A general discussion on thermochromic windows. *Scientific Reports, 4*, 6427. doi:10.1038/srep06427

https://www.nature.com/articles/srep06427#supplementary-information

Loonen, R. C. G. M. (2018). *Approaches for computational performance optimization of innovative adaptive façade concepts* (Ph.D.). Technische Universiteit Eindhoven, Eindhoven, the Netherlands.

Loonen, R. C. G. M., Favoino, F., Hensen, J. L. M., & Overend, M. (2017). Review of current status, requirements and opportunities for building performance simulation of adaptive facades. *Journal of Building Performance Simulation, 10*(2), 205-223. doi:10.1080/19401493.2016.1152303

Loonen, R. C. G. M., Singaravel, S., Trčka, M., Cóstola, D., & Hensen, J. L. M. (2014). Simulation-based support for product development of innovative building envelope components. *Automation in Construction, 45*, 86-95. doi:https://doi.org/10.1016/j.autcon.2014.05.008

Loonen, R. C. G. M., Trcka, M., Costla, D., & Hensen, J. L. M. (2013). Climate adaptive building shells: State-of-the-art and future challenges. *Renewable & Sustainable Energy Reviews, 25*, 483-493. doi:10.1016/j.rser.2013.04.016

López, F. P., Jensen, R. L., Heiselberg, P., & Ruiz de Adana Santiago, M. (2012). Experimental analysis and model validation of an opaque ventilated facade. *Building and Environment, 56*, 265-275. doi:https://doi.org/10.1016/j.buildenv.2012.03.017

Ma, Y., Kelman, A., Daly, A., & Borrelli, F. (2012). Predictive Control for Energy Efficient Buildings with Thermal Storage: Modeling, Stimulation, and Experiments. *IEEE Control Systems Magazine, 32*(1), 44-64. doi:10.1109/MCS.2011.2172532

Ma, Y., Li, Y., & Zhu, B. (2012). Analysis of the thermal properties of air-conditioning-type building materials. *Solar Energy, 86*(10), 2967-2974. doi:https://doi.org/10.1016/j.solener.2012.07.001

Ma, Y., Zhu, B., & Wu, K. (2000). Preparation of reversible thermochromic building coatings and their properties. *Journal of Coatings Technology, 72*(911), 67-71. doi:10.1007/BF02720527

Mahdavi, A., & Mahattanatawe, P. (2003). *Enclosure systems design and control support via dynamic simulation-assisted optimization*. Paper presented at the Eighth International IBPSA Conference, Eindhoven, Netherlands.

Mahmood, M. H., Sultan, M., Miyazaki, T., Koyama, S., & Maisotsenko, V. S. (2016). Overview of the Maisotsenko cycle – A way towards dew point evaporative cooling. *Renewable and Sustainable Energy Reviews, 66*, 537-555. doi:https://doi.org/10.1016/j.rser.2016.08.022

Mandal, J., Fu, Y., Overvig, A. C., Jia, M., Sun, K., Shi, N. N., . . . Yang, Y. (2018). Hierarchically porous polymer coatings for highly efficient passive daytime radiative cooling. *Science, 362*(6412), 315. doi:10.1126/science.aat9513

Mankins, J. C. (2009). Technology readiness assessments: A retrospective. *Acta Astronautica, 65*(9), 1216-1223. doi:https://doi.org/10.1016/j.actaastro.2009.03.058

Marler, R. T., & Arora, J. S. (2004). Survey of multi-objective optimization methods for engineering. *Structural and Multidisciplinary Optimization, 26*(6), 369-395. doi:10.1007/s00158-003-0368-6

MathWorks. (2019). *MATLAB® Primer*. Retrieved from https://www.mathworks.com/help/pdf_doc/matlab/getstart.pdf

Mattingley, J., Wang, Y., & Boyd, S. (2011). Receding Horizon Control. *IEEE Control Systems Magazine, 31*(3), 52-65. doi:10.1109/MCS.2011.940571

May-Ostendorp, P., Henze, G. P., Corbin, C. D., Rajagopalan, B., & Felsmann, C. (2011). Model-predictive control of mixed-mode buildings with rule extraction. *Building and Environment, 46*(2), 428-437. doi:https://doi.org/10.1016/j.buildenv.2010.08.004

Maydanik, Y. F. (2005). Loop heat pipes. *Applied Thermal Engineering, 25*(5), 635-657. doi:https://doi.org/10.1016/j.applthermaleng.2004.07.010

Menzies, G. F., & Wherrett, J. R. (2005). Multiglazed windows: potential for savings in energy, emissions and cost. *Building Services Engineering Research and Technology, 26*(3), 249-258. doi:10.1191/0143624405bt132tn

Minitab LLC. (2019). Mnitab. Retrieved from https://www.minitab.com/en-us/

Morari, M., & H. Lee, J. (1999). Model predictive control: past, present and future. *Computers & Chemical Engineering, 23*(4), 667-682. doi:https://doi.org/10.1016/S0098-1354(98)00301-9

Nabil, A., & Mardaljevic, J. (2006). Useful daylight illuminances: A replacement for daylight factors. *Energy and Buildings, 38*(7), 905-913. doi:https://doi.org/10.1016/j.enbuild.2006.03.013

National Renewable Energy Laboratory. (2019). OpenStudio. Retrieved from https://www.openstudio.net/

Nielsen, M. V., Svendsen, S., & Jensen, L. B. (2011). Quantifying the potential of automated dynamic solar shading in office buildings through integrated simulations of energy and daylight. *Solar Energy, 85*(5), 757-768. doi:https://doi.org/10.1016/j.solener.2011.01.010

Noie, S. H. (2005). Heat transfer characteristics of a two-phase closed thermosyphon. *Applied Thermal Engineering, 25*(4), 495-506. doi:https://doi.org/10.1016/j.applthermaleng.2004.06.019

Norton, B., Eames, P. C., Mallick, T. K., Huang, M. J., McCormack, S. J., Mondol, J. D., & Yohanis, Y. G. (2011). Enhancing the performance of building integrated photovoltaics. *Solar Energy, 85*(8), 1629-1664. doi:https://doi.org/10.1016/j.solener.2009.10.004

Oh, S. J., Chun, W., Han, H., Kim, J. T., & Chen, K. (2008). Overview of several novel thermodiode designs and their application in buildings. *International Journal of Low-Carbon Technologies, 3*(2), 83-100. doi:10.1093/ijlct/3.2.83

Oral, G. K., Yener, A. K., & Bayazit, N. T. (2004). Building envelope design with the objective to ensure thermal, visual and acoustic comfort conditions. *Building and Environment, 39*(3), 281-287. doi:10.1016/S0360-1323(03)00141-0

Ozel, M. (2011). Effect of wall orientation on the optimum insulation thickness by using a dynamic method. *Applied Energy, 88*(7), 2429-2435. doi:https://doi.org/10.1016/j.apenergy.2011.01.049

Pacific Northwest National Laboratory. (2013, July 11, 2013). Residential Prototype Building Models. Retrieved from https://www.energycodes.gov/development/residential/iecc_models

Pacific Northwest National Laboratory. (2018, October 24, 2018). Commercial Prototype Building Models. Retrieved from https://www.energycodes.gov/development/commercial/prototype_models

Palmero-Marrero, A. I., & Oliveira, A. C. (2010). Effect of louver shading devices on building energy requirements. *Applied Energy, 87*(6), 2040-2049. doi:https://doi.org/10.1016/j.apenergy.2009.11.020

Papaefthimiou, S., Syrrakou, E., & Yianoulis, P. (2006). Energy performance assessment of an electrochromic window. *Thin Solid Films, 502*(1), 257-264. doi:https://doi.org/10.1016/j.tsf.2005.07.294

Park, C.-S., Augenbroe, G., Sadegh, N., Thitisawat, M., & Messadi, T. (2004). Real-time optimization of a double-skin façade based on lumped modeling and occupant preference. *Building and Environment, 39*(8), 939-948. doi:https://doi.org/10.1016/j.buildenv.2004.01.018

Pasquay, T. (2004). Natural ventilation in high-rise buildings with double facades, saving or waste of energy. *Energy and Buildings, 36*(4), 381-389. doi:https://doi.org/10.1016/j.enbuild.2004.01.018

Pflug, T., Kuhn, T. E., Nörenberg, R., Glück, A., Nestle, N., & Maurer, C. (2015). Closed translucent façade elements with switchable U-value—A novel option for energy management via the facade. *Energy and Buildings, 86*, 66-73. doi:https://doi.org/10.1016/j.enbuild.2014.09.082

Pikas, E., Thalfeldt, M., & Kurnitski, J. (2014). Cost optimal and nearly zero energy building solutions for office buildings. *Energy and Buildings, 74*, 30-42. doi:https://doi.org/10.1016/j.enbuild.2014.01.039

Plotner, S. C., Babbitt, C., Charest, A. C., Elsmore, C., & Gomes, J. (2015). *RSMeans Building Construction Cost Data 2016*. Rockland, MA, US: RSMeans.

Raman, A. P., Anoma, M. A., Zhu, L., Rephaeli, E., & Fan, S. (2014). Passive radiative cooling below ambient air temperature under direct sunlight. *Nature, 515*, 540. doi:10.1038/nature13883

Riangvilaikul, B., & Kumar, S. (2010). An experimental study of a novel dew point evaporative cooling system. *Energy and Buildings, 42*(5), 637-644. doi:https://doi.org/10.1016/j.enbuild.2009.10.034

Rogdakis, E., & Tertipis, D. (2015). Maisotsenko cycle: technology overview and energy-saving potential in cooling systems. *Energy and Emission Control Technologies, 3*, 15-22. doi:https://doi.org/10.2147/EECT.S62995

Roth, K., Lawrence, T., & Brodrick, J. (2007). Double-skin facades. *Ashrae Journal, 49*(10), 70-72.

Sadineni, S. B., Madala, S., & Boehm, R. F. (2011). Passive building energy savings: A review of building envelope components. *Renewable & Sustainable Energy Reviews, 15*(8), 3617-3631. doi:10.1016/j.rser.2011.07.014

Saeli, M., Piccirillo, C., Parkin, I. P., Binions, R., & Ridley, I. (2010). Energy modelling studies of thermochromic glazing. *Energy and Buildings, 42*(10), 1666-1673. doi:https://doi.org/10.1016/j.enbuild.2010.04.010

SageGlass®. Performance & Acoustical Data. In *Internet*.

Sbar, N., Badding, M., Budziak, R., Cortez, K., Laby, L., Michalski, L., . . . Urbanik, K. (1999). Progress toward durable, cost effective electrochromic window glazings. *Solar Energy Materials and Solar Cells, 56*(3), 321-341. doi:https://doi.org/10.1016/S0927-0248(98)00141-X

Shameri, M. A., Alghoul, M. A., Sopian, K., Zain, M. F. M., & Elayeb, O. (2011). Perspectives of double skin façade systems in buildings and energy saving. *Renewable and Sustainable Energy Reviews, 15*(3), 1468-1475. doi:https://doi.org/10.1016/j.rser.2010.10.016

Shurcliff, W. A. (1980). *Thermal shutters and shades: over 100 schemes for reducing heat-loss through windows*. Baltimore, US: Brick House Pub. Co.

Snyman, J. A. (2005). *Practical Mathematical Optimization: An Introduction to Basic Optimization Theory and Classical and New Gradient-Based Algorithms*. Boston, MA, USA: Springer.

Stribling, D., & Stigge, B. (2009). *A critical review of the energy savings and cost payback issues of double façades.* Paper presented at the CIBSE/ASHRAE Conference.

Syrrakou, E., Papaefthimiou, S., & Yianoulis, P. (2005). Environmental assessment of electrochromic glazing production. *Solar Energy Materials and Solar Cells, 85*(2), 205-240. doi:https://doi.org/10.1016/j.solmat.2004.03.005

Taylor, B. J., Cawthorne, D. A., & Imbabi, M. S. (1996). Analytical investigation of the steady-state behaviour of dynamic and diffusive building envelopes. *Building and Environment, 31*(6), 519-525. doi:https://doi.org/10.1016/0360-1323(96)00022-4

Taylor, B. J., & Imbabi, M. S. (1998). The application of dynamic insulation in buildings. *Renewable Energy, 15*(1), 377-382. doi:https://doi.org/10.1016/S0960-1481(98)00190-6

Teowee, G., Gudgel, T., McCarthy, K., Agrawal, A., Allemand, P., & Cronin, J. (1999). User controllable photochromic (UCPC) devices. *Electrochimica Acta, 44*(18), 3017-3026. doi:https://doi.org/10.1016/S0013-4686(99)00015-8

Torcellini, P., Pless, S., Deru, M., Griffith, B., Long, N., & Judkoff, R. (2006). *Lessons learned from case studies of six high-performance buildings*. Retrieved from

U.S. Department of Energy. (2015). Testing and Validation | EnergyPlus. Retrieved from https://energyplus.net/testing

U.S. Department of Energy. (2016a). *EnergyPlus™ Version 8.6 Documentation -- Application Guide for EMS*. Retrieved from

U.S. Department of Energy. (2016b). *EnergyPlus™ Version 8.6 Documentation -- Engineering Reference*. Retrieved from

U.S. Department of Energy. (2016c). *EnergyPlus™ Version 8.6 Documentation -- External Interface(s) Application Guide*. Retrieved from

U.S. Department of Energy. (2016d). *EnergyPlus™ Version 8.6 Documentation -- Input Output Reference*. Retrieved from

U.S. Energy Information Administration. (2019a). Average Price of Electricity to Ultimate Customers by End-Use Sector. Retrieved from https://www.eia.gov/electricity/monthly/epm_table_grapher.php?t=epmt_5_6_a

U.S. Energy Information Administration. (2019b). Heat Content of Natural Gas Consumed. Retrieved from https://www.eia.gov/dnav/ng/ng_cons_heat_a_EPG0_VGTH_btucf_a.htm

U.S. Energy Information Administration. (2019c). U.S. Price of Natural Gas Delivered to Residential Consumers. Retrieved from https://www.eia.gov/dnav/ng/hist/n3010us3m.htm

Vance, A. (2018). Saudi-Backed Vision Fund Invests $1.1 Billion in a Maker of 'Smart Window' Glass. Retrieved from https://www.bloomberg.com/news/articles/2018-11-02/saudi-backed-vision-fund-invests-1-1-billion-in-a-maker-of-smart-window-glass

Vergaz, R., Sánchez-Pena, J.-M., Barrios, D., Vázquez, C., & Contreras-Lallana, P. (2008). Modelling and electro-optical testing of suspended particle devices. *Solar Energy Materials and Solar Cells, 92*(11), 1483-1487. doi:https://doi.org/10.1016/j.solmat.2008.06.018

Wang, W., Rivard, H., & Zmeureanu, R. (2005). An object-oriented framework for simulation-based green building design optimization with genetic algorithms. *Advanced Engineering Informatics, 19*(1), 5-23. doi:https://doi.org/10.1016/j.aei.2005.03.002

Wang, Y., Runnerstrom, E. L., & Milliron, D. J. (2016). Switchable Materials for Smart Windows. *Annual Review of Chemical and Biomolecular Engineering, 7*(1), 283-304. doi:10.1146/annurev-chembioeng-080615-034647

Wani, C., Ghodke, S., & Shrivastava, C. (2012). A review on potential of Maisotsenko cycle in energy saving applications using evaporative cooling. *International Journal of Advanced Research in Science, Engineering and Technology, 1*, 15-20.

Wesoff, E. (2018). Tintable-Glass Unicorn Gets Massive $1.1 Billion Investment From SoftBank Vision Fund. Retrieved from https://www.greentechmedia.com/articles/read/view-gets-massive-1-1-billion-investment-from-softbank?utm_medium=email&utm_source=Daily&utm_campaign=GTMDaily#gs.KvT0YSNi

Wetter, M. (2016). *Building Controls Virtual Test Bed Manual*. Retrieved from http://simulationresearch.lbl.gov/bcvtb/releases/latest/doc/manual/index.xhtml

Wong, J. M., Glasser, F. P., & Imbabi, M. S. (2007). Evaluation of thermal conductivity in air permeable concrete for dynamic breathing wall construction. *Cement and Concrete Composites, 29*(9), 647-655. doi:https://doi.org/10.1016/j.cemconcomp.2007.04.008

Wright, J., & Mourshed, M. (2009). *Geometric optimization of fenestration*. Paper presented at the Eleventh International IBPSA Conference, Glasgow, Scotland.

Wright, J. A., Brownlee, A., Mourshed, M. M., & Wang, M. (2014). Multi-objective optimization of cellular fenestration by an evolutionary algorithm. *Journal of Building Performance Simulation, 7*(1), 33-51. doi:10.1080/19401493.2012.762808

Xu, C., Liu, L., Legenski, S. E., Ning, D., & Taya, M. (2004). Switchable window based on electrochromic polymers. *Journal of Materials Research, 19*(7), 2072-2080. doi:10.1557/JMR.2004.0259

Ye, H., Long, L., Zhang, H., & Gao, Y. (2014). The energy saving index and the performance evaluation of thermochromic windows in passive buildings. *Renewable Energy, 66*, 215-221. doi:https://doi.org/10.1016/j.renene.2013.12.008

Ye, H., Meng, X., Long, L., & Xu, B. (2013). The route to a perfect window. *Renewable Energy, 55*, 448-455. doi:https://doi.org/10.1016/j.renene.2013.01.003

Zeng, R., Wang, X., Di, H., Jiang, F., & Zhang, Y. (2011). New concepts and approach for developing energy efficient buildings: Ideal specific heat for building internal thermal mass. *Energy and Buildings, 43*(5), 1081-1090. doi:https://doi.org/10.1016/j.enbuild.2010.08.035

Zhai, Y., Ma, Y., David, S. N., Zhao, D., Lou, R., Tan, G., . . . Yin, X. (2017). Scalable-manufactured randomized glass-polymer hybrid metamaterial for daytime radiative cooling. *Science, 355*(6329), 1062. doi:10.1126/science.aai7899

Zhang, J., Zou, Q., & Tian, H. (2013). Photochromic Materials: More Than Meets The Eye. *Advanced Materials, 25*(3), 378-399. doi:10.1002/adma.201201521

Zhao, X., Liu, S., & Riffat, S. B. (2008). Comparative study of heat and mass exchanging materials for indirect evaporative cooling systems. *Building and Environment, 43*(11), 1902-1911. doi:https://doi.org/10.1016/j.buildenv.2007.11.009

Zheng, S., Xu, Y., Shen, Q., & Yang, H. (2015). Preparation of thermochromic coatings and their energy saving analysis. *Solar Energy, 112*, 263-271. doi:https://doi.org/10.1016/j.solener.2014.09.049

Zhou, J., & Chen, Y. (2010). A review on applying ventilated double-skin facade to buildings in hot-summer and cold-winter zone in China. *Renewable and Sustainable Energy Reviews, 14*(4), 1321-1328. doi:https://doi.org/10.1016/j.rser.2009.11.017

Zhu, L., Raman, A., & Fan, S. (2013). Color-preserving daytime radiative cooling. *Applied Physics Letters, 103*(22), 223902. doi:10.1063/1.4835995